2009

Hemoprotein-Mediated Activation of Nitroalkanes

Ling Li
Cleveland State University

HEMOPROTEIN-MEDIATED ACTIVATION OF NITROALKANES

LING LI

Bachelor of Science in Applied Chemistry

Tianjin University, China

July, 1995

Submitted in partial fulfillment of requirements for the degree

DOCTOR OF PHILOSOPHY IN CLINICAL AND BIOANALYTICAL CHEMISTRY

at the

CLEVELAND STATE UNIVERSITY

June, 2009

This dissertation has been approved

For the Department of CHEMISTRY

and the College of Graduate Studies by

_____

Thesis/Dissertation Chairperson, *Dr. Mekki Bayachou*

_____

Department & Date

_____

Dr. Alan Riga

_____

Department & Date

_____

Dr. Robert Wei

_____

Department & Date

_____

Dr. Stan Duraj

_____

Department & Date

_____

Dr. Tobili Sam-Yellowe

_____

Department & Date

ACKNOWLEDGEMENTS

To stand where I am today would not be possible without my parents Xinghua Li and Lifeng Xu. I could not express my gratitude enough for your encouragement and support in pursuit of my education. I am thankful to my wife Yin Xu, who always gives me support and help, and also brought us our lovely daughter Qingcheng.

I would not become who I am today without my advisor, Dr. Mekki Bayachou. Thank you for taking me as your student and giving me the opportunity to work in your lab. Thank you for paying attention to my weaknesses and guiding me through every obstacle in my study. You showed me the amazing world of science and the value of my research.

I am thankful to my committee members, Dr. Alan Riga, Dr. Stan Duraj, Dr. Robert Wei, and Dr. Tobili Sam-Yellowe, for you thoughtful suggestions and guidance.

Last but not least, I thank all my labmates who are always warm-hearted and helpful. You are like my family, Dr. Pingang He, Dr. Serban Peteu, Dr. Chunyeon Lee, Dr Jean Boutros, Dr. Indika Perera, Dr. John Moran, Dr. Charbel Abou-Diwan, Pubudu Peiris, Reshani Perera, Saleem A. Bani Hani, and Bhagya Gunasekera, it is always a pleasure working with you.

HEMOPROTEIN-MEDIATED ACTIVATION OF NITROALKANES

LING LI

ABSTRACT

Chemicals and drugs are known to be metabolized mostly by Cytochrome P450 xenobiotic metabolizing enzymes. However, the detailed mechanism of nitro-compounds metabolism is still unclear. The activation of nitro-xenobiotics by heme-P450 enzymes is a potential explanation for the origin of nitro-compound carcinogenesis. Investigating the interaction of simple nitro-compounds with redox activity of heme enzymes is therefore critical to explore the mechanism and products of activation.

In this study, multiple analytical methods and instrumentations are employed and graphic and simulation software such as Origin® and Digisim® are utilized to quantitatively derive parameters from experimental raw data. This study shows that myoglobin, iron-protoporphyrin-IX (hemin), and the oxygenase domain of inducible nitric oxide synthase (iNOSoxy) act as efficient electrocatalysts for nitroalkane reductions in the surfactant films on pyrolytic graphite electrodes.

In the study using myoglobin as a model electrocatalyst for the electroreduction of nitromethane, the catalytic activity is evaluated using Michaelis-Menten kinetics. The apparent K_m and the turnover number k_{cat} are derived from non-linear regression of Michaelis-Menten plot using Origin software. The reductive products of catalytic electroreduction of nitromethane are identified by a mass spectrometric method. We also identified a ferrous heme-nitrosomethane as the intermediate in the catalytic process using UV-Vis spectroscopy and electrochemical techniques. We show the

electrochemical signature of a nitrosoalkane-heme complex that is possibly involved in the mechanism of activation of aliphatic nitro-compounds xenobiotics. A possible heme-mediated electroreductive pathway is proposed.

In this work, we also explored the comparative study of the electroreduction of nitromethane using myoglobin, hemin, and iNOSoxy as the electrocatalysts. We discussed the role of the protein shell in the activation process. We also studied four different aliphatic nitroalkanes as substrates to study their electro activation using hemin and iNOSoxy as electrocatalysts, and used a mass spectrometric method to identify the reduction products. By comparing the catalysis of each nitroalkane substrate and by varying experimental conditions such as scan rate of cyclic voltametry, substrate concentration, and pH, we discussed the effects caused by the physical and chemical properties of the substrates on their electrocatalytic reductions.

TABLE OF CONTENTS

Page

LIST OF TABLES

Table **Page**

LIST OF FIGURES

Figure **Page**

Appendix

LIST OF SCHEMES

Scheme **Page**

GENERAL INTRODUCTION

Due to their widespread use, the human body is frequently exposed to nitro-compounds. Nitroalkanes are recognized as carcinogens[1, 2], genotoxicant,[2, 3] and are suspected as cardiovascular toxins and neurotoxins.[4-6] The detailed mechanism of nitroalkane-induced carcinogenesis is still unclear. It is believed that nitro-compound activation may take place in the liver, catalyzed by xenobiotic enzymes under anaerobic conditions through catalytic electron transfer.[7, 8] Research has shown that cytochrome P450 participates in the reductive metabolism of nitro-compounds.[9] It also has been reported that 2-nitropropane reductive metabolite, N-isopropylhydroxylamine (IPHA), frequently causes DNA damage at thymine.[2] The formation of 8-hydroxydeoxyguanosine (8-OHdG) induced by IPHA is speculated to be involved in oxidative stress-related carcinogenesis.[10] To better comprehend the carcinogenesis of nitro-compounds, it is important to understand the fundamental reductive pathways catalyzed by heme-base proteins and enzymes.

Chemicals (including drugs) involve two-phase reactions in the metabolism. Phase I reactions are nonsynthetic reactions, including reduction, oxidation, and hydrolysis. Phase II reactions are known as conjugation reactions, and usually involve the interactions of the metabolites from phase I. This process usually detoxicates the chemicals. These reactions are catalyzed by a family of enzymes called xenobiotic metabolizing Cytochrome P450s. The metabolizing process will result in toxication or detoxication, also called activation and deactivation. The mechanisms of cytochrome P450 catalysis and inhibition have been the subject of intense studies in recent years. [11-14] Carcinogen and mutagen activations which occur in phase I are closely related to the

activity of Cytochrome P450s. Therefore, Cytochrome P450s became vital enzymes for the study of the mechanism of formation of carcinogenic metabolites.

Traditional methods of enzyme activity study include assays on initial rate, progress curve and transient kinetics through varying techniques such as spectrophotometric methods, light scattering methods, fluorometric methods, chemiluminescent methods, calorimetric methods, chromatographic methods, and radiometric methods. These methods can resolve enzyme mechanisms in concentration and time domain by measuring concentration change of substrate or product versus time, but little information can be obtained on the mechanism of catalytic reaction at the molecular level.

Most commonly used analytical techniques in recent investigations of P450 enzymes and their activation of xenobiotic compounds or their metabolites are HPLC, UV-Vis, Mass Spectrometry, and Electrochemical methods. Electrochemical methods show the advantages of being quantitative, sensitive and relatively uncomplicated.

Since more than 30% of enzymes are oxidoreductases including P450 heme enzymes, their activities involve electron transfer coupled with substrate transformation at the catalytic site that can be monitored electrochemically. This dynamic voltammetric approach obtains not only the kinetic information of enzymatic reactivity, but also the electrochemical potential, which defines the oxidation states and the rate of catalytic reaction.

The voltammetric electrochemical method on biomolecules such as proteins showed its potential first in the late 1970's when the direct (unmediated) voltammetry of cytochromes was obtained at solid electrodes.[15] This approach was enhanced when enzymes or other molecules of interest are attached or absorbed on the electrode surface.

The techniques of immobilization includes covalent attachment, self assembled monolayers (SAM), and bilayer thin film methods or layer-by-layer assembly. The commonly used materials used for these applications as solid electrodes are platinum, gold, silver, or even indium doped tin oxide transparent electrodes.

In our study, we use mostly the lipid bilayer thin film method. The catalysts or enzymes under investigation are embedded in a biomembrane-like surfactant bilayer structure on the surface of pyrolytic graphite electrode. The electrochemical studies of the enzymatic activity are combined with other analytical chemical techniques, such as spectrophotometric methods and mass spectrometric methods, in effort to understand the underlying mechanism of enzymatic or heme-based catalytic nitroalkane electroreduction.

CHAPTER I

CURRENT METHODS OF INVESTIGATING THE METABOLISMS OF NITROCOMPOUNDS

1.1 Introduction

Nitroalkanes are widely used as solvents, chemical intermediates or fuel in racing cars or rockets. Large amounts of nitroalkanes are released into the environment and result in environmental contamination. Chronic intake of these compounds may cause neuropathy,[4] DNA damage,[2, 3] and cancer.[16, 17]

As other xenobiotics, the metabolism of nitroalkanes is catalyzed by a superfamily of enzymes called Cytochrome P450s (CYPs). Human CYPs are mostly membrane-associated enzymes, located either in the endoplasmic reticulum or in the inner membrane of mitochondria of cells, and some CYPs exit in cytosol as well. CYPs are in charge of metabolizing thousands of exogenous and endogenous compounds. Most CYPs can metabolize multiple substrates, and many can catalyze multiple reactions, which enable them to catalyze the transformation and degradation a large variety of molecules.

Cytochromes are proteins that carry a heme protoporphyrin IX group as their prosthetic group, Figure 1.1. The heme group is a highly conjugated ring with an iron atom in the center. The oxidation states of iron readily interconverts between +2 and +3 through electron transfer. It can perform as either an electron source or an electron sink. This characteristic makes it capable to catalyze either oxidations or reductions.

Cytochromes P450 serve crucial functions in humans. The subfamily that act as xenobiotic-metabolizing enzymes is a prime target in pharmacology and drug development.[18]. The name P450 comes from its characteristic Soret peak at 450 nm of the reduced carbon monoxide-bound complex[19, 20]. P450 enzymes catalyze the activation of a variety of xenobiotics including almost all drugs and chemicals. For example, P450 enzymes metabolize organic nitrates, [21, 22] lauric acid and ethanol. [23] Cytochrome P450 belongs to a multi-gene family; so far more than 6,400 distinct Cytochrome P450 sequences are known from all variants of life, including mammals, plants, and even bacteria. There are 57 genes and 59 pseudogenes recognized so far coded for different Cytochrome P450s in the human genome.

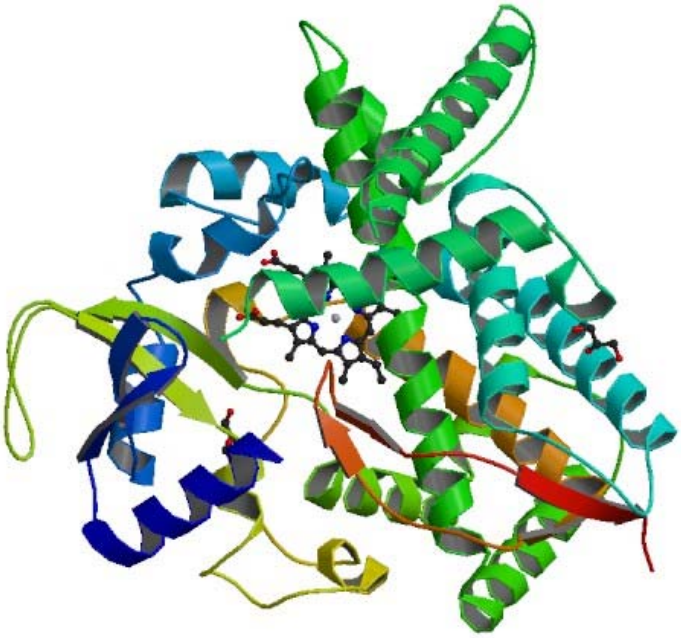

Figure 1.1 Crystal Structure of human cytochrome P450 46A1

Image from PDB 2Q9G

There is a structural diversity among Cytochrome P450s. Nonetheless, they share many common features: 1) Cytochrome P450s have a heme group as the active site. 2) The iron in the heme is coordinated to a cysteine thiolate ligand at the proximal site. This cysteine and many other peptides in the enzyme are highly conserved over all known Cytochrome P450s. 3) The catalytic function of cytochrome P450 needs other partner proteins such as Cytochrome P450 reductase or ferredoxins to donate and shuttle reducing equivalents (electrons) to the heme Fe(III) center.

The mechanisms of cytochrome P450 catalysis and inhibition have been the subject of intense studies in recent years. [11-14] Carcinogen and mutagen activations which occur in phase I are closely related to the activity of Cytochrome P450s. Therefore, Cytochrome P450s became vital enzymes for the study of the mechanism of formation of carcinogenic metabolites.

The general mechanism of the cytochrome P450 aerobic catalytic cycle is well known (Scheme 1.1). [24] It involves heme activation (Fe^{3+} reduces to Fe^{2+}), oxygen binding and activation, and then hydroxylation of the substrate.

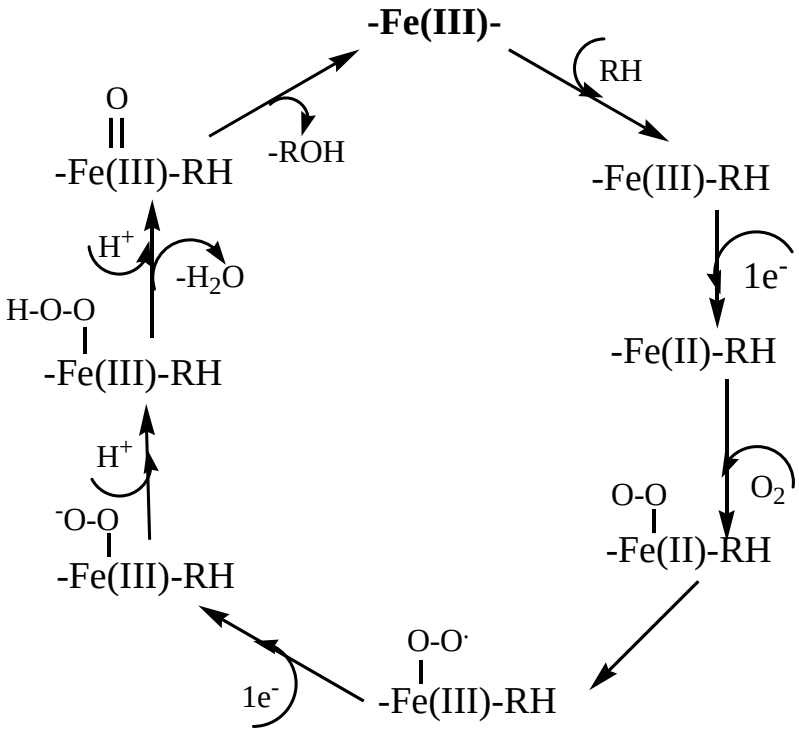

Scheme 1.1 Mechanism of Cytochrome P450 aerobic catalysis[24]

However, not all xenobiotics take the oxidative metabolic pathway. Some nitro-compounds can be reductively activated by Cytochrome P450s.[25] Nitroalkanes can either be reduced or oxidized by different enzymes. They could be oxidized by P450 enzymes under aerobic conditions initiated by electron transfer, and oxygen activation [7]. They could also be reduced by Cytochrome P450s under anaerobic conditions through catalytic electron transfer. [7-9] The primary product of nitroalkane reduction is alkyl hydroxylamine [26]. Fitzpatrick's group reported their work on a FAD-containing enzyme called nitroalkane oxidase from fungus, and stated that the oxidation products of nitroalkanes are aldehydes or ketones with nitrite and hydrogen peroxide as side products [27].

Cytochrome P450s are responsible for the metabolism of almost all kinds of chemicals including drugs. The activation of drugs by P450s can either lead to non-toxic metabolites or cytotoxicants, genotoxicants, and carcinogens; hence, CYPs are key enzymes for studying the metabolism and potential toxicity of drugs. A number of investigations have been carried out to study the effects of nitro-compounds on animal models or human samples, and there are also reports of cases showing health problems caused by the exposure to these chemicals. The techniques that have been commonly used in the studies are the following including spectroscopic methods such as UV-Vis spectroscopy, infrared spectroscopy, high performance liquid chromatography (HPLC) coupled UV-Vis or mass spectroscopy (MS), biological techniques such as gel electrophoresis, comet assay (single cell electrophoresis), Ames mutagenicity test, and electrochemical methods which are primarily used in our study.

UV-Vis spectroscopy has been commonly used to determine the concentration of protein samples, quantitatively measure the change of the reactive species, and monitor

the formation of new species. Because of its capability, this technique is constantly applied to the studies of cytochrome P450s catalyzed nitro-compound metabolism.

H.G. Jonen used UV-Vis spectroscopic method to study the nitrofurantoin metabolism in rat liver under aerobic and anaerobic conditions.[28, 29] His results showed that nitrofurantoin can be rapidly eliminated under anaerobic condition through a reductive metabolism. Under aerobic condition, the hepatic clearance of this chemical is slow. 4-hydroxylation of nitrofurantoin is catalyzed by 3-methylcholanthrene-inducible cytochrome P450.

Mansuy's group studied the interaction between hemoproteins including P450 enzyme and nitroalkanes and their metabolites under reducing conditions, and found out that nitroalkanes and hemoproteins form stable ferrous heme nitrosoalkane complexes under reducing condition using UV-Vis spectroscopic methods[30, 31]. Also N-hydroxylamines can react with Cytochrome P450 under oxidative condition to form the same type of complexes.[32]

Christopher Kohl *et al* reported on the toxicity of the genotoxicant and hepacarcinogen, 2-nitropropane.[33] The results showed that the nitro-aci tautomerism of 2-nitropropane catalyzed by rodent or human liver cytosol might be the reason for its toxicity. The study of 1-nitropyrene activation catalyzed by Human Hepatoblastoma Cell Line was also reported by Kimberley J. Silvers *et al.* [34] Their HPLC results showed that only nitroreduction pathway of 1-nitropyrene by HepG2 could form the DNA adduct, N-(2'-deoxyguanosin-8-yl)-l-aminopyrene (dG-CS-AP), and the cytochrome P450-mediated C-oxidative pathways are detoxification pathways.

In a recent study of the hepatoxicity of an anti-tumor prodrug 5-(Aziridin-1-yl)-2,4-dinitrobenzamide (CB 1954), HPLC coupled to mass spectrometry showed that the major metabolite, 4-hydroxylamine was formed,[35] a potent DNA cross-linking cytotoxin. 2-hydroxylamine and 2-amine metabolites were also detected and both of them exhibited high cytotoxicity. Another study reported on the metabolism of a nitro-containing drug, N1-phenyl-3,5-dinitro-N4,N4-di-n-butylsulfanilamide (GB-II-150), and showed that the drug underwent nitroreduction when administered orally. [36]

Comet assay is useful to study the genotoxicant by monitoring the DNA damage. An investigation of 2-nitroproapne-induced DNA damage using animal model by Xin-Sheng Deng *et al*[37] utilized this method and found out that DNA damage happened in bone marrow cells thus indicated that 2-ntiropropane could be leukemogenic.

Ames test was used in an investigation carried out by Peter P. Fu *et al* on the mutagenesis of nitrobenzo[a]pyrenes (NBaPs).[38] The results indicate that isomeric NBaPs are activated to DNA adducts and mutagenic derivatives by nitroreduction, ring-oxidation, or by a combination of these two pathways. Another report using the same approach to study the mutagenicity of various nitrocompound was conducted by S. G. Salamanca-Pinzon et al.[39] The results illustrated that the mutagenicity of the nitrocompound metabolites related to nitroreductase proficiency. All nitrocompound showed more mutagenic after metabolic activation by nitroreductase.

1.2 Electrochemical methods

The metabolic mechanisms of chemicals catalyzed by cytochrome P450 (CYP) enzymes involve electron transfer. In biological systems, enzymes such as CYPs have to use electron donors such as NADPH or NADH to perform their enzymatic activity, and they are affected by electron transfer mediators such as flavin nucleotides. The advantage of direct electrochemical methods are that if enzymes such as CYP can be connected to a solid electrode surfaces by a bridge, and the active site of CYP, a heme group, can exchange electrons with the underlying electrode, there is no need to have the electron donors or mediators in the system. We can thus study the enzymatic reactions by providing electrons directly from the electrode.

The current response on the electrode is directly related to the rate of the reaction and the amount substrate being processed. Hence it is a quantitative method. When using dynamic voltammetric technique, electrode potential can reflect thermodynamic information of the enzyme as well as enzymatic kinetics. High sensitivity is the nature of electrochemical method; therefore the amount of enzyme sample can be very small.

There are numbers of electrochemical techniques available. Because of the advantages, electrochemical techniques of studing metalloeproteins especailly CYP heme enzymes have drawn more and more attention in the last couple of decads. In the appendix we describe the common methods that we used throughout this work.

Cyclic voltammetry (CV) is probably the most versatile electrochemical technique for the mechanistic study of redox active systems. Direct electrochemistry of P450 enzyme was reported in the literature that have protein shows typically a reversible Fe^{III}/Fe^{II} redox couple of the prosthetic heme group.[40-43]

1.3 Protein immobilization methods

Before the development of biomolecule immobilization methodology, the electrochemical studies of proteins or enzymes were carried out in solution and the signal obtained directly at the working electrode was facilitated by small mediators. This approach not only requires large amount of enzyme or proteins, but the signal is also very weak. The protein immobilization method confines the protein on the surface of working electrodes instead of in solution. This approach not only saves lot of protein sample, but also enhanced the electrochemical current signal. Since direct (non-mediated) electron transfer through metalloprotein was achieved, the electrochemical study of metalloproteins began to attract the interest of investigators and became more and more popular.

The techniques of immobilizing native proteins on working electrodes are critical in the research and various methods of immobilization are developed for different applications.

1.3.1 Adsorption

Proteins such as Cytochrome P450s can be directly deposited on the metal or graphite electrode. Purified CYP solution can be spread on a basal plane pyrolytic graphite surface, [44] and the film is formed simply by evaporating water naturely. Protein or peptide modification can also be done electrochemically by cycling a gold electrode at reducing potentials in the peptide solution as described by J. Kazlauskaite *et al*.[45]

Besides direct adsorption, co-adsorbates such as polyamines,[46] neomycin[47-49], and polymyxin[50-55] have been used for protein immobilization. These polyamines can bind to

negatively charged parts of protein under neutral pH and form salt bridges between protein and electrode surface.

Other adsorption methods involves nano-particles[56] such as titanate nanotubes,[57] carbon nanotubes,[58-70], gold nanoparticles,[71, 72] and silver nanoparticles.[73]

1.3.2 Hydrogel or clay entrapment

The electron transfer between the electrode and protein is usually low for a protein-modified electrode by absorption. Therefore application of substances that facilitates electron transfer may enhance the intensity of the signal and the stability of the protein film. There are a numbers of choices of film-forming materials such as colloid size clay,[74, 75] hexagonal mesoporous silica (HMS),[76] polyacrylamide (PAM) hydrogel films,[77, 78] and carboxymethyl cellulose films,[79] to cite a few.

1.3.3 Lipid bilayer thin films

Some amphiphilic compounds (surfactants) such as didodecyl dimethyl ammonium bromide (DDAB) can form a water-insoluble bilayered film structure that resembles bio-membranes on solid electrode surfaces, Figure 1.2. Both hydrophilic and hydrophobic proteins or other molecules can be embedded into these surfactant thin films. This method of protein immobilization promotes the electron transfer between the protein and the electrode. Research had shown that the film is fairly stable in aqueous environment and the proteins could maintain their native structure in the lipid thin film.[80-82] This method is suitable for applications such as biosensors and bioreactors, and also widely used in the electrochemical investigations of catalytic mechanisms of enzymes and other proteins.[80, 81, 83-86]

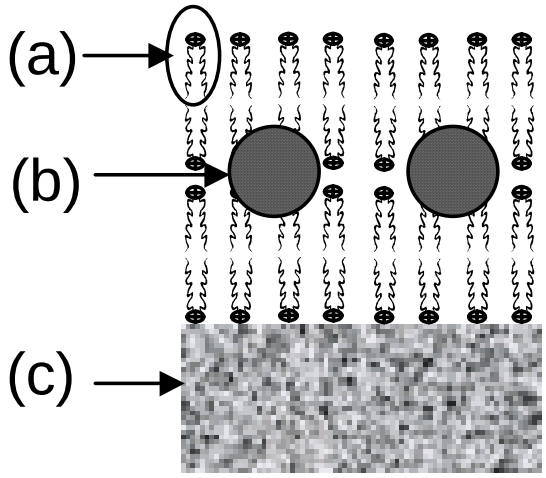

Figure 1.2 Protein immobilized in bio-membrane like lipid film on pyrolytic graphite (PG) electrode. (a) Lipid molecule (b) Protein moleclue (c) Pyrolytic graphite (PG) electrode

1.3.4 Covalent attachment

Biomolecules such as proteins can form covalent bonds with specific chemical groups on the electrode surface. This usually involves a step called functionalization of the electrode surface. The desired chemical group(s) is covalently attached to the electrode surface usually through defined chemical reactions.

Functionalized alkyl thiols can be spontaneously adsorbed onto Au, Pt, and Ag surface to generate self-assembled monolayers (SAM) with the functional groups pointing away from the electrode so that it can engage the protein molecules, Figure 1.3.

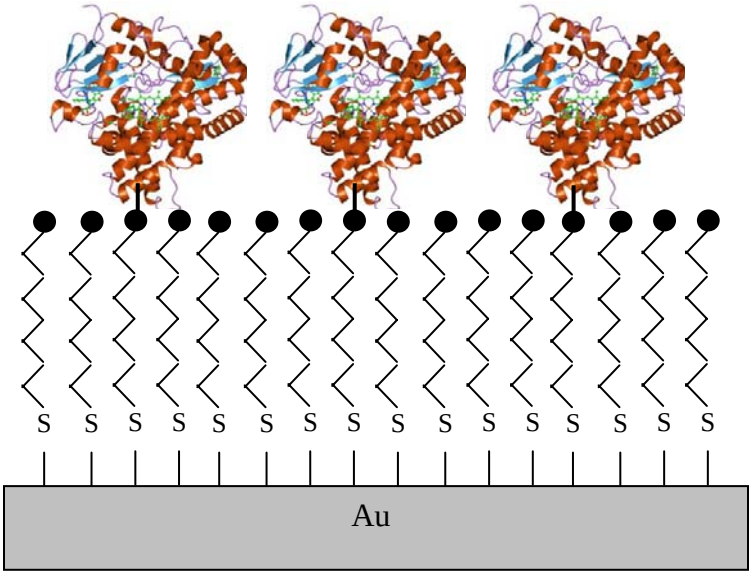

Figure 1.3 Immobilization via covalent attachment of proteins

1.3.5 Layer-by-layer polyion protein adsorption

Electrostatic coupling can be used to deposit charged compounds onto a charged electrode surface. Layer-by-layer (LBL) deposition is a technique of thin film fabrication. The method consists of applying oppositely charged polyions respectively with washing step in between. Just like the name indicates, the resulting film has alternative layers of negatively charged and positively charged polyions. The number of layer and the thickness of the film can be well controlled, Figure 1.4. Proteins can bear different surface charge at different pHs. Therefore this method is used for protein immobilization. Some multi-charged matrices such as poly(diallyl dimethyl ammonium chloride) (PDDA) can be used to couple with negatively charged polyions or proteins to form protein-containing LBL films.

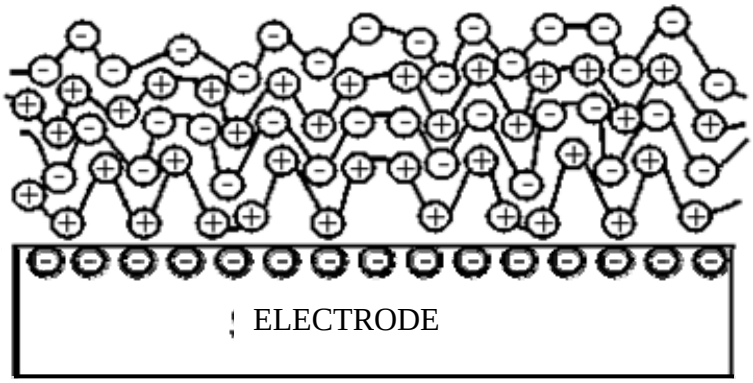

Figure 1.4 Layer-by-layer polyion adsorption

1.4 The approach we took in our study

The electrochemical technique using surface confined metalloprotein especially enzymes, may not only apply to substrate-specific biosensors and bioreactors, but can also be used commonly to study enzymatic activity of metalloenzymes. Since the majority of cytochrome P450 enzymes are located in hydrophobic environments such as the reticulum of cells or cell membranes, the study of such type of enzymes needs to mimic the physiological environments. In this work, we select well-known lipid thin film immobilization methods to retain our enzymes on the basal plane pyrolytic graphite working electrode surface. The lipid bilayer structure provides a biomembrane-like environment in which the protein molecule is embedded. We use electrochemical techniques as the major tools to characterize the redox activity of the heme group as well as electro activation of nitroalkane substrates.

In addition to electrochemistry, UV-Vis spectroscopy is routinely used to monitor the concentration and integrity of hemoproteins. It is also employed to characterize possible reaction intermediates of heme-mediated catalytic nitroalkane electroreduction.

Final products of electroreductions mediated by immobilized hemoproteins, as well as their distribution are needed to shed light on the complex activation pathways, and to identify the plausible mechanism. To analyze the final electroreduction products, we used bulk electrolysis (i.e. exhaustive reduction at the potential of the catalytic wave on the heme or (protein)-modified electrode) and analyze the products at different times using mass spectrometry (MS). The setup that allows for bulk electrolysis and analysis of products been developed in the past[87-90]. The system is adapted to this work.

1.5 References

1. Page, E. H. a. P., Aurora K.b; Arnold, Thomas C.c; Fincher, Allene R.d; Goddard, Mark J.e, Peripheral neuropathy in workers exposed to nitromethane. *American Journal of Industrial Medicine* **2001,** 40, (1), 107-113.

2. Sakano, K.; Oikawa, S.; Murata, M.; Hiraku, Y.; Kojima, N.; Kawanishi, S., Mechanism of metal-mediated DNA damage induced by metabolites of carcinogenic 2-nitropropane. *Mutat Res* **2001,** 479, (1-2), 101-11.

3. Deng, X. S.; Tuo, J.; Poulsen, H. E.; Loft, S., 2-Nitropropane-induced DNA damage in rat bone marrow. *Mutat Res* **1997,** 391, (3), 165-9.

4. Page, E. H.; Pajeau, A. K.; Arnold, T. C.; Fincher, A. R.; Goddard, M. J., Peripheral neuropathy in workers exposed to nitromethane. *Am J Ind Med* **2001,** 40, (1), 107-13.

5. Toxicology and carcinogenesis studies of nitromethane (CAS No. 75-52-5) in F344/N rats and B6C3F1 mice. (Inhalation studies). *National Toxicology Program Technical Report Series* **1997**, (461), 284.

6. Lewis, T. R.; Ulrich, C. E.; Busey, W. M., Subchronic inhalation toxicity of nitromethane and 2-nitropropane. *J Environ Pathol Toxicol* **1979,** 2, (5), 233-49.

7. Mansuy, D., The great diversity of reactions catalyzed by cytochromes P450. *Comparative Biochemistry and Physiology -- Part C: Pharmacology, Toxicology & Endocrinology* **1998,** 121, (1-3), 5-14.

8. Jiang, Y.; Kuo, C. L.; Pernecky, S. J.; Piper, W. N., The detection of cytochrome P450 2E1 and its catalytic activity in rat testis. *Biochem Biophys Res Commun* **1998,** 246, (3), 578-83.

9. Harada, N.; Omura, T., Participation of cytochrome P-450 in the reduction of nitro compounds by rat liver microsomes. *J Biochem (Tokyo)* **1980,** 87, (5), 1539-54.

10. Floyd, R. A., The role of 8-hydroxyguanine in carcinogenesis. *Carcinogenesis* **1990,** 11, (9), 1447-50.

11. Wang, Y.; Yang, C.; Wang, H.; Han, K.; Shaik, S., A New Mechanism for Ethanol Oxidation Mediated by Cytochrome P450 2E1: Bulk Polarity of the Active Site Makes a Difference. *Chembiochem* **2007,** 8, (3), 277-281.

12. Tsalkova, T. N.; Davydova, N. Y.; Halpert, J. R.; Davydov, D. R., Mechanism of interactions of alpha-naphthoflavone with cytochrome P450 3A4 explored with an engineered enzyme bearing a fluorescent probe. *Biochemistry* **2007,** 46, (1), 106-19.

13. Obach, R. S.; Walsky, R. L.; Venkatakrishnan, K., Mechanism-based inactivation of human cytochrome p450 enzymes and the prediction of drug-drug interactions. *Drug Metab Dispos* **2007,** 35, (2), 246-55.

14. Yamada, H.; Ishii, Y.; Yamamoto, M.; Oguri, K., Induction of the hepatic cytochrome P450 2B subfamily by xenobiotics: research history, evolutionary aspect, relation to tumorigenesis, and mechanism. *Curr Drug Metab* **2006,** 7, (4), 397-409.

15. Eddowes, M. J.; Elzanowska, H.; Hill, H. A., Electrochemistry of cytochrome c3 from Desulfovibrio desulphuricans (Norway) [proceedings]. *Biochem Soc Trans* **1979,** 7, (4), 735-7.

16. Conaway, C. C.; Nie, G.; Hussain, N. S.; Fiala, E. S., Comparison of oxidative damage to rat liver DNA and RNA by primary nitroalkanes, secondary nitroalkanes, cyclopentanone oxime, and related compounds. *Cancer Res* **1991,** 51, (12), 3143-7.

17. Hadidian, Z.; Fredrickson, T. N.; Weisburger, E. K.; Weisburger, J. H.; Glass, R. M.; Mantel, N., Tests for chemical carcinogens. Report on the activity of derivatives of aromatic amines, nitrosamines, quinolines, nitroalkanes, amides, epoxides, aziridines, and purine antimetabolites. *J Natl Cancer Inst* **1968,** 41, (4), 985-1036.

18. Haining, R. L.; Nichols-Haining, M., Cytochrome P450-catalyzed pathways in human brain: metabolism meets pharmacology or old drugs with new mechanism of action? *Pharmacol Ther* **2007,** 113, (3), 537-45.

19. Klingenberg, M., Pigments of rat liver microsomes. *Arch Biochem Biophys* **1958,** 75, (2), 376-86.

20. Murray, G. I., The role of cytochrome P450 in tumour development and progression and its potential in therapy. *J Pathol* **2000,** 192, (4), 419-26.

21. Minamiyama, Y.; Takemura, S.; Yamasaki, K.; Hai, S.; Hirohashi, K.; Funae, Y.; Okada, S., Continuous administration of organic nitrate decreases hepatic cytochrome P450. *J Pharmacol Exp Ther* **2004,** 308, (2), 729-35.

22. Minamiyama, Y.; Takemura, S.; Nishino, Y.; Okada, S., Organic nitrate tolerance is induced by degradation of some cytochrome P450 isoforms. *Redox Rep* **2002,** 7, (5), 339-42.

23. Orellana, M.; Varela, N.; Guajardo, V.; Araya, J.; Rodrigo, R., Modulation of rat liver cytochrome P450 activity by prolonged red wine consumption. *Comp Biochem Physiol C Toxicol Pharmacol* **2002,** 131, (2), 161-6.

24. Guengerich, F. P., Cytochrome P450: what have we learned and what are the future issues? *Drug Metab Rev* **2004,** 36, (2), 159-97.

25. Kappers, W. A.; van Och, F. M.; de Groene, E. M.; Horbach, G. J., Comparison of three different in vitro mutation assays used for the investigation of cytochrome P450-mediated mutagenicity of nitro-polycyclic aromatic hydrocarbons. *Mutat Res* **2000,** 466, (2), 143-59.

26. Boutros, J.; Bayachou, M., Myoglobin as an efficient electrocatalyst for nitromethane reduction. *Inorg Chem* **2004,** 43, (13), 3847-53.

27. Gadda, G.; Fitzpatrick, P. F., Mechanism of nitroalkane oxidase: 2. pH and kinetic isotope effects. *Biochemistry* **2000,** 39, (6), 1406-10.

28. Jonen, H. G., Reductive and oxidative metabolism of nitrofurantoin in rat liver. *Naunyn Schmiedebergs Arch Pharmacol* **1980,** 315, (2), 167-75.

29. Jonen, H. G.; Oesch, F.; Platt, K. L., 4-Hydroxylation of nitrofurantoin in the rat. A 3-methylcholanthrene-inducible pathway of a relatively nontoxic compound. *Drug Metab Dispos* **1980,** 8, (6), 446-51.

30. Mansuy, D.; Gans, P.; Chottard, J. C.; Bartoli, J. F., Nitrosoalkanes as Fe(II) ligands in the 455-nm-absorbing cytochrome P-450 complexes formed from nitroalkanes in reducing conditions. *Eur J Biochem* **1977,** 76, (2), 607-15.

31. Mansuy, D.; Chottard, J. C.; Chottard, G., Nitrosoalkanes as Fe(II) ligands in the hemoglobin and myoglobin complexes formed from nitroalkanes in reducing conditions. *Eur J Biochem* **1977,** 76, (2), 617-23.

32. Mansuy, D.; Rouer, E.; Bacot, C.; Gans, P.; Chottard, J. C.; Leroux, J. P., Interaction of aliphatic N-hydroxylamines with microsomal cytochrome P450: nature of the different derived complexes and inhibitory effects on monoxygenases activities. *Biochem Pharmacol* **1978,** 27, (8), 1129-37.

33. Kohl, C.; Gescher, A., Catalysis of nitro-aci tautomerism of the genotoxicant 2-nitropropane by cytosol from rodent and human liver. *Chem Biol Interact* **1996,** 99, (1-3), 219-26.

34. Silvers, K. J.; Couch, L. H.; Rorke, E. A.; Howard, P. C., Role of nitroreductases but not cytochromes P450 in the metabolic activation of 1-nitropyrene in the HepG2 human hepatoblastoma cell line. *Biochem Pharmacol* **1997,** 54, (8), 927-36.

35. Tang, M. H.; Helsby, N. A.; Wilson, W. R.; Tingle, M. D., Aerobic 2- and 4-nitroreduction of CB 1954 by human liver. *Toxicology* **2005,** 216, (2-3), 129-39.

36. Wu, D.; George, T. G.; Hurh, E.; Werbovetz, K. A.; Dalton, J. T., Pre-systemic metabolism prevents in vivo antikinetoplastid activity of N1,N4-substituted 3,5-dinitro sulfanilamide, GB-II-150. *Life Sci* **2006,** 79, (11), 1081-93.

37. Xin-Sheng Deng, J. T., Henrik E. Poulsen, Steffen loft, 2-nitroproapne-induced DNA damage in rat bone marrow. *Mutation Research* **1997,** 391, 165-169.

38. Fu, P. P.; Qui, F. Y.; Jung, H.; Von Tungeln, L. S.; Zhan, D. J.; Lee, M. J.; Wu, Y. S.; Heflich, R. H., Metabolism of isomeric nitrobenzo[a]pyrenes leading to DNA adducts and mutagenesis. *Mutat Res* **1997,** 376, (1-2), 43-51.

39. Salamanca-Pinzon, S. G.; Camacho-Carranza, R.; Hernandez-Ojeda, S. L.; Espinosa-Aguirre, J. J., Nitrocompound activation by cell-free extracts of nitroreductase-proficient Salmonella typhimurium strains. *Mutagenesis* **2006,** 21, (6), 369-74.

40. Fantuzzi, A.; Fairhead, M.; Gilardi, G., Direct electrochemistry of immobilized human cytochrome P450 2E1. *J Am Chem Soc* **2004,** 126, (16), 5040-1.

41. Udit, A. K.; Hill, M. G.; Gray, H. B., Electrochemistry of cytochrome P450 BM3 in sodium dodecyl sulfate films. *Langmuir* **2006,** 22, (25), 10854-7.

42. Sultana, N.; Schenkman, J. B.; Rusling, J. F., Protein film electrochemistry of microsomes genetically enriched in human cytochrome p450 monooxygenases. *J Am Chem Soc* **2005,** 127, (39), 13460-1.

43. Oku, Y.; Ohtaki, A.; Kamitori, S.; Nakamura, N.; Yohda, M.; Ohno, H.; Kawarabayasi, Y., Structure and direct electrochemistry of cytochrome P450 from the thermoacidophilic crenarchaeon, Sulfolobus tokodaii strain 7. *J Inorg Biochem* **2004,** 98, (7), 1194-9.

44. Barry D. Fleming, S. G. B., Luet-Lok Wong, Alan M. Bond, The electrochemistry of a heme-containing enzyme, CYP199A2, adsorbed directly onto a pyrolytic graphite electrode. *Journal of Electroanalytical Chemistry* **2007,** 611, 149-154.

45. Kazlauskaite, J.; Hill, H. A.; Wilkins, P. C.; Dalton, H., Direct electrochemistry of the hydroxylase of soluble methane monooxygenase from Methylococcus capsulatus (Bath). *Eur J Biochem* **1996,** 241, (2), 552-6.

46. Vincent, K. A.; Tilley, G. J.; Quammie, N. C.; Streeter, I.; Burgess, B. K.; Cheesman, M. R.; Armstrong, F. A., Instantaneous, stoichiometric generation of powerfully reducing states of protein active sites using Eu(II) and polyaminocarboxylate ligands. *Chem Commun (Camb)* **2003**, (20), 2590-1.

47. Armstrong, J. S.; Jones, D. P., Glutathione depletion enforces the mitochondrial permeability transition and causes cell death in Bcl-2 overexpressing HL60 cells. *FASEB J* **2002,** 16, (10), 1263-5.

48. Bruno, J. G.; Parker, J. E.; Kiel, J. L., Plant nitrate reductase gene fragments enhance nitrite production in activated murine macrophage cell lines. *Biochem Biophys Res Commun* **1994,** 201, (1), 284-9.

49. Armstrong, F. A.; George, S. J.; Cammack, R.; Hatchikian, E. C.; Thomson, A. J., Electrochemical and spectroscopic characterization of the 7Fe form of ferredoxin III from Desulfovibrio africanus. *Biochem J* **1989,** 264, (1), 265-73.

50. Ludwig, M.; Cracknell, J. A.; Vincent, K. A.; Armstrong, F. A.; Lenz, O., Oxygen-tolerant H2 oxidation by membrane-bound [NiFe] hydrogenases of ralstonia species. Coping with low level H2 in air. *J Biol Chem* **2009,** 284, (1), 465-77.

51. Goldet, G.; Wait, A. F.; Cracknell, J. A.; Vincent, K. A.; Ludwig, M.; Lenz, O.; Friedrich, B.; Armstrong, F. A., Hydrogen production under aerobic conditions by membrane-bound hydrogenases from Ralstonia species. *J Am Chem Soc* **2008,** 130, (33), 11106-13.

52. Vincent, K. A.; Cracknell, J. A.; Clark, J. R.; Ludwig, M.; Lenz, O.; Friedrich, B.; Armstrong, F. A., Electricity from low-level H2 in still air--an ultimate test for an oxygen tolerant hydrogenase. *Chem Commun (Camb)* **2006**, (48), 5033-5.

53. Vincent, K. A.; Cracknell, J. A.; Lenz, O.; Zebger, I.; Friedrich, B.; Armstrong, F. A., Electrocatalytic hydrogen oxidation by an enzyme at high carbon monoxide or oxygen levels. *Proc Natl Acad Sci U S A* **2005,** 102, (47), 16951-4.

54. Jones, A. K.; Lamle, S. E.; Pershad, H. R.; Vincent, K. A.; Albracht, S. P.; Armstrong, F. A., Enzyme electrokinetics: electrochemical studies of the anaerobic interconversions between active and inactive states of Allochromatium vinosum [NiFe]-hydrogenase. *J Am Chem Soc* **2003,** 125, (28), 8505-14.

55. Leger, C.; Jones, A. K.; Roseboom, W.; Albracht, S. P.; Armstrong, F. A., Enzyme electrokinetics: hydrogen evolution and oxidation by Allochromatium vinosum [NiFe]-hydrogenase. *Biochemistry* **2002,** 41, (52), 15736-46.

56. Liu, G.; Lin, Y. Y.; Wang, J.; Wu, H.; Wai, C. M.; Lin, Y., Disposable electrochemical immunosensor diagnosis device based on nanoparticle probe and immunochromatographic strip. *Anal Chem* **2007,** 79, (20), 7644-53.

57. Liu, A.; Wei, M.; Honma, I.; Zhou, H., Direct electrochemistry of myoglobin in titanate nanotubes film. *Anal Chem* **2005,** 77, (24), 8068-74.

58. Kang, X.; Wang, J.; Tang, Z.; Wu, H.; Lin, Y., Direct electrochemistry and electrocatalysis of horseradish peroxidase immobilized in hybrid organic-inorganic film of chitosan/sol-gel/carbon nanotubes. *Talanta* **2009,** 78, (1), 120-5.

59. Zhang, L.; Tian, D. B.; Zhu, J. J., Direct electrochemistry and electrochemical catalysis of myoglobin-TiO2 coated multiwalled carbon nanotubes modified electrode. *Bioelectrochemistry* **2008,** 74, (1), 157-63.

60. Lojou, E.; Luo, X.; Brugna, M.; Candoni, N.; Dementin, S.; Giudici-Orticoni, M. T., Biocatalysts for fuel cells: efficient hydrogenase orientation for H2 oxidation at electrodes modified with carbon nanotubes. *J Biol Inorg Chem* **2008,** 13, (7), 1157-67.

61. Cao, Z.; Jiang, X.; Xie, Q.; Yao, S., A third-generation hydrogen peroxide biosensor based on horseradish peroxidase immobilized in a tetrathiafulvalene-tetracyanoquinodimethane/multiwalled carbon nanotubes film. *Biosens Bioelectron* **2008,** 24, (2), 222-7.

62. Pumera, M.; Smid, B., Redox protein noncovalent functionalization of double-wall carbon nanotubes: electrochemical binder-less glucose biosensor. *J Nanosci Nanotechnol* **2007,** 7, (10), 3590-5.

63. Manesh, K. M.; Kim, H. T.; Santhosh, P.; Gopalan, A. I.; Lee, K. P., A novel glucose biosensor based on immobilization of glucose oxidase into multiwall carbon

nanotubes-polyelectrolyte-loaded electrospun nanofibrous membrane. *Biosens Bioelectron* **2008,** 23, (6), 771-9.

64. Kang, X.; Mai, Z.; Zou, X.; Cai, P.; Mo, J., A novel glucose biosensor based on immobilization of glucose oxidase in chitosan on a glassy carbon electrode modified with gold-platinum alloy nanoparticles/multiwall carbon nanotubes. *Anal Biochem* **2007,** 369, (1), 71-9.

65. Alonso-Lomillo, M. A.; Rudiger, O.; Maroto-Valiente, A.; Velez, M.; Rodriguez-Ramos, I.; Munoz, F. J.; Fernandez, V. M.; De Lacey, A. L., Hydrogenase-coated carbon nanotubes for efficient H2 oxidation. *Nano Lett* **2007,** 7, (6), 1603-8.

66. Heering, H. A.; Williams, K. A.; de Vries, S.; Dekker, C., Specific vectorial immobilization of oligonucleotide-modified yeast cytochrome C on carbon nanotubes. *Chemphyschem* **2006,** 7, (8), 1705-9.

67. Lee, Y. M.; Kwon, O. Y.; Yoon, Y. J.; Ryu, K., Immobilization of horseradish peroxidase on multi-wall carbon nanotubes and its electrochemical properties. *Biotechnol Lett* **2006,** 28, (1), 39-43.

68. Lenihan, J. S.; Gavalas, V. G.; Wang, J.; Andrews, R.; Bachas, L. G., Protein immobilization on carbon nanotubes through a molecular adapter. *J Nanosci Nanotechnol* **2004,** 4, (6), 600-4.

69. Davis, J. J.; Coleman, K. S.; Azamian, B. R.; Bagshaw, C. B.; Green, M. L., Chemical and biochemical sensing with modified single walled carbon nanotubes. *Chemistry* **2003,** 9, (16), 3732-9.

70. Azamian, B. R.; Davis, J. J.; Coleman, K. S.; Bagshaw, C. B.; Green, M. L., Bioelectrochemical single-walled carbon nanotubes. *J Am Chem Soc* **2002,** 124, (43), 12664-5.

71. Xu, Q.; Mao, C.; Liu, N. N.; Zhu, J. J.; Sheng, J., Direct electrochemistry of horseradish peroxidase based on biocompatible carboxymethyl chitosan-gold nanoparticle nanocomposite. *Biosens Bioelectron* **2006,** 22, (5), 768-73.

72. Yin, X. B.; Qi, B.; Sun, X.; Yang, X.; Wang, E., 4-(Dimethylamino)butyric acid labeling for electrochemiluminescence detection of biological substances by increasing sensitivity with gold nanoparticle amplification. *Anal Chem* **2005,** 77, (11), 3525-30.

73. Ren, X.; Meng, X.; Chen, D.; Tang, F.; Jiao, J., Using silver nanoparticle to enhance current response of biosensor. *Biosens Bioelectron* **2005,** 21, (3), 433-7.

74. Lei, C.; Wollenberger, U.; Bistolas, N.; Guiseppi-Elie, A.; Scheller, F. W., Electron transfer of hemoglobin at electrodes modified with colloidal clay nanoparticles. *Anal Bioanal Chem* **2002,** 372, (2), 235-9.

75. Lei, C.; Wollenberger, U.; Jung, C.; Scheller, F. W., Clay-bridged electron transfer between cytochrome p450(cam) and electrode. *Biochem Biophys Res Commun* **2000,** 268, (3), 740-4.

76. Dai, Z.; Xu, X.; Ju, H., Direct electrochemistry and electrocatalysis of myoglobin immobilized on a hexagonal mesoporous silica matrix. *Anal Biochem* **2004,** 332, (1), 23-31.

77. Lu, H.; Li, Z.; Hu, N., Direct voltammetry and electrocatalytic properties of catalase incorporated in polyacrylamide hydrogel films. *Biophys Chem* **2003,** 104, (3), 623-32.

78. Li, Y.-z. H., Ning; Ci, Yun-xiang, Mimicry of peroxidase by immobilization of hemin on N-isopropylacrylamide-based hydrogel. *The Analyst* **1998,** 123, (2), 359-364.

79. Huang, H.; He, P.; Hu, N.; Zeng, Y., Electrochemical and electrocatalytic properties of myoglobin and hemoglobin incorporated in carboxymethyl cellulose films. *Bioelectrochemistry* **2003,** 61, (1-2), 29-38.

80. Nassar, A. E.; Rusling, J. F.; Kumosinski, T. F., Salt and pH effects on electrochemistry of myoglobin in thick films of a bilayer-forming surfactant. *Biophys Chem* **1997,** 67, (1-3), 107-16.

81. Nassar, A. E.; Willis, W. S.; Rusling, J. F., Electron transfer from electrodes to myoglobin: facilitated in surfactant films and blocked by adsorbed biomacromolecules. *Anal Chem* **1995,** 67, (14), 2386-92.

82. Guto, P. M. R., James F., Myoglobin retains iron heme and near-native conformation in DDAB films prepared from pH 5 to 7 dispersions. *Electrochemistry Communications* **2006,** 8, (3), 455-459.

83. Carrero, H.; Rusling, J. F., Analysis of haloacetic acid mixtures by HPLC using an electrochemical detector coated with a surfactant-nafion film. *Talanta* **1999,** 48, (3), 711-8.

84. Wang, F.; Chen, X.; Xu, Y.; Hu, S.; Gao, Z., Enhanced electron transfer for hemoglobin entrapped in a cationic gemini surfactant films on electrode and the fabrication of nitric oxide biosensor. *Biosens Bioelectron* **2007,** 23, (2), 176-82.

85. Shimomura, T.; Itoh, T.; Sumiya, T.; Mizukami, F.; Ono, M., Amperometric determination of choline with enzyme immobilized in a hybrid mesoporous membrane. *Talanta* **2009,** 78, (1), 217-20.

86. Tani, Y.; Tanaka, K.; Yabutani, T.; Mishima, Y.; Sakuraba, H.; Ohshima, T.; Motonaka, J., Development of a D-amino acids electrochemical sensor based on immobilization of thermostable D-proline dehydrogenase within agar gel membrane. *Anal Chim Acta* **2008,** 619, (2), 215-20.

87. Lin, R. B., Mekki; Greaves, John; Farmer, Patrick J., Nitrite Reduction by Myoglobin in Surfactant Films. *Journal of the American Chemical Society* **1997,** 119, (51), 12689-12690.

88. Bayachou, M. L., Rong; Cho, William; Farmer, Patrick J., Electrochemical Reduction of NO by Myoglobin in Surfactant Film: Characterization and Reactivity of the Nitroxyl (NO-) Adduct. *Journal of the American Chemical Society* **1998,** 120, (38), 9888-9893.

89. Immoos, C. E.; Chou, J.; Bayachou, M.; Blair, E.; Greaves, J.; Farmer, P. J., Electrocatalytic reductions of nitrite, nitric oxide, and nitrous oxide by thermophilic cytochrome P450 CYP119 in film-modified electrodes and an analytical comparison of its catalytic activities with myoglobin. *J Am Chem Soc* **2004,** 126, (15), 4934-42.

90. Bayachou, M.; Elkbir, L.; Farmer, P. J., Catalytic two-electron reductions of N2O and N3- by myoglobin in surfactant films. *Inorg Chem* **2000,** 39, (2), 289-93.

CHAPTER II

STUDY OF MYOGLOBIN-MEDIATED NITROMETHANE ELECTRO-REDUCTION AND THE CATALYTIC REACTION MECHANISM

2.1 Introduction

Nitromethane is the simplest aliphatic nitroalkane. It is recognized as a carcinogen, and is suspected to be a cardiovascular toxin and neurotoxin.[1, 2] Nitromethane transformation in human body is believed to be catalyzed by P450-type xenobiotic enzymes under anaerobic conditions through catalytic electron transfer.[3, 4]

Nitromethane is electroactive and can be electroreduced to methyl hydroxylamine at electrode surface. The process can be simplified as in Equation 1. This electrochemical reaction consists of 4 electrons and 4 protons uptake in addition to a break of N-O bond and involves a complex mechanism.[5]

$$CH_3NO_2 + 4H^+ \xrightarrow{4e^-} CH_3NHOH + H_2O \qquad (1)$$

The active sites of cytochrome P450s (CYPs) are heme groups. Chemicals and drugs transformations are catalyzed by the heme groups in P450s. Electrons in CYP-catalyzed chemical metabolism come from cytochrome P450 reductases involves a subfamily of

flavoproteins designed to provide electrons to CYPs. Electrochemical study has the advantage that proteins can get electrons directly from the electrode, hence the electron provider CPR and the cofactor NADPH are not required.

Although there are large varieties of CYPs, the active site of the enzyme is highly conservative. The iron in the heme group is tethered through a thiol ligand from a cysteine residue, this cysteine and some other amino acid residues around it are also highly conserved. We chose a simple hemoprotein (myoglobin) to start our study on the interaction between nitroalkane with heme group. Myoglobin is easily available and had been electrochemically studied extensively.[6-15] Previously published work in this lab has shown that myoglobin is an efficient catalyst in electroreduction of nitromethane.[16]

Myoglobin is a primary oxygen-carrying protein in muscle tissues, Figure 2.1. The crystal structure of myoglobin[17] showed that the N^{ϵ} atom of the proximal histidine residue (His93 in horse heart myoglobin) acts as the fifth coordination of the iron atom of the porphyrin ring, and leave only the distal (or trans-axial) side of the porphyrin plane accessible to ligands such as oxygen. There is another histidine residue (His64 in horse heart myoglobin) at the distal side which helps stabilize the binding of the ligand through hydrogen bonding.

Some electrochemical studies of surface confined myoglobin focused on the electrochemical characteristics of myoglobin,[8, 15] and others also focused on the myoglobin catalyzed electroreductions.[6, 11, 18, 19] In this work, we study the myoglobin-mediated nitromethane reduction.

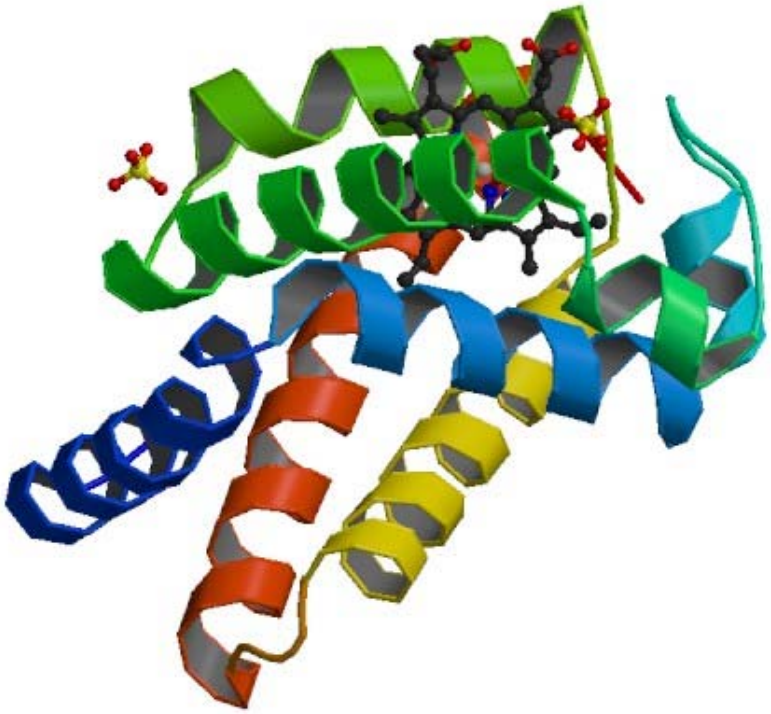

Figure 2.1 Structure of nitromethane modified horse heart myoglobin

Image from: PDB 2NSR

Traditionally potentiometric titration [20-23] was the main approach to investigate the thermodynamics and sometimes the mechanisms of electron transfer of in enzymatic processes. This method is not suitable for studying kinetics of reactions. Another drawback is that this approach requires relatively large quantity of enzyme samples. More recently, direct electrochemistry [24-26] of metalloproteins became more popular because of the speed and wealth of inforamtion that it provides. This approach is much more versatile and powerful; if not only gives access to thermodynamic data, but it also provides information on the kinetics of electron transfer.

Direct electrochemical study of metalloproteins requires direct electron transfer between protein and electrode surface. The surfactant thin film methodology [27, 28] was developed to study a variety of metalloproteins. The film-forming surfactant employed in our work and widely used in other investigations [16, 28-31] is didodecyl dimethyl ammonium bromide (DDAB).

2.2 Experimental Design

2.2.1 Materials

Horse heart myoglobin is purchased from Sigma. Myoglobin is purified as in reference[32] before use. Didodecyldimethyl-ammonium bromide (DDAB) and nitromethane are from Acros Organics.

Nitrogen gas is purchased from PRAXAIR. Deionized water is obtained from a Barnstead Nanopure system with a resistivity greater than 18 MΩ· cm. Pyrolytic graphite (Advanced Ceramics) is the material for working electrodes. Homemade working electrodes are prepared as in reference,[16] and the fabrication process is described below.

2.2.2 Fabrication of the pyrolytic graphite (PG) working electrode

A pyrolytic graphite block is cut perpendicularly to the basal plane using a diamond core drill bit to make a cylinder of the graphite with diameter of ~3.2mm. The cylinder lock is then cut into small cylinders with a scalpel blade along the basal plane to make each cylinder about 3 mm tall. A piece of copper wire (precut 15 cm) is connected to one end of the graphite cylinder using conductive epoxy, and allowed to dry. The graphite cylinder is then inserted in a glass tubing (ID=4mm) and set in place with non-conductive epoxy and allowed to dry, figure in appendix B. The non-conductive epoxy is also used to seal the gaps between graphite and glass. The finished electrode is then polished and cleaned.

2.2.3 Electrode modification

Myoglobin (Mb) is immobilized in DDAB surfactant film on a basal-plane pyrolytic graphite (PG) disc electrode[28, 33] (surface area is ~0.08 cm^2), (Mb/DDAB/PG). Before film casting, the PG electrode is polished using 400-grit sandpaper followed by 0.3μm alumina slurry. The polished electrode is then rinsed and sonicated in distilled water. Mb/DDAB surfactant film is prepared by casting 10μl of 10mM DDAB in H_2O followed by 10μl 0.4mM myoglobin solution. The modified PG electrode is then allowed to dry in air for more than 12 hours. DDAB emulsion is prepared by dissolving DDAB powder in deionized water. The emulsion is then sonicated for at least 2 hours or until the solution becomes clear. Myoglobin buffer solution is prepared by dissolving myoglobin in 0.1M acetate buffer (pH 5.5) or in other suitable buffers.

2.2.4 Procedures and Apparatus

2.2.4.1 Electrochemical Measurement

Cyclic voltammetry (CV) is an excellent tool to study the heme iron redox activity through electron transfer. Another electrochemical technique that we use is rotating disk voltammetry (RDV). This hydrodynamic electrochemical method can provide steady state current needed to measure true values of the catalytic current. Therefore, it is routinely used in electrochemical study of enzyme catalysis.[34-36]

All electrochemical experiments are conducted using a three-electrode system (Figure 2.2) on a BAS 100B electrochemical workstation or CH Instrument. Ag/AgCl (3M KCl) is used as reference electrode and all potentials are reported versus this reference. A platinum wire is employed as the auxiliary electrode. Modified PG electrodes are used as working electrodes of course.

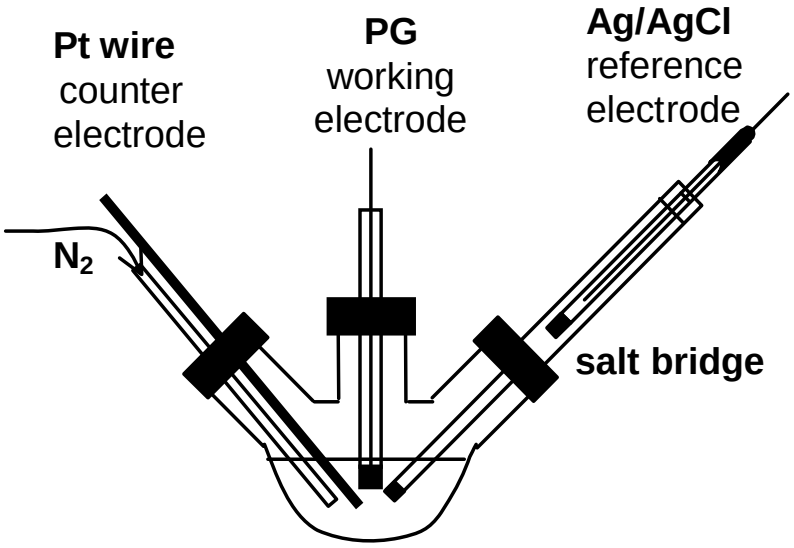

Figure 2.2 Electrochemical setup

All electrochemical experiments are performed in 0.1M acetate buffer (pH 5.5) containing 0.1M sodium bromide. The solution in the cell is purged with purified nitrogen for at least 15 min prior to experiments to remove oxygen from the solution. A nitrogen blanket is maintained to prevent contamination with oxygen from air.

2.2.4.2 Bulk Electrolysis

Bulk electrolysis is performed using a modified large area PG electrode as working electrodes. The electrode is poised at the potential where the electro catalysis occurs. Constant stirring is maintained to ensure mass transfer during electrolysis. The amount of substrate converted during the process is calculated using initial and final concentrations.

2.2.4.3 Mass Spectrometry

A sample of the solution after bulk electrolysis is infused into a Micromass Quattro II electro-spray triple quadrupole mass spectrometer (ESI-MS) to identify and quantify the products of the catalytic nitromethane electroreduction. The calibrations of the possible products are conducted using triethylamine as an internal standard.

2.3 Results and Discussion

2.3.1 Electrochemistry of Mb/DDAB/PG

A cyclic voltammogram of Mb/DDAB/PG in pH5.5 acetate buffer, Figure 2.3, shows a pair of well-defined reversible redox couples; the first couple, R1/O1 (Equation 2), is assigned to Fe^{III}/Fe^{II} with a formal potential –0.180V vs. Ag/AgCl. The R2/O2 couple, (Equation 3) with formal potential –1.052V vs. Ag/AgCl is tentatively assigned to Fe^{II}/Fe^{I}.[16, 29, 32]

$$Mb-Fe^{III}- + 1e^{-1} \underset{O1}{\overset{R1}{\rightleftharpoons}} Mb-Fe^{II}- \quad (2)$$

$$Mb-Fe^{II}- + 1e^{-1} \underset{O2}{\overset{R2}{\rightleftharpoons}} Mb-Fe^{I}- \quad (3)$$

As has been shown in a number of reports the heterogeneous electron transfer is greatly enhanced in the surfactant film. In fact, as shown in Figure 2.4, when peak splitting ΔEp for the Fe^{III}/Fe^{II} is plotted as a function of scan rate, the ΔEp stays unchanged in the range of scan rates from 0.001V/s to 1V/s, and then increases as expected at higher scan rates (i.e. shorter time frame) where electron transfer is kinetically challenged. Simulation of this behavior provides an estimate of the electron transfer rate. We find a k_s of 0.01 cm/s indicating a fast electron transfer for this large protein.

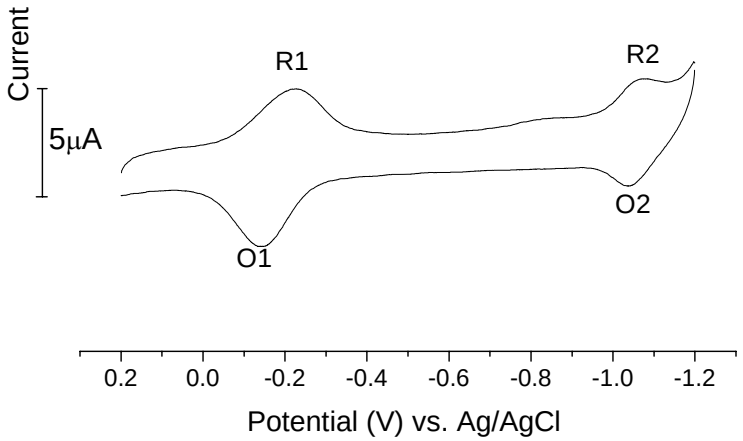

Figure 2.3 Cyclic voltammogram of Mb/DDAB/PG in pH5.5 acetate buffer at 0.15 V/s.

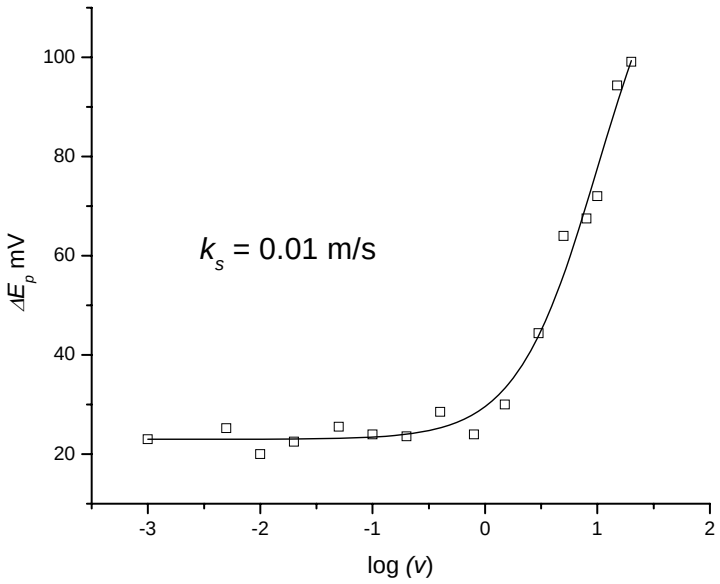

Figure 2.4 Plot of ΔE_p as a function of scan rate using Mb/DDAB/PG electrode in pH 5.5 buffer

2.3.2 Electrocatalytic reduction of nitromethane

The cyclic voltammogram as described earlier dramatically changes after introducing nitromethane. Figure 2.5a shows the typical voltammogram of Mb/DDAB/PG electrode in pH5.5 buffer in absence of nitromethane. There are 2 pairs of redox couples assigned to Fe^{III}/Fe^{II} (formal potential at -0.18V vs. Ag/AgCl) and Fe^{II}/Fe^{I} (formal potential at -1.06V vs. Ag/AgCl), respectively. Upon addition of nitromethane, a new peak, R_c, appears at -1.0V vs. Ag/AgCl in parallel with the disappearance of the Fe^{II}/Fe^{I} (Figure 2.5b). A control experiment (Figure 2.5c) is conducted with a DDAB/PG electrode without embedded Mb as working electrode under the same conditions. The R_c peak current is significantly higher than that of the control experiment and the R_c peak potential is more positive compared to the control voltammogram (-1.16V in Figure 2.5c). The new Rc peak appearing at potentials more positive than Fe^{II}/Fe^{I} redox couple and the disappearance of the later are both indicative of an electro catalytic process mediated by myoglobin.

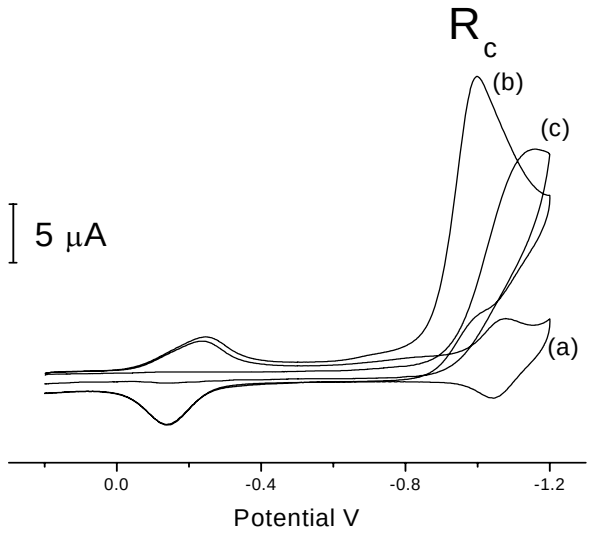

Figure 2.5 Cyclic voltammograms of DDAB/PG and Mb/DDAB/PG electrode in pH 5.5 acetate buffer solution at the scan rate 0.15V/s. (a) Mb/DDAB/PG without nitromethane, (b) Mb/DDAB/PG with 0.4 mM nitromethane, (c) DDAB/PG with 0.4 mM nitromethane.

Literatures showed that myoglobin maintains its native structure in a certain pH range when immobilized in the surfactant films such as DDAB.[15, 32, 37] However, other investigations claimed different results. Some reports state that heme is released from myoglobin in DDAB surfactant film,[38, 39] and the electrochemical signals of myoglobin arise actually from the free heme.

In our hands and under our conditions, myoglobin maintains a native-like structure and the redox activity observed comes from its intact form. In fact, cyclic voltammetry performed with chemically denatured (SDS treated) myoglobin on the electrode surface gives a different behavior. The voltammogram (Figure 2.6a) shows that the previously well defined 2 redox couples (Figure 2.5a) has drastically changed. Also in support of our results, the catalytic function of the denatured protein is lost in the presence of nitromethane substrate. The reductive wave at –1.1V (Figure 2.6b) is the direct electroreduction of nitromethane. Our results are in support of the fact that myoglobin retains its native-like structure in our surfactant films.

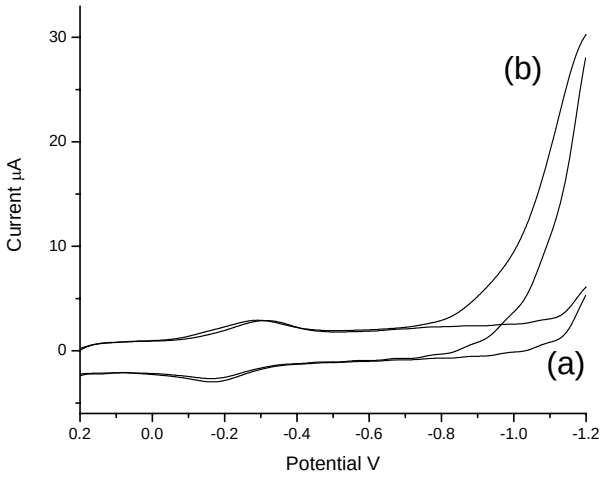

Figure 2.6 Cyclic voltammograms of SDS denatured* myoglobin electrode in pH5.5 buffer. (a) 0 mM nitromethane (b) 0.4 mM nitromethane.

*Myoglobin solution was treated with 1% SDS solution prior to electrode modification. 10μl of the SDS treated myoglobin suspension after vortexing was used along with 10μl DDAB solution to modify a PG electrode (procedure refer to section 2.2.3).

2.3.3 Effect of nitromethane concentration

The catalytic reduction current obtained from cyclic voltammetry can provide quantitative information of on turnover and other kinetic aspects in the thin film. Figure 2.7A shows myoglobin-mediated nitromethane reduction catalytic currents at different substrate concentrations. Catalytic current I_{cat} as a function of substrate concentration [S] is shown in Figure 2.7B. The plot exhibits linear relationship between I_{cat} and [S] when [S] is smaller than 0.6 mM. The plot starts to curve down greater concentrations, which is typical for enzyme saturation kinetics. The plot can be fit to Michaelis-Menten kinetics, Equation 4.

$$V = \frac{V_{\max} \times [S]}{K_m + [S]} \text{ (Michaelis-Menten Equation)} \quad (4)$$

Equation 5 shows the scheme of enzyme-catalyzed substrate transformation. E symbolizes the enzyme, S the substrate, ES is enzyme-substrate complex, and P is product.

$$E + S \underset{k_{-1}}{\overset{k_1}{\rightleftharpoons}} ES \xrightarrow{k_2} E + P \quad (5)$$

$$Km = \frac{k_{-1} + k_2}{k_1} \quad (6)$$

K_m, as defined in Equation 6, is an indication of the constant of the formation of enzyme-substrate complex. It also reflects the catalytic constant k_2 or k_{cat}, the turnover number.

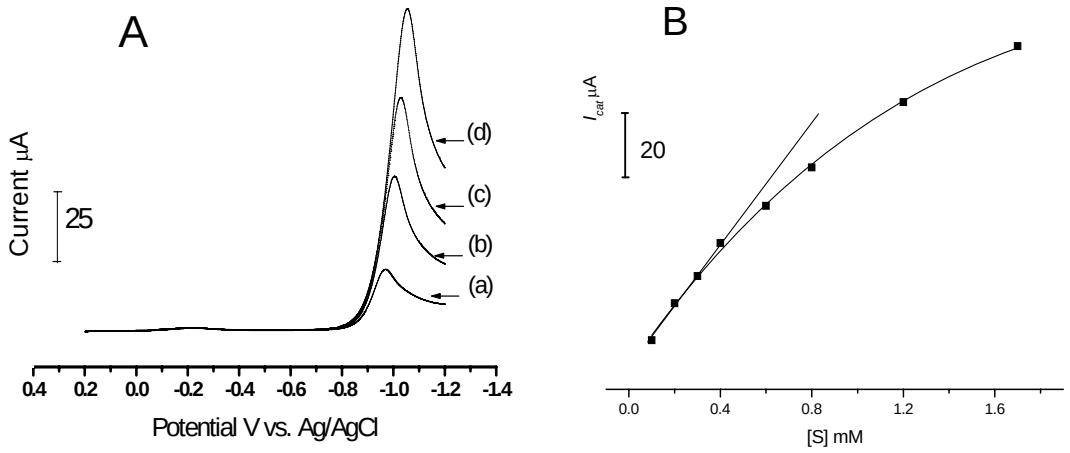

Figure 2.7A Voltammograms of Mb/DDAB/PG electrode in pH 5.5 acetate buffer solution at a scan rate of 0.15V/s in the presence of (a) 0.3 mM, (b) 0.8 mM, (c) 1.3 mM, (d) 2.0 mM nitromethane.

Figure 2.7B Catalytic current of nitromethane catalytic reduction by Mb/DDAB/PG as a function of nitromethane concentration.

To quantify K_m and k_{cat} electrochemically, we need to use the electrochemical form of Michaelis-Menten equation can be expressed by Equation 7 [40] under steady-state conditions:

$$I_{cat} = \frac{nFA\Gamma k_{cat} \times [S]}{K_m + [S]} \quad (7)$$

where Γ is the surface concentration of catalyst, F is Faraday's constant, A is the surface area of the electrode, [S] is substrate concentration, K_m and k_{cat} are the usual Michaelis-Menten parameters.

To calculate the total amount of active catalyst on the electrode surface we typically use an electrochemical technique based on current integration (i.e. charge measurement) of voltammograms taken at very slow scans.[15] The integration of the reductive peak of Fe^{III}-heme/ Fe^{II}-heme from a linear potential scan at 5mV/s gives the amount of active heme proteins in the surfactant films, Figure 2.8. The average value for Mb/DDAB is around 21.2 picomoles; accordingly the surface concentration is 2.65×10^{-10} mole/cm^2, which is in the same range of the value reported in the literature.[15]

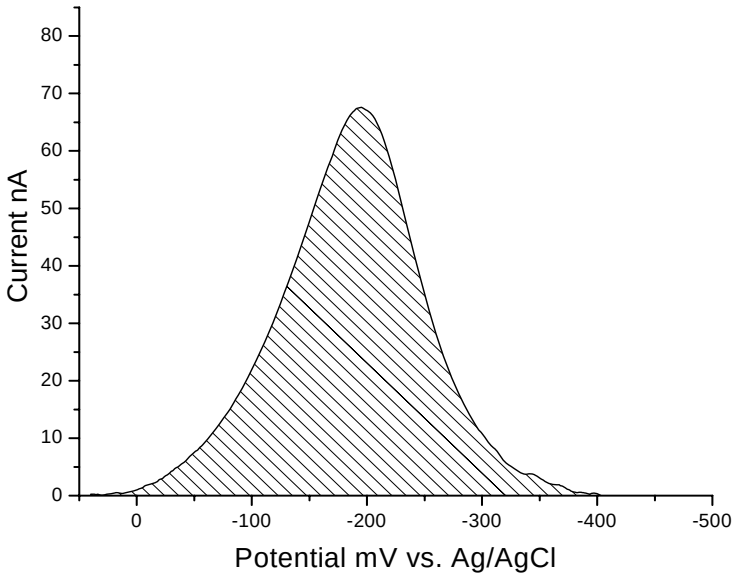

Figure 2.8 Typical linear voltammogram of Mb/DDAB/PG electrode in pH5.5 acetate buffer at scan rate 5mV/s; Integrated area under the voltammogram is shown as filled.

Figure 2.9 shows the plots of normalized catalytic current, $I_{cat} / nFA\Gamma$, versus substrate concentration [S] plot of Mb/DDAB-catalyzed reaction. Non-linear fitting the plots (Figure 2.9) using Equation 7 gives the regression parameters k_{cat} and K_m. The parameters are shown in Table 2.1.

Table 2.1 Regression parameters from Figure 2.9

	K_m (mM)	k_{cat} (s^{-1})	k_{cat} / K_m ($s^{-1} \cdot mM^{-1}$)
Myoglobin	1.9 ± 0.2	20.9 ± 1.8	11.2 ± 2.1

The parameter V_{max} / K_m (or k_{cat} / K_m) is the rate of catalysis at the substrate concentration [s] close to 0, equation 7, and is usually used to define the catalytic ability or efficiency of an enzyme.

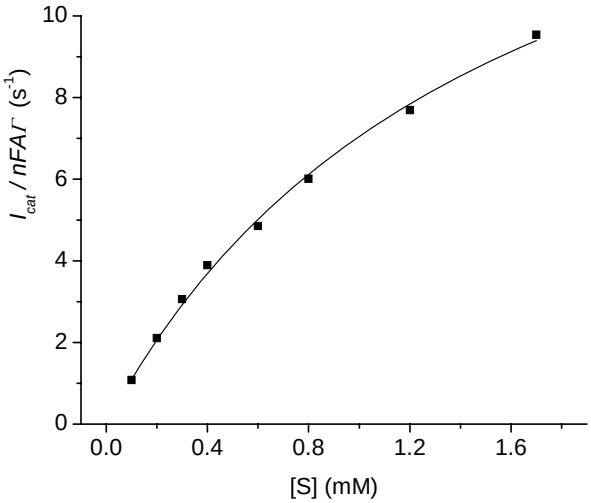

Figure 2.9 Catalytic current of Mb/DDAB/PG normalized by catalyst surface concentration as a function of nitromethane concentration.

2.3.4 Effect of scan rate

One can study the electron transfer and mass transfer kinetics using diffusion-controlled technique such as cyclic voltammetry. Increasing scan rate shortens the timescale within which the catalytic reaction is monitored. As expected the catalytic efficiency, defined by the ratio I_{cat}/I_0 [29] is larger at small scan rate and gradually drops as the scan rate increase, Figure 2.10. This behavior is typical of electrocatalytic process and can be used to extract kinetic information.

The peak potential of the catalytic wave is plotted as a function of scan rate, Figure 2.11. The figure shows that the catalytic peak shifts negatively with increasing scan rate. Since the catalysis is triggered within the time scale defined by the scan rate, this shift is an indication that more energy is required for the catalysis to occur in a higher scan rate. A chemical and/or an electrochemical step(s) in the catalytic reaction could be rate determine during the catalysis.

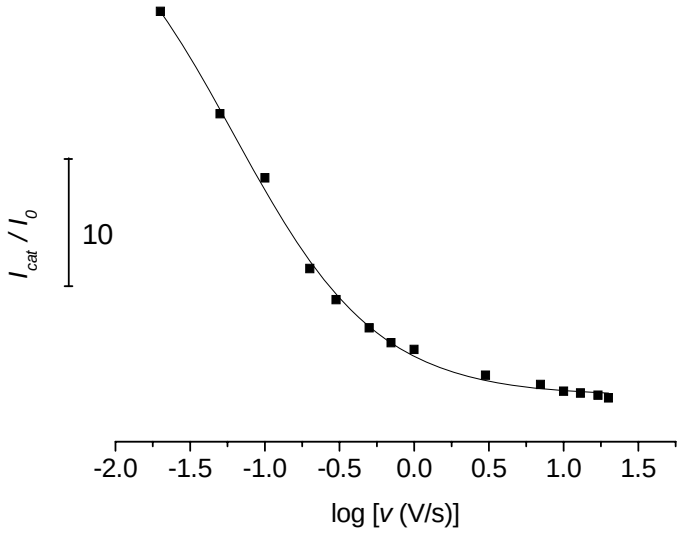

Figure 2.10 Catalytic efficiency as a function of scan rate.

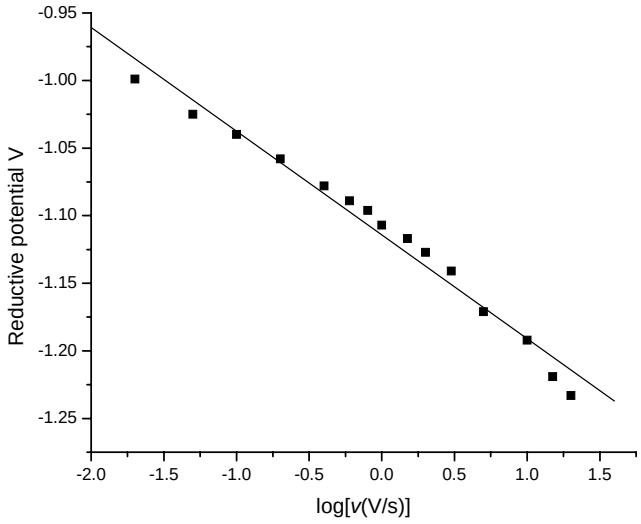

Figure 2.11 Catalytic peak potential as a function of scan rate

2.3.5 Effect of pH

The electroreduction of nitromethane involves protons uptake.[5] The catalytic reduction is also a proton-coupled process, which we will discuss later in the mechanistic study. Therefore, the availability of protons will affect the catalytic process. We conduct cyclic voltammetry under a series of pH values to monitor the effect of proton availability on the myoglobin-mediated reduction of nitromethane.

Figure 2.12A shows that the catalytic current drops with increasing pH. Figure 2.12B shows that the catalytic current changes slowly from pH 5.5 to pH 9, and then sharply from pH 9 to pH 11. Studies have shown that nitromethane is polar and exists in different forms under different pHs.[41] The aci-nitro tautomerism of nitroalkane shows the equilibria of nitronic acid, $R_1R_2C{=}NO_2H$ (aci form), nitroalkane, and the nitronate anion $R_1R_2C{=}NO_2^-$ in neutral or basic medium, Equation 8.[41]

$$R_1R_2C{=}NO_2H \underset{k_{-2}}{\overset{k_2}{\rightleftharpoons}} R_1R_2C{=}NO_2^- + H^+ \underset{k_1}{\overset{k_{-1}}{\rightleftharpoons}} R_1R_2CH\text{-}NO_2 \qquad (8)$$

Nitromethane stays in nitro-from under acidic pH and transforms to aci-form in basic media. The dissociation constant of the *aci* form of nitromethane to the nitronate anion.[42] It is known that the formation of the anion of the *aci* form of nitromethane in alkaline solution prevents the reduction.[42] This can partially explain the sharp decrease of catalysis when pH is greater than 9, Figure 2.12B.

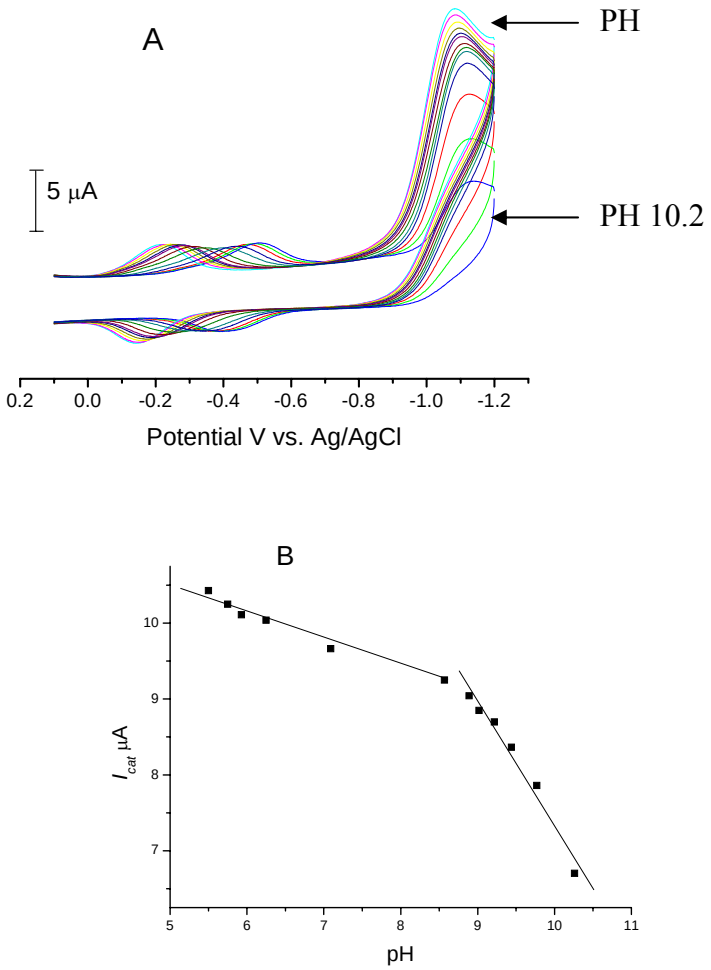

Figure 2.12A Cyclic Voltammograms of Mb/DDAB electrode in the presence of 0.1mM of nitromethane in different pH solution.

Figure 2.12B Catalytic current, I_{cat}, as a function of pH.

It is known that water is the heme ligand in acidic environments and hydroxide becomes the ligand under basic conditions.[27] Thus the fast drop of catalysis is not only caused by the availability of proton, but also the competitively binding of nitromethane with hydroxide ion to the heme iron.[27] At pH 11, the catalytic current is not observed, indicating that the proton concentration cannot support the catalysis.

The catalytic peak potential is affected by the pH, Figure 2.13. The shift of reduction potential with pH may reflect the change of ligand binding properties to the heme as well as the change of proton availability that drives the catalysis. There is also a clear turning point at pH 9.5 in Figure 2.13, which shows a change of the slope of pH dependency. The sharp decrease of catalytic peak potentials can be partially due to the intrinsic dissociation of nitronic acid to nitronate anion, which is difficult to reduce.

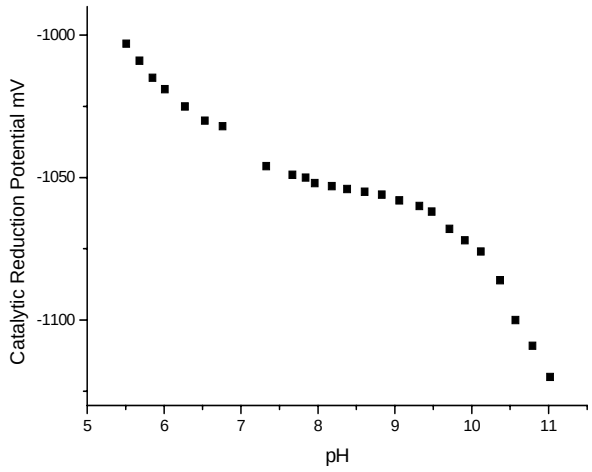

Figure 2.13 Potential of the catalytic reduction of 0.1 mM nitromethane on Mb/DDAB/PG electrode as a function of pH.

2.3.6 Number electrons per nitromethane molecule in myoglobin-mediated catalysis

We used the bulk electrolysis method to measure how many electrons pass through Mb/DDAB/PG and how much nitromethane is consumed. Bulk electrolysis is performed at the level of the catalytic peak at -1.0 V vs. Ag/AgCl under constant stirring. A large surface PG electrode modified with Mb/DDAB is used as a working electrode. The starting concentration of nitromethane is 1.96 mM in 5 mL of solution, and the concentration of nitromethane after the process is measured by an electrochemical calibration method. The consumption of nitromethane is then derived, and the total number of nitromethane molecules consumed can be calculated. The total charge passed during the electrolysis is recorded by the electrochemical station. The electrons per nitromethane molecule can therefore be acquired.

The stoichiometric study derived that the ratio of total charges to the reduced molecules is close to 4:1, implying 4 electrons per nitromethane molecule consumed, and implies that nitromethane electroreduction yields mainly methyl hydroxylamine. Table 2.2 shows the results of the number of electrons per molecule after bulk electrolysis for various trials.

Table 2.2 Calculation of number of electron per nitromethane molecule

	Total electrons passed	Total nitromethane molecules reduced	Electrons per molecule	Average (mean ± SD)
Trial 1	7.20×10^{18}	1.54×10^{18}	4.68	
Trial 2	7.33×10^{18}	1.65×10^{18}	4.44	4.45 ± 0.23
Trial 3	7.62×10^{18}	1.80×10^{18}	4.23	

2.3.7 The products of catalytic reduction of nitromethane

In order to identify the products of the catalytic reduction, which is critical for the understanding of the reaction mechanism, we used a mass spectrometric method. The mass spectrometric technique we used to analyze the products of electrolysis of nitromethane electroreduction is semi-quantitative. Calibration curves (Figure 2.14) of the possible products are prepared using authentic compounds with triethylamine as the internal standard. The mass spectrometry analysis of the solution after bulk electrolysis shows that methyl hydroxylamine is the dominant product; the other possible reductive product methylamine was not detectable by the MS technique used (the detection limit is below 1 μM for this compound, Figure 2.14b).

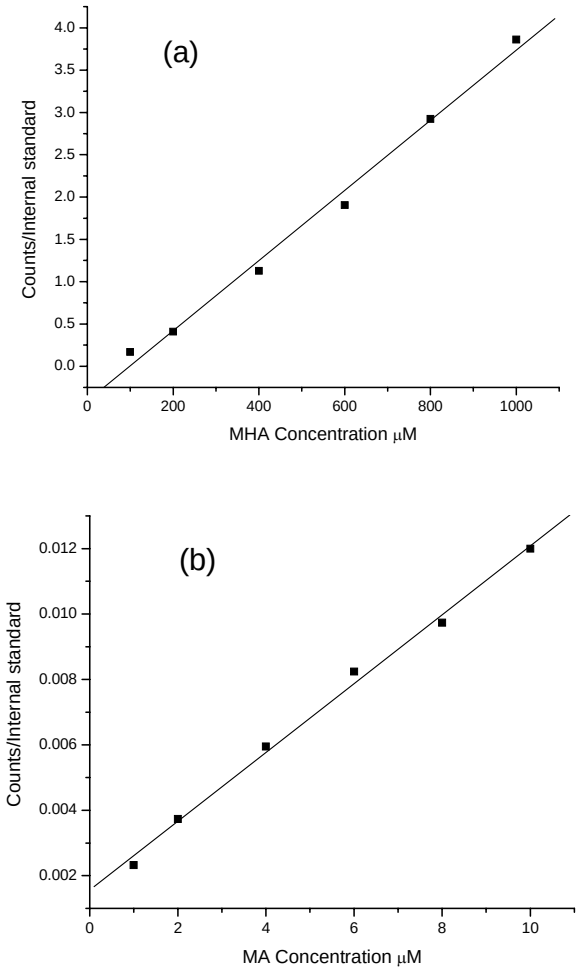

Figure 2.14 Calibration curve of methyl hydroxylamine (a) and methylamine (b) using QQQ-ESI mass spectrometer

2.3.8 Characterization of the intermediate of the catalytic reaction

2.3.8.1 UV-vis spectroscopy

We resorted to UV-vis spectroscopy to investigate the reaction between nitromethane and heme group and characterize possible intermediates complexes during the catalytic reduction of nitromethane. Mb-Fe^{III} (Soret at 409nm, data not shown) is reduced to Mb-Fe^{II} (Soret at 434nm, Figure 2.15) by adding excess amount of sodium hydrosulfite. The addition of nitromethane causes an absorption decrease at 434nm with concurrent absorption increase at 424nm giving an isosbestic point at around 430nm. The species with 424nm absorption is identical to that of ferrous myoglobin-nitrosomethane complex characterized in solution.[43-45]

The heme(Fe^{II})-nitrosomethane complex was studied by Mansuy's group in their investigation of the reaction of aliphatic nitro compounds with myoglobin and hemoglobin under reducing conditions.[46] Other reports[43, 47] also stated that ferrous hemoproteins bind to nitrosoalkanes to form stable complexes that were characterized by UV-vis spectroscopy.

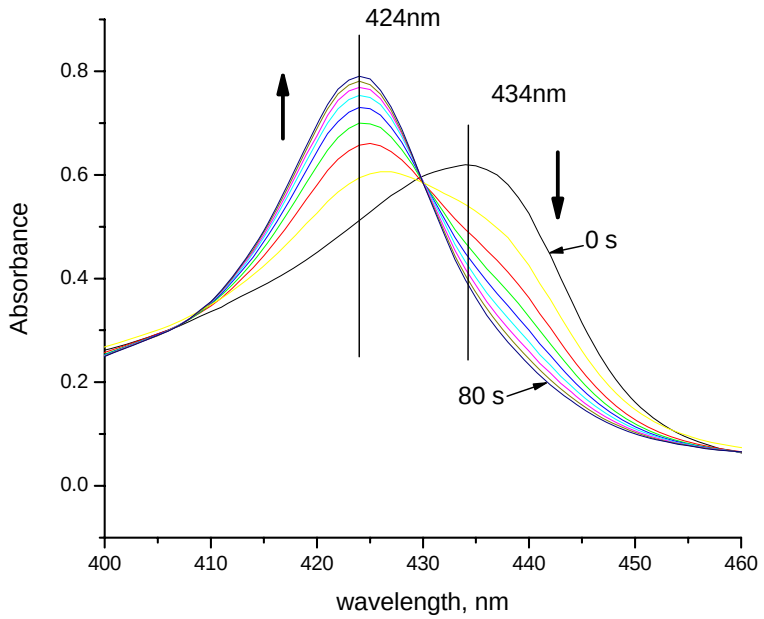

Figure 2.15 Evolution of the absorption spectra of reduced 10μM of Mb solution after addition of 25 mM nitromethane. Spectra were taken every 10s.

Nitromethane itself bind neither to Heme(Fe^{III}) and nor to Heme(Fe^{II}).[45] Consistent with these results, UV-vis experiments show no reaction between nitromethane and Heme(Fe^{III}) (Figure 2.16A) or Heme(Fe^{II}) (Figure 2.16B).

To examine if the myoglobin ferrous nitrosomethane complex forms during our heme-mediated electroreduction process, we poised a DDAB/PG electrode at –0.8 V in pH5.5 acetate buffer in the presence of nitromethane and Mb(Fe^{II}). The direct electroreduction of nitromethane at PG electrode will transform nitromethane to potentially nitrosomethane under these conditions; the latter should bind to Mb(Fe^{II}) to form the complex if any. UV-vis spectrum is taken before the catalysis and every 2 minutes during the electrolysis. A complex with UV-vis features similar to those assigned by Mb-nitrosomethane forms during our reduction process triggered electrochemically. The results confirm that the myoglobin ferrous nitrosomethane complex is formed after the electrolysis, Figure 2.17.

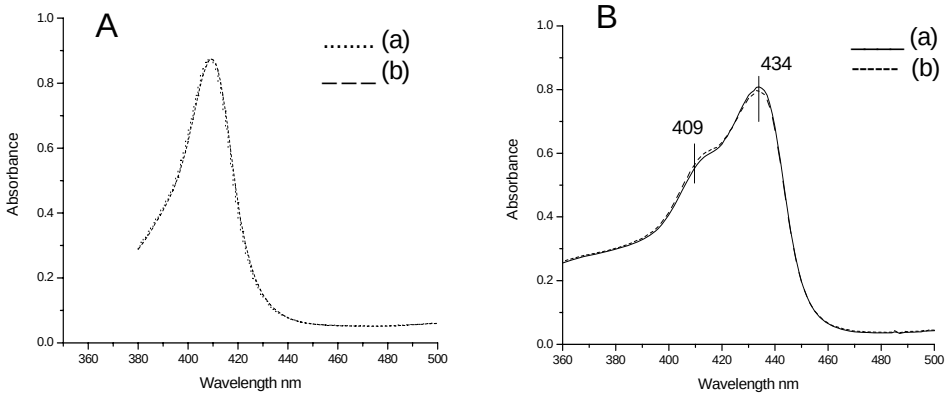

Figure 2.16A UV-vis spectra of myoglobin in pH 5.5 buffer. (a) 0 mM of nitromethane, (b) 2 mM of nitromethane.

Figure 2.16B UV-vis spectra of reduced myoglobin in pH 5.5 buffer. (a) 0 mM of nitromethane, (b) 2 mM of nitromethane.

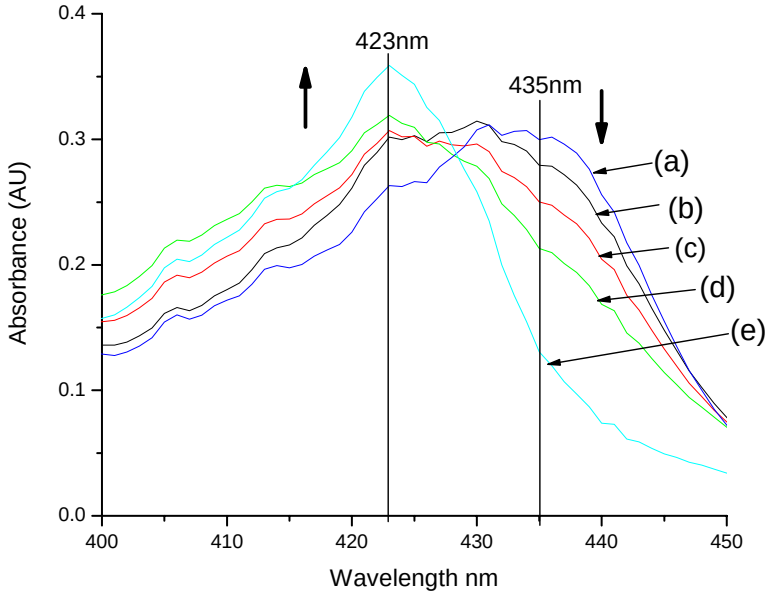

Figure 2.17 UV-vis spectra of Mb(Fe^{II}) with nitromethane in pH 5.5 buffer solution. (a) Mb(Fe^{II}) + nitromethane before electrolysis, (b) after 2 minutes of electrolysis, (c) after 4 minutes of electrolysis, (d) after 6 minutes of electrolysis, and (e) after 15 minutes of electrolysis.

2.3.8.2 Electrochemical signature of the heme ferrous nitrosomethane complex

Since the ferrous nitrosomethane complex of myoglobin forms under our experimental conditions, we asked whether we could characterize it electrochemically. Under anaerobic condition, we preformed the nitrosomethane-heme(Fe^{II}) by reacting myoglobin solution with nitromethane in the presence of excess amount of dithionite. The reaction product was then used to modify our PG electrode under N_2. The modification procedure refers to section 2.2.3. We performed cyclic voltammetry in pH 6 buffer in the range of –0.8 to –1.1 V at a scan rate of 0.8 V/s. The myoglobin and nitrosomethane is expected to separate if Mb-nitrosomethane complex is oxidized.[16] Hence, all our experiments are performed under N_2, and potential scan starts at –0.8 V to avoid the chemical or electrochemical oxidation of the Mb-nitrosomethane complex. Fast scan prevents the electroreduction from completion, which will cause dissociation of the complex and irreversibility. We were able to observe a reversible redox couple at the potential of –0.924 V (Figure 2.18) for this complex inside a narrow electrochemical window. The possible reaction of this reversible electrochemical reaction is showed in Equation 9.

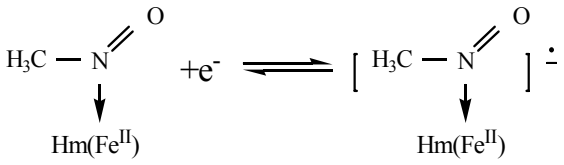

(9)

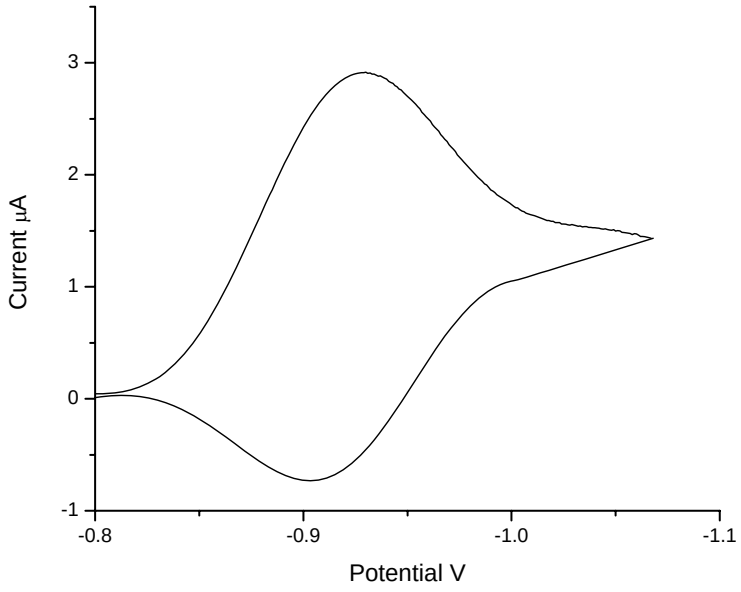

Figure 2.18 Baseline-subtracted cyclic voltammogram of Mb(Fe^{II})-nitrosomethane/DDAB/PG electrode in pH6 buffer solution at a scan rate of 0.8 V/s.

2.3.9 Mechanistic insights on the heme-mediated catalytic electroreduction of nitromethane

According to the fact that neither ferric myoglobin nor ferrous myoglobin can bind nitromethane, and the myoglobin as the catalyst in the process needs to interact with substrate, the nitromethane substrate should change its state before the catalysis can happen. It is known that the first step of direct electroreduction of nitromethane forms nitrosomethane, which is the substrate for $Mb(Fe^{II})$ to form the myoglobin-nitrosomethane complex as we discussed before. Another evidence is that the myoglobin-mediated electroreduction peak starts at -0.75 V as shown in Figure 2.5, and the direct reduction peak of nitromethane on a DDAB only electrode starts also at -0.75 V vs. Ag/AgCl, Figure 2.19. It is an indication that the catalytic process is also triggered by the direct electroreduction of nitromethane. The following step will be the formation of $Mb(Fe^{II})$-nitrosomethane intermediate. The electroreduction of the intermediate will be the next step. Based on the voltammetric behavior observed, the proposed catalytic reduction pathway is as follow:

(a) heme reduction:

$$Heme(Fe^{III}) + e^- \rightarrow Heme(Fe^{II}) \qquad (10)$$

(b) Heme-mediated nitromethane electroreduction:

$$CH_3NO_2 + 2\ e^- + 2\ H^+ \underset{k_{-1}}{\overset{k_1}{\rightleftharpoons}} CH_3N{=}O + H_2O \qquad (11)$$

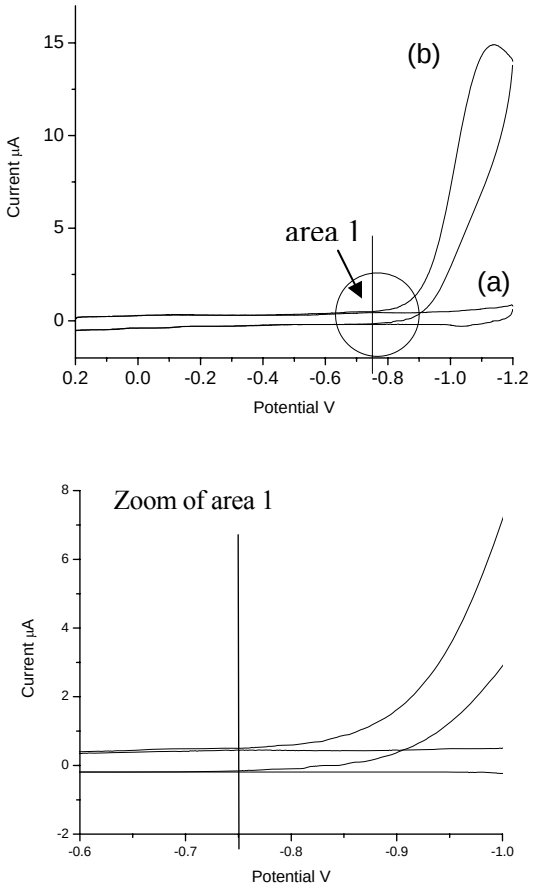

Figure 2.19 Cyclic voltammograms of DDAB/PG electrode in pH 5.5 acetate buffer solution at the scan rate 0.15V/s. (a) 0 mM nitromethane (b) 0.2 mM of nitromethane

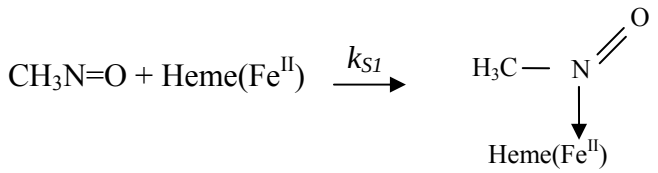

(12)

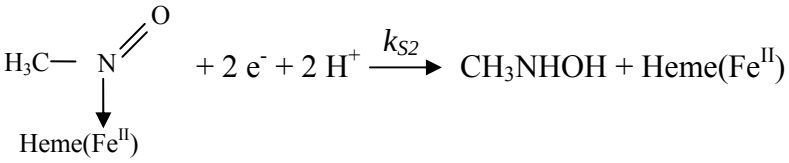

(13)

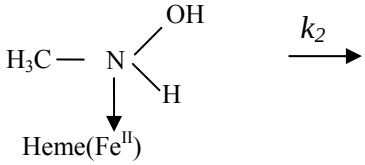

(14)

In step (a), Heme-Fe(III) gains electrons and reduces to Heme-Fe(II), Equation 10. Step (b) shows the catalytic reduction of nitromethane using Heme-Fe(II) as a catalyst. During the negative potential scan of the cyclic voltammetry, nitromethane gains 2 electrons from the electrode coupled with 2 protons and forms an unstable nitrosomethane $CH_3N=O$, Equation 11.

Nitrosomethane binds to typical hemoproteins irreversibly.[43] The lone pair electrons on the nitrogen of the nitrosomethane readily coordinate the ferrous heme to from a stable ferrous-nitrosomethane complex, Equation 12. It is this intermediate that was characterized spectroscopically and electrochemically in this work. A further 2-electron process coupled to two protons reduces this intermediate to regenerates the catalyst along with the reduced product, Equation 13. A dissociation step gives out the final product, methyl hydroxylamine, with the release of the catalyst at the Fe^{II} state, Equation 14.

2.3.10 Heterogeneous and homogeneous reaction rates

The proposed heme-mediated nitromethane electroreduction pathway involves chemical and electrochemical reactions; the determination of the kinetic parameters of the processes can be obtained by simulation of cyclic voltammograms using Digisim software package (BAS).

One of the chemical reactions in the catalytic process is described in Equation 11 with the forward rate constant k_1, and the backward rate constant k_{-1}, and the other is described in Equation 14 with rate constant k_2. The electrochemical reactions include direct electroreduction of nitromethane, displayed in Equation 11, with the heterogeneous electron transfer rate constant k_{S1} and the catalytic electrochemical process given in Equation 13 with an electron transfer rate constant k_{S2}. The simulated parameters are shown in table 2.3 using our proposed mechanism.

By definition, k_2 is equal to k_{cat} and K_m is equal to $(k_{-1} + k_2) / k_1$. The parameters of simulation k_1, k_{-1}, and k_2 shown in Table 2.3 are in agreement with the Michaelis-Menten parameters k_{cat} and K_m listed in Table 2.1. The simulated voltammograms fit the experimental data properly and are shown in Figure 2.20. Digisim simulations validate the k_{cat} and K_m values derived from catalytic current data and further confirm our proposed mechanism of the heme-mediated catalysis.

Table 2.3 Digisim® simulation parameters of myoglobin-catalyzed nitromethane electroreduction

	k_1 ($s^{-1} \cdot M^{-1}$)	k_{-1} (s^{-1})	k_2 (s^{-1})	k_{S1} (cm/s)	k_{S2} (cm/s)
Myoglobin	1×10^4	0.1	20	3.8×10^{-7}	0.01

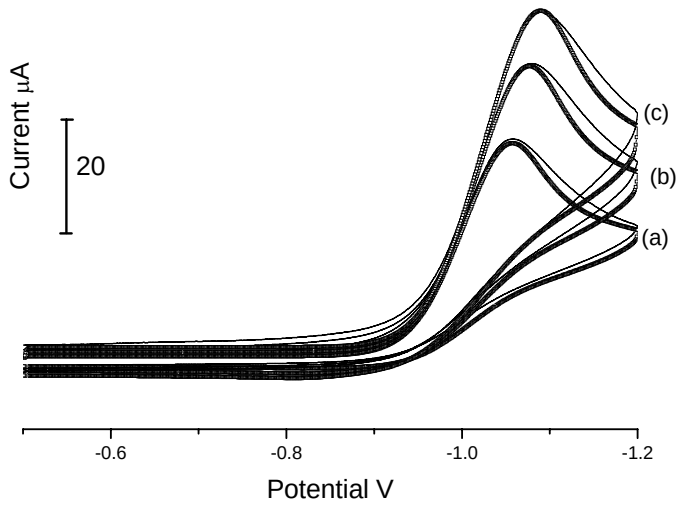

Figure 2.20 Digisim® simulation of cyclic voltammograms. (□) simulated voltammograms, (—) experimental voltammograms using the proposed mechanism.

Cyclic voltammogram of Mb/DDAB/PG is obtained in the presence of 0.4 mM nitromethane in pH5.5 buffer solution at (a) 200 mV/s, (b) 400 mV/s, and (c) 600 mV/s.

2.4 Conclusion

Myoglobin can be used to study the catalytic activation of xenobiotic carcinogens such as nitromethane. The DDAB surfactant thin film method is suitable for metalloprotein immobilization. Myoglobin and cytochrome P450s share some common characteristics that come from the iron center of the porphyrin. Our mechanistic investigation showed the existence of a ferrous nitroso complex as the intermediate during Mb-mediated catalytic reduction of nitromethane. The product of Mb-mediated electroreduction of nitromethane is methyl hydroxylamine, and the catalysis is a 4-electron process. The catalytic reduction process is examined under the experimental conditions such as scan rate, substrate concentration and pH. The kinetic information of the catalysis was extracted from our electrochemical experimental data. The Digisim software can be used to obtain the heterogeneous and homogeneous reaction rate constants using the cyclic voltammograms from our experiments.

2.5 References

1. Toxicology and carcinogenesis studies of nitromethane (CAS No. 75-52-5) in F344/N rats and B6C3F1 mice. (Inhalation studies). *National Toxicology Program Technical Report Series* **1997**, (461), 284.

2. Lewis, T. R.; Ulrich, C. E.; Busey, W. M., Subchronic inhalation toxicity of nitromethane and 2-nitropropane. *J Environ Pathol Toxicol* **1979,** 2, (5), 233-49.

3. Mansuy, D., The great diversity of reactions catalyzed by cytochromes P450. *Comparative Biochemistry and Physiology -- Part C: Pharmacology, Toxicology & Endocrinology* **1998,** 121, (1-3), 5-14.

4. Jiang, Y.; Kuo, C. L.; Pernecky, S. J.; Piper, W. N., The detection of cytochrome P450 2E1 and its catalytic activity in rat testis. *Biochem Biophys Res Commun* **1998,** 246, (3), 578-83.

5. Perter B. Mills, W. J. A., Francisco Prieto, John A. Alden, Richard G. Compton, Heterogenerous ECE Processes at Channel Electrodes: Voltammetric Waveshape Theory. Application to the Reduction of Nitromethane at Platinum Electrodes. *J. Phys. Chem. B* **1998,** 102, (34), 6573-6578.

6. Dai, Z.; Xu, X.; Ju, H., Direct electrochemistry and electrocatalysis of myoglobin immobilized on a hexagonal mesoporous silica matrix. *Anal Biochem* **2004,** 332, (1), 23-31.

7. Guo, Z.; Chen, J.; Liu, H.; Cha, C., Direct electrochemistry of hemoglobin and myoglobin at didodecyldimethylammonium bromide-modified powder microelectrode and application for electrochemical detection of nitric oxide. *Anal Chim Acta* **2008,** 607, (1), 30-6.

8. Zhang, H. M.; Li, N. Q., The direct electrochemistry of myoglobin at a DL-homocysteine self-assembled gold electrode. *Bioelectrochemistry* **2001,** 53, (1), 97-101.

9. Dai, Z.; Xiao, Y.; Yu, X.; Mai, Z.; Zhao, X.; Zou, X., Direct electrochemistry of myoglobin based on ionic liquid-clay composite films. *Biosens Bioelectron* **2009,** 24, (6), 1629-34.

10. Liu, A.; Wei, M.; Honma, I.; Zhou, H., Direct electrochemistry of myoglobin in titanate nanotubes film. *Anal Chem* **2005,** 77, (24), 8068-74.

11. Wang, L.; Hu, N., Electrochemistry and Electrocatalysis with Myoglobin in Biomembrane-Like DHP-PDDA Polyelectrolyte-Surfactant Complex Films. *J Colloid Interface Sci* **2001,** 236, (1), 166-172.

12. Hu, Y.; Hu, N.; Zeng, Y., Electrochemistry and electrocatalysis with myoglobin in biomembrane-like surfactant-polymer 2C(12)N(+)PA(-) composite films. *Talanta* **2000,** 50, (6), 1183-95.

13. Liu, C. Y.; Hu, J. M., Hydrogen peroxide biosensor based on the direct electrochemistry of myoglobin immobilized on silver nanoparticles doped carbon nanotubes film. *Biosens Bioelectron* **2009,** 24, (7), 2149-54.

14. Shen, L.; Huang, R.; Hu, N., Myoglobin in polyacrylamide hydrogel films: direct electrochemistry and electrochemical catalysis. *Talanta* **2002,** 56, (6), 1131-9.

15. Nassar, A. E.; Rusling, J. F.; Kumosinski, T. F., Salt and pH effects on electrochemistry of myoglobin in thick films of a bilayer-forming surfactant. *Biophys Chem* **1997,** 67, (1-3), 107-16.

16. Boutros, J.; Bayachou, M., Myoglobin as an efficient electrocatalyst for nitromethane reduction. *Inorg Chem* **2004,** 43, (13), 3847-53.

17. Copeland, D. M.; West, A. H.; Richter-Addo, G. B., Crystal structures of ferrous horse heart myoglobin complexed with nitric oxide and nitrosoethane. *Proteins* **2003,** 53, (2), 182-92.

18. Kumar, S. A.; Chen, S. M., Direct electrochemistry and electrocatalysis of myoglobin on redox-active self-assembling monolayers derived from nitroaniline modified electrode. *Biosens Bioelectron* **2007,** 22, (12), 3042-50.

19. Zhang, L.; Tian, D. B.; Zhu, J. J., Direct electrochemistry and electrochemical catalysis of myoglobin-TiO2 coated multiwalled carbon nanotubes modified electrode. *Bioelectrochemistry* **2008,** 74, (1), 157-63.

20. Sligar, S. G.; Cinti, D. L.; Gibson, G. G.; Schenkman, J. B., Spin state control of the hepatic cytochrome P450 redox potential. *Biochem Biophys Res Commun* **1979,** 90, (3), 925-32.

21. Thomas, H.; Sagelsdorff, P.; Molitor, E.; Skripsky, T.; Waechter, F., Bromopropylate: induction of hepatic cytochromes P450 and absence of covalent binding to DNA in mouse liver. *Toxicol Appl Pharmacol* **1994,** 129, (1), 155-62.

22. Shen, A. L.; Kasper, C. B., Role of Ser457 of NADPH-cytochrome P450 oxidoreductase in catalysis and control of FAD oxidation-reduction potential. *Biochemistry* **1996,** 35, (29), 9451-9.

23. Pikuleva, I. A.; Bjorkhem, I.; Waterman, M. R., Studies of distant members of the P450 superfamily (P450scc and P450c27) by random chimeragenesis. *Arch Biochem Biophys* **1996,** 334, (2), 183-92.

24. Shumyantseva, V. V.; Bulko, T. V.; Rudakov, Y. O.; Kuznetsova, G. P.; Samenkova, N. F.; Lisitsa, A. V.; Karuzina, II; Archakov, A. I., Electrochemical

properties of cytochroms P450 using nanostructured electrodes: Direct electron transfer and electro catalysis. *J Inorg Biochem* **2007,** 101, (5), 859-65.

25. Udit, A. K.; Hagen, K. D.; Goldman, P. J.; Star, A.; Gillan, J. M.; Gray, H. B.; Hill, M. G., Spectroscopy and electrochemistry of cytochrome P450 BM3-surfactant film assemblies. *J Am Chem Soc* **2006,** 128, (31), 10320-5.

26. Shumyantseva, V. V.; Bulko, T. V.; Samenkova, N. F.; Kuznetsova, G. P.; Usanov, S. A.; Schulze, H.; Bachmann, T. T.; Schmid, R. D.; Archakov, A. I., A new format of electrodes for the electrochemical reduction of cytochromes P450. *J Inorg Biochem* **2006,** 100, (8), 1353-7.

27. Nassar, A.-E. F. Z., Zhe; Hu, Naifei; Rusling, James F.; Kumosinski, Thomas F., Proton-Coupled Electron Transfer from Electrodes to Myoglobin in Ordered Biomembrane-like Films. *journal of physical chemistry B* **1997,** 101, (12), 2224-2231.

28. Nassar, A.-E. F. B., J. M.; Stuart, J. D.; Rusling, J. F., Catalytic Reduction of Organohalide Pollutants by Myoglobin in a Biomembrane-like Surfactant Film. *Journal of the American Chemical Society* **1995,** 117, (44), 10986-10993.

29. Bayachou, M.; Elkbir, L.; Farmer, P. J., Catalytic two-electron reductions of N2O and N3- by myoglobin in surfactant films. *Inorg Chem* **2000,** 39, (2), 289-93.

30. Immoos, C. E.; Chou, J.; Bayachou, M.; Blair, E.; Greaves, J.; Farmer, P. J., Electrocatalytic reductions of nitrite, nitric oxide, and nitrous oxide by thermophilic cytochrome P450 CYP119 in film-modified electrodes and an analytical comparison of its catalytic activities with myoglobin. *J Am Chem Soc* **2004,** 126, (15), 4934-42.

31. Mimica, D. Z., José H.; Bedioui, Fethi, Electroreduction of nitrite by hemin, myoglobin and hemoglobin in surfactant films. *Journal of Electroanalytical Chemistry* **2001,** 497, (1-2), 106 - 113.

32. Nassar, A. E.; Willis, W. S.; Rusling, J. F., Electron transfer from electrodes to myoglobin: facilitated in surfactant films and blocked by adsorbed biomacromolecules. *Anal Chem* **1995,** 67, (14), 2386-92.

33. Alatorre Ordaz, A. B., Fethi, The electrocatalytic reduction of organohalides by myoglobin and hemoglobin in a biomembrane-like film and its application to the electrochemical detection of pollutants: new trends and discussion. *Sensors and Actuators B: Chemical* **1999,** 59, (2-3), 128-133.

34. Honeychurch, M. J.; Bernhardt, P. V., On the steady-state assumption and its application to the rotating disk voltammetry of adsorbed enzymes. *J Phys Chem B Condens Matter Mater Surf Interfaces Biophys* **2005,** 109, (12), 5766-73.

35. Argese, E.; De Carli, B.; Orsega, E.; Rigo, A.; Rotilio, G., A rotating disk electrode for kinetic studies of superoxide dismutases: applicability in a wide pH range and for continuous monitoring of enzyme inactivation. *Anal Biochem* **1983,** 132, (1), 110-4.

36. Shu, F. R.; Wilson, G. S., Rotating ring-disk enzyme electrode for surface catalysis studies. *Anal Chem* **1976,** 48, (12), 1679-86.

37. Guto, P. M. R., James F., Myoglobin retains iron heme and near-native conformation in DDAB films prepared from pH 5 to 7 dispersions. *Electrochemistry Communications* **2006,** 8, (3), 455-459.

38. de Groot, M. T.; Merkx, M.; Koper, M. T., Heme release in myoglobin-DDAB films and its role in electrochemical NO reduction. *J Am Chem Soc* **2005,** 127, (46), 16224-32.

39. de Groot, M. T.; Merkx, M.; Koper, M. T., Evidence for heme release in layer-by-layer assemblies of myoglobin and polystyrenesulfonate on pyrolitic graphite. *J Biol Inorg Chem* **2007,** 12, (6), 761-6.

40. Sucheta, A.; Cammack, R.; Weiner, J.; Armstrong, F. A., Reversible electrochemistry of fumarate reductase immobilized on an electrode surface. Direct voltammetric observations of redox centers and their participation in rapid catalytic electron transport. *Biochemistry* **1993,** 32, (20), 5455-65.

41. Feuer, H., The chemistry of nitro and nitroso groups. *Robert E. Krieger Publishing Company, Huntington, New York* **1981,** Chapter 7, 349-486.

42. Henning Lund, O. H., Organic Electrochemistry. *Marcel Derkker, Inc. New York. Basel* **2000**, (4th Edition), 380.

43. Stone, J. R.; Marletta, M. A., The ferrous heme of soluble guanylate cyclase: formation of hexacoordinate complexes with carbon monoxide and nitrosomethane. *Biochemistry* **1995,** 34, (50), 16397-403.

44. Mansuy, D.; Battioni, P.; Chottard, J. C.; Lange, M., Nitrosoalkanes as new ligands of iron(II) porphyrins and hemoproteins. *J Am Chem Soc* **1977,** 99, (19), 6441-3.

45. Mansuy, D.; Chottard, J. C.; Chottard, G., Nitrosoalkanes as Fe(II) ligands in the hemoglobin and myoglobin complexes formed from nitroalkanes in reducing conditions. *Eur J Biochem* **1977,** 76, (2), 617-23.

46. Mansuy D., C. J. C., Chottard G., Nitrosoalkanes as Fe(II) ligands in the hemoglobin and myoglobin complexes formed from nitroalkanes in reducing conditions. *European journal of biochemistry / FEBS* **1977,** 76, (2), 617-623.

47. Sakurai, H. H., G.; Ruf, H. H.; Ullrich, V., The interaction of aliphatic nitro compounds with the liver microsomal monooxygenase system. *Biochemical Pharmacology* **1980,** 29, (3), 341-345.

CHAPTER III

CATALYTIC ACTIVATION OF NITROMETHANE USING VARIOUS HEMOPROTEINS AND HEMIN

3.1 Introduction

The study of myoglobin-catalyzed nitromethane electroreduction gave us a general understanding of how hemoprotein can facilitate the electro activation of nitromethane. But what is the function of the protein parts of myoglobin, and whether there are differences between using myoglobin and using a real P450 enzyme in this catalytic process are still open questions. In this part of study, we use heme group without protein (hemin) and nitric oxide synthase (NOS), an enzyme that has a proximal cysteine thiolate akin to P450 enzymes, to catalyze the electroactivation of nitromethane and compare the results of myoglobin-mediated processes. Through the comparison, we may evaluate the effect of the protein shell and the effects of different heme ligands in different hemoproteins.

Hemin is the bare heme group and the prosthetic group in all heme proteins. It may have the catalytic properties of heme proteins without a protein shell (Figure 3.1). Understanding the intrinsic catalytic activation of nitromethane by hemin is of critical importance in order to better understand the role of the protein part of P450s.

In the absence of protein structure, iron in hemin does not have the fifth ligand, therefore the ligand binding to heme and its open structure may bring different electron transfer, mass transport, and overall kinetics. Some studies reveal its ability to electro-catalyze hydrogen peroxide, nitrite, nitric oxide, nitrous oxide, other nitro-compounds, and organic halides reduction. [1-5]

We also chose the nitric oxide synthase oxygenase (NOSoxy, Figure 3.2) to catalyze the electro-activation of nitromethane. Compared to hemin molecule, NOSoxy has the protein shell, and the heme group is held by a cysteine thiolate coordination at the proximal site just like P450 enzymes. Those differences could affect substrate accessibility and substrate binding affinity to the heme, therefore change the catalytic process. Also, the catalytic activation of nitroalkane needs protons, hence we can observe the effect of protein structure on proton transfer.

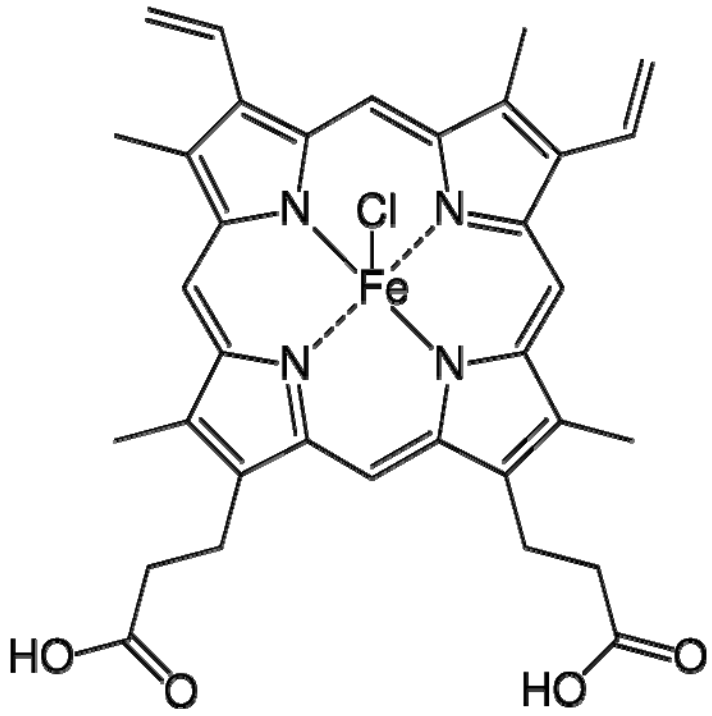

Figure 3.1 Structure of Hemin

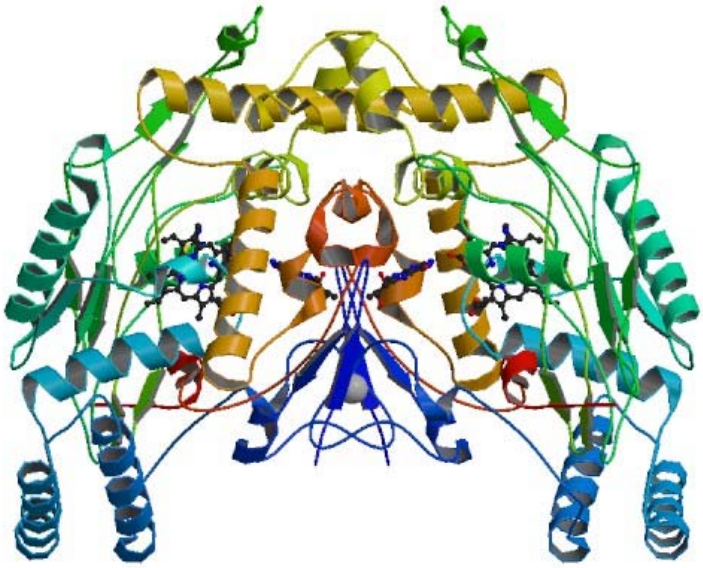

Figure 3.2 Murine inducible nitric oxide synthase oxygenase domain with inhibitor

Image from: PDB 1DF1

NOS is a very important enzyme responsable for nitric oxide biological production. Three isoforms of nitric oxide synthase are currently known; the family includes inducible NOS (iNOS), neuronal NOS (nNOS), and endothelial NOS (eNOS). We chose inducible NOS in our study, which is used by the immune system to produce NO to fight pathogens.

Full-length NOS enzymes are heme flavoproteins belonging to the P450 superfamily [6]. Their structure contains two domains on the same polypeptide: 1) an oxygenase domain, with specific binding sites for the heme active center, the tetrahydrobiopterin (BH_4) cofactor, and arginine substrate [7], and 2) a reductase domain, which contains binding sites for nicotinamide adenine dinucleotide phosphate (NADPH), flavin adenine dinucleotide (FAD), and flavin mononucleotide (FMN) [7].

Cytochrome P450 Reductase (CPR) and the NOS reductase domain both have the same prosthetic group FAD and FMN and the NADPH binding site.[8] The oxygenase domain of NOS is also a heme-containing protein like cytochrome P450s. The biological functions of these two proteins are different but the basic catalytic functions of the functional groups are similar. FAD and FMN in reductase domain shuttle electrons from NADPH to heme group in oxygenase domain to activate heme, and the activated heme will perform the transition of substrate to product. Under aerobic condition, similar to other monooxygenases, NOS catalytic NO production is initiated by activation of molecular oxygen by NOS-heme to form an oxyferroheme complex[9] (Scheme 3.1), just like cytochrome P450 (Scheme 1.1). So this enzyme can closely mimic cytochrome P450 catalytic activity.

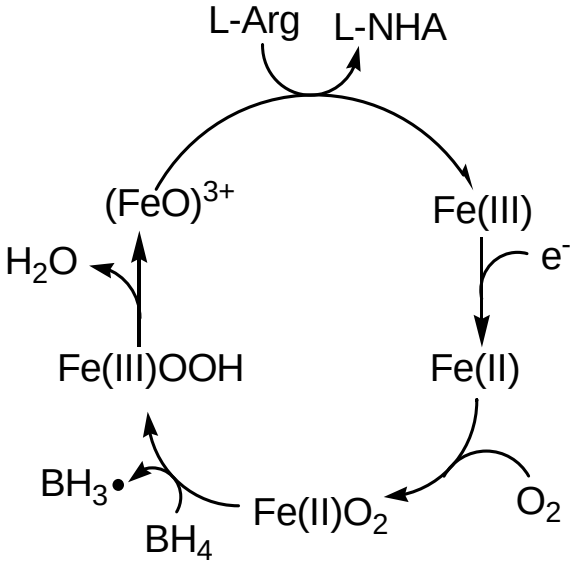

Scheme 3.1 Monooxygenation step of biological NO production by NOS[9]

In this study, we chose only oxygenase domain of NOS to study P450 enzyme activity because the electrons needed to activate heme are provided by the electrode.

NOS enzymes structurally resemble the nitroalkane-metabolizing P450 enzymes, and nitroalkanes could be potential substrates for NOS too. Evidence shows that nitroalkanes or their metabolites such as hydroxylamines could interact with NOS-heme [10]. Nitroalkane can also be oxidized by oxygen catalyzed by a flavoprotein [11]. In addition, hydroxylamines have shown to have vasodilatory properties [12, 13], possibly through a metabolic path leading to NO release.

In this work, hemin and NOS are immobilized on PG electrodes in DDAB thin film as we did with myoglobin in the previous study. The electrocatalysis is characterized electrochemically and the differences of enzymatic activities are discussed.

3.2 Experimental design

3.2.1 Materials

Hemin is purchased from Sigma and used without further process. Didodecyldimethyl-ammonium bromide (DDAB) and nitromethane are from Acros Organics. Oxygenase domain of inducible nitric oxide synthase (iNOSoxy) is expressed and purified in our laboratory.

Nitrogen, compressed from PRAXAIR. Deionized water is obtained from a Barnstead Nanopure system with a resistivity greater than 18 MΩ · cm. Pyrolytic graphite (Advanced Ceramic) is the material for the working electrodes. Homemade working electrodes are prepared as in reference.[5]

3.2.1.1 Expression and Purification of Recombinant iNOSoxy

The expression and purification of the oxygenase domain is conducted in house using classic *Escherichia coli* expression systems.

The experimental protocol that we use is for $iNOS_{oxy}$ expression has been described in the literature [14]; it was adopted as such but with minor modification. Briefly, recombinant wild-type iNOSoxy proteins with a His_6 tag attached to their carboxyl terminus are overexpressed in Escherichia coli strain BL21 (DE3) using a modified pCWori vector. The expression of the protein is typically induced when the culture reaches an optical density of 0.6 at 600 nm. The cells are harvested after (12-24) hours induction and then suspended in the lysis buffer. After sonication, the suspension is centrifuged and the crude extract is loaded into a Ni-nitrilotriacetate-Sepharose 4B column. Bound protein was eluted with elution buffer (160 mM Imidazole, 10μM

H_4B/AA, 1mM L-Arginine, 1mM PMSF/ethanol). The collected fractions containing iNOSoxy are then pooled and concentrated. The final concentrated protein solution is then dialyzed at 4°C to desalt and stored in aliquots (10% glycerol added) at -80°C.

3.2.2 Electrode modification

Hemin (Hm) or iNOSoxy is immobilized in the surfactant film on a basal-plane pyrolytic graphite (PG) disc electrode[4, 15] (surface area is 0.08 cm^2), and the modified electrodes are referred to as Hm/DDAB/PG and iNOSoxy/DDAB/PG. Before coating, the PG electrode is polished using 400 grit sandpaper followed by 0.3μm alumina. The polished electrode is then rinsed and sonicated in distilled water. Hm/DDAB surfactant film is prepared by casting 10μl Hm/DDAB surfactant solution on the PG electrode and dried in air for more than 12 hours. Hm/DDAB surfactant solution is prepared by mixing 0.4 mM hemin solution with 10mM DDAB H_2O emulsion is a 1:1 volume ratio. DDAB solution is prepared by dissolving DDAB powder in deionized water and sonicating for 2 hours. Hemin solution is prepared by sonicating hemin in 0.1M acetate buffer (pH 5.5, 0.05 M NaBr is added) for 2 hours to make a homogeneous dispersion. The hemin dispersion is mixed with DDAB emulsion immediately after sonication. iNOSoxy/DDAB surfactant film is prepared by casting 5μl of 10mM DDAB H_2O solution followed by 5μl of iNOSoxy buffer solution. iNOSoxy buffer solution is prepared using the protocol described above.

3.2.3 Electrochemistry

The electrochemical techniques used in this work are the same as in the previous study. The apparatus keeps the same.

3.2.4 UV-Vis spectroscopy

UV-Vis spectroscopy is used in this work to determine the concentration and structure character of iNOSoxy protein.

3.3 Results and discussion

3.3.1 Spectroscopic characterization of $iNOS_{oxy}$/DDAB film

Prior to electrochemical measurements, we first studied whether the native form of $iNOS_{oxy}$ is conserved in the surfactant environment. To this end, we used UV-Vis spectroscopic characterization using the typical Soret band (Figure 3.3), as well as Fourier Transform Infrared Spectroscopy (FTIR) using the amide I and amide II IR bands (results not shown). A mixture of equal volumes of a purified sample of enzyme (~60 μM) and DDAB suspension (10 mM) is cast on transparent indium tin oxide (ITO) glass slide to prepare the $iNOS_{oxy}$/DDAB film. As with graphite electrode preparation, the cast film on ITO is typically left to dry slowly in a closed vessel overnight, and then in open air. For iNOS heme domain, the typical low-spin iron-heme Soret bands is at around 422 nm [16]. Our results show that both $iNOS_{oxy}$/DDAB on ITO slide and the control $iNOS_{oxy}$ in pH 7 phosphate buffer show the characteristic Soret absorption at 421 nm, Figure 3.4. These results show that the native form of iNOSoxy is mainly conserved in the DDAB surfactant film. Also, addition of arginine, which binds above the Fe-heme at the active site switches the spin state of the iron center from low to high spin. This process can be easily monitored through a typical shift of the Soret band to about 396 nm. We observe similar shift with iNOSoxy immobilized in the bilayered DDAB film. This indicates clearly that the substrate arginine specifically recognizes its binding site in the film environment. These spectroscopic results show that the native structure of the embedded iNOSoxy enzyme is still conserved.

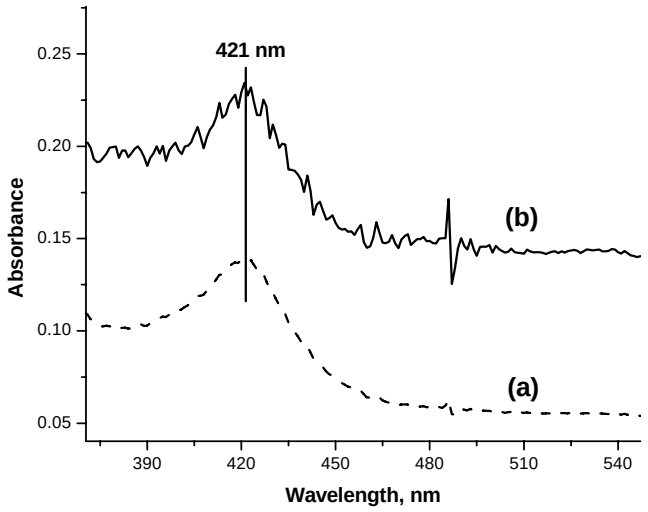

Figure 3.3 UV-vis absorption spectra of (a) iNOSoxy in buffer solution and (b) iNOSoxy/DDAB film on a transparent ITO slides.

To further confirm the native form of NOS in the DDAB environment, we analyzed the effect of DDAB on the position and shape of the amide I and amide II, which typically reflect the state of the secondary structure of globular proteins. To this end, we used FTIR spectroscopy on films cast on a diamond crystal. Our results show that the shape and position amide I and II are not affected by the presence of DDAB (results not shown).

Together, our spectroscopic characterizations of iNOSoxy/DDAB films, confirm that the native structure of iNOSoxy in the surfactant thin film is conserved, and that the immobilized enzyme can still interact and recognize analytes added in the solution bulk.

3.3.2 Electrochemistry of Hm/DDAB/PG, iNOSoxy/DDAB/PG, and Mb/DDAB/PG

Figure 3.4 shows the voltammograms of Hm/DDAB/PG, iNOSoxy/DDAB/PG, and Mb/DDAB/PG in buffer solution. The direct electrochemistry of each electrode shows two fast and reversible redox couples that are characteristics of the heme redox centers. The formal potentials of Fe^{III}/Fe^{II} and Fe^{II}/Fe^{I} redox couples for Hm/DDAB are –0.195V and –1.038V vs. Ag/AgCl respectively, for iNOSoxy/DDAB these couples are at –0.184V and –1.055V, respectively, and for Mb/DDAB these are found at –0.180V and –1.052V. The iNOSoxy/DDAB results are comparable with Udit's work using a similar experimental approach[17]. The difference in redox potential can be only due to the different residues or ligands in the heme vicinity of hemoprotein or hemin.

Although we try to use the same concentration of heme (or protein) solutions to modify the electrodes, the surface concentration of heme group for each type of electrode will be different. As can be seen the reductive or oxidative peak area of Fe^{III}/Fe^{II} redox

couple of the Hm/DDAB electrode is bigger than that of iNOSoxy/DDAB or Mb/DDAB electrode. The peak area is proportional to the amount of electroactive species in the film. Therefore, the surface concentration of heme for Hm/DDAB electrode is higher than that of iNOSoxy/DDAB or Mb/DDAB electrode. iNOSoxy/DDAB and Mb/DDAB electrodes show similar surface concentration of heme group. The difference in surface concentrations can be a problem when comparing the catalytic currents for different catalysts because the amount of catalyst that participates in the catalysis is not the same. To eliminate the effect of concentration differences, the catalytic current is normalized by dividing the catalytic peak by the reductive or oxidative peak area (or peak height if the peak widths are similar) of Fe^{III}/Fe^{II} redox couple of the same electrode. It also eliminates the deviation among the same type of electrodes.

To quantify total amount of active catalyst on the electrode surface we use the method described in previous study. The results show that The average values for Hm/DDAB and iNOSoxy/DDAB film are around 38.1 picomoles and 19.0 picomoles, respectively; accordingly the surface concentrations are 4.76×10^{-10} mole/cm^2 for Hm/DDAB/PG and 2.37×10^{-10} mole/cm^2 for iNOSoxy/DDAB/PG. The average surface concentration of active heme for Mb/DDAB/PG is 2.65×10^{-10} mole/cm^2 from previous research.

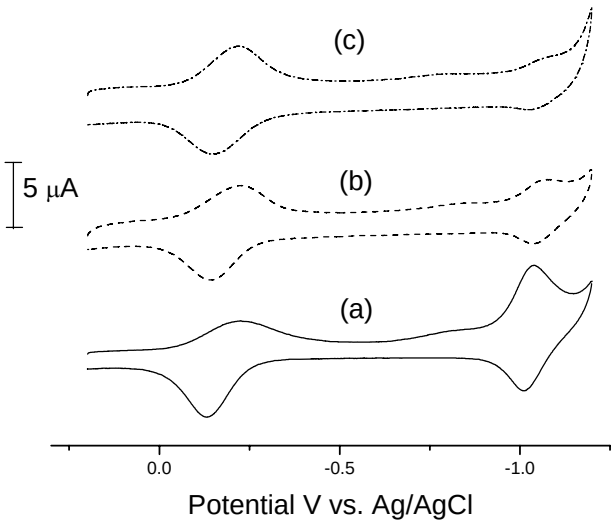

Figure 3.4 Cyclic voltammograms of heme(protein)-modified PG electrode in pH 5.5 buffer at 0.15V/s. (a) Hm/DDAB/PG, (b) Mb/DDAB/PG, and (c) iNOSoxy/DDAB/PG.

Not only the formal potentials and the amount of active heme are different for each heme (or protein), the electron transfer kinetics also differs between Hm/DDAB and Mb/DDAB. To compare the electron transfer kinetic of Hm/DDAB electrode within the film with that of Mb/DDAB electrode, cyclic voltammetry is conducted from 0.2V to –0.6V for 2 continuous cycles, and only the second cycle of the voltammogram is used to obtain peak separation data (ΔEp) used in kinetic assessments.

When we compare the 2 curves in Figure 3.5, we see that both $\Delta Ep_{(Mb)}$ and $\Delta Ep_{(Hm)}$ stay unchanged in the range of scan rate from 0.001V/s to 1V/s, indicating fast reversible electron transfer kinetics. The electron transfer tat is typically measured at the onset of the abrupt increase of ΔE_ps at high scan rates. Hemin shows higher ΔE_p in every scan rate we tested. At the scan rate that is lower than 1V/s, the ΔE_ps of Hm/DDAB and Mb/DDAB are 50-60mV and 22-25mV, respectively. In the high scan rate (greater than 1V/s) region, Hm/DDAB system displays increasing ΔE_p with a relatively steeper increase than from Mb/DDAB electrode. These data suggest that Hm/DDAB have lower heterogeneous electron transfer rate than that of Mb/DDAB within the thin film.

The same experiment with iNOSoxy/DDAB was performed. However, due to the poor stability of the protein film under the condition of extremely low scan rate, full set of data could not be obtained. Hence, the iNOSoxy/DDAB data was not included in the comparison above.

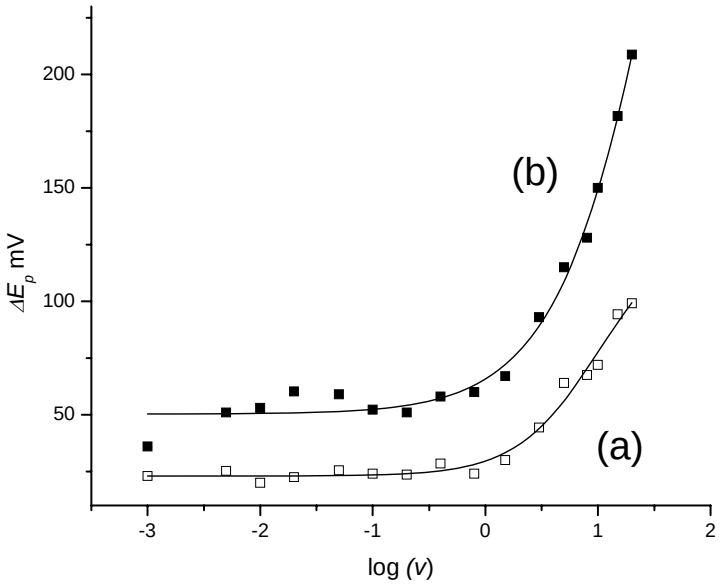

Figure 3.5 ΔE_p as a function of scan rate. (a) Mb/DDAB/PG; (b) Hm/DDAB/PG

3.3.3 Comparison of iNOSoxy-mediated nitromethane electroactivation with myoglobin-mediated, and bare heme-mediated activations.

3.3.3.1 Electroreduction of nitromethane by the different heme-based catalysts

The Hm/DDAB and iNOSoxy/DDAB systems can also catalyze the electroreduction of nitromethane as Mb/DDAB did in the previous study. Figure 3.6A(b) shows the catalytic reduction peak R_c of Hm/DDAB at –0.964 V in the presence of 0.4 mM of nitromethane. As a bare hemin-mediated catalysis, the catalytic current of Hm/DDAB is the highest among the 3 catalysts. The high surface concentration of heme group is an obvious reason. However, once normalized with the amount of heme, Hm/DDAB still exhibits the highest turnover rate; this will be discussed later. Figure 3.6B(b) shows the catalytic reduction peak R_c of iNOSoxy/DDAB at –1.060 V. It displays a notable higher catalytic current compared to the catalysis mediated by Mb/DDAB (Figure 3.6C) even with slightly lower amount of heme group in the film. The factor that contributes to this might be the protein structure difference; so the accessibility to heme for iNOSoxy may be easier than that of myoglobin. Therefore, the mass transport is faster in iNOSoxy/DDAB system than in Mb/DDAB.

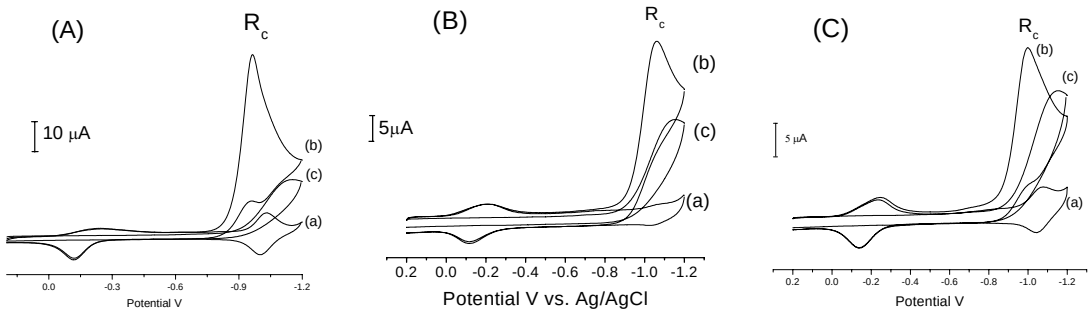

Figure 3.6A Cyclic voltammograms of DDAB/PG and Hm/DDAB/PG electrode in pH 5.5 acetate buffer solution at the scan rate 0.15V/s. (a) Hm/DDAB/PG without nitromethane, (b) Hm/DDAB/PG with 0.4 mM nitromethane, (c) DDAB/PG with 0.4 mM nitromethane.

Figure 3.6B Cyclic voltammograms of DDAB/PG and iNOSoxy/DDAB/PG electrode in pH 5.5 acetate buffer solution at the scan rate 0.15V/s. (a) iNOSoxy/DDAB/PG electrode without nitromethane, (b) iNOSoxy/DDAB/PG electrode with 0.4 mM nitromethane, and (c) DDAB/PG electrode with 0.4 mM nitromethane.

Figure 3.6C Cyclic voltammograms of DDAB/PG and Mb/DDAB/PG electrode in pH 5.5 acetate buffer solution at the scan rate 0.15V/s. (a) Mb/DDAB/PG without nitromethane, (b) Mb/DDAB/PG with 0.4 mM nitromethane, (c) DDAB/PG with 0.4 mM nitromethane.

Some reports claim that the electronic signal from a hemoprotein modified electrode is from hemin that is released from hemoprotein. We already tested SDS denatured myoglobin electrode in the previous study, and here we apply the same treatment to a hemin-modified electrode, and the results are shown in Figure 3.7B. The electrochemical activity of Hm/DDAB (Figure 3.7A) is not changed with or without nitromethane substrate. Therefore, hemoproteins should be intact when being modified to PG electrode to perform catalysis.

Some previous electrochemical investigations report on critical residues around the active site of hemoprotein.[18] Also, a pH study of myoglobin-modified electrodes has shown that the electrochemical activity is closely related to the pk_as of key residues of the protein.[19-21] These results have showed that the protein and hydrogen-bonding network that it provides are involved in the electron transfer process.

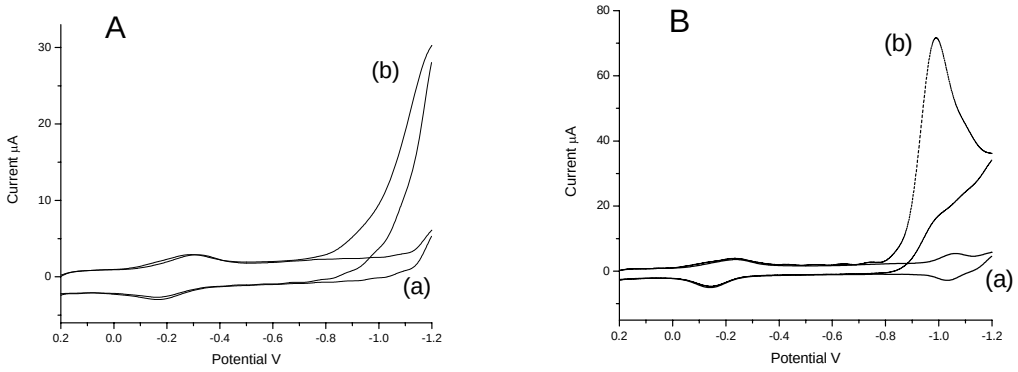

Figure 3.7A Cyclic voltammograms of SDS denatured myoglobin electrode in pH5.5 buffer. (a) 0 mM nitromethane (b) 0.4 mM nitromethane.

Figure 3.7B Cyclic voltammograms of SDS treated hemin electrode in pH5.5 buffer. (a) 0 mM nitromethane (b) 0.4 mM nitromethane.

3.3.3.2 The effect of nitromethane concentration

We collected data from the experiments with iNOSoxy, hemin, and myoglobin, and plotted the normalized catalytic current as a function of substrate concentration (Michaelis-Menten plot, Figure 3.8) for these three different catalysts. The hyperbolic plot of each catalyst is then fitted into the electrochemical form of Michaelis-Menten equation (Equation 2.7) to obtain the parameters of kinetics.

After data processing (Table 3.1), iNOSoxy shows the highest catalytic ability and the lowest catalyst-substrate dissociation constant K_m for the catalytic reaction. On the contrary, hemin has the highest K_m and highest turnover number K_{cat} (more than two times higher than that of iNOSoxy), but the overall catalytic ability is not better than iNOSoxy. iNOSoxy and myoglobin have similar catalyst-substrate stability, maybe because of the structural similarity of the substrate binding site of their heme centers. Hemin, on the other hand, lack the proximal fifth ligand and the protein shell, which may affect binding affinity and substrate accessibility to the heme iron.

Table 3.1. Non-linear regression parameters from Figure 3.8

	K_m (mM)	k_{cat} (s^{-1})	k_{cat} / K_m ($s^{-1} \cdot mM^{-1}$)
Hemin	4.4 ± 0.5	68.3 ± 6.3	15.6
iNOSoxy	1.7±0.2	28.1 ± 2.2	16.5
Myoglobin	1.9 ± 0.2	20.9 ± 1.8	11

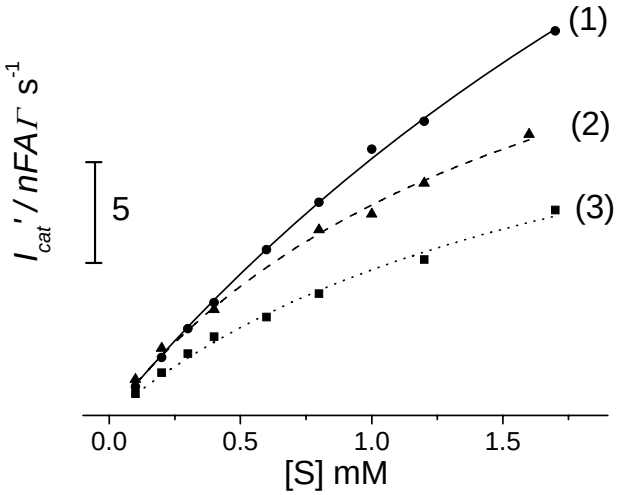

Figure 3.8 Normalized catalytic current as a function of substrate concentration. (Michaelis-Menten plot) (1) Hm/DDAB, (2) iNOSoxy/DDAB, and (3) Mb/DDAB.

I_{cat}' is the catalytic current measured at the scan rat of 150 mV/s.

3.3.3.3 The effect of scan rate

From the scan rate dependency studies of these three heme-based catalyst, one can see that NOS-mediated reaction has the steepest drop of catalytic efficiency compared to the hemin- and myoglobin-mediated ones in the scan rate range from 5mV/s to 1V/s, Figure 3.9. In the range from 1V/s to 20V/s, the catalytic efficiency of NOS or myoglobin-mediated reaction drops only slightly. The protein shell is iNOSoxy may play a role in the steep drop of catalytic efficiency in the 5 mV/s to 1 V/s range. In fact, protein shell controls substrate access to the active site, and thus directly affects mass transport. This is in line with the behavior of myoglobin, with relatively open active site compared to iNOSoxy, and which exhibits a moderate drop in catalytic current. At the other extreme, bare hemin, with a complete open access, exhibits only a gradual drop in catalytic current.

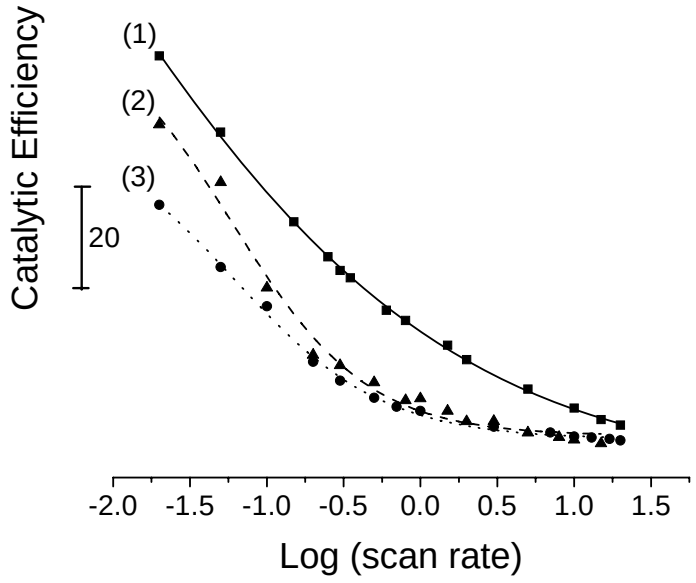

Figure 3.9 Catalytic efficiency as a function of scan rate. (1) Hm/DDAB/PG (2) iNOSoxy/DDAB/PG (3) Mb/DDAB/PG.

3.3.3.4 The effect of pH

The pH dependency studies show clear proton dependency for hemin and heme-protein-mediated catalysis, Figure 3.10. Hemin-mediated reaction exhibits the fastest dropping of catalytic efficiency with increasing pH, and NOS- or myoglobin-mediated reaction has a slower dropping rate. Literature suggests that the large number of hydrogen bonds within the protein molecule may provide extremely efficient means of proton transfer,[22] and protonation and deprotonation of the amino acids surrounding the heme group of hemoprotein has been shown to affect proton coupled electron transfer process.[19, 23-27] Also, the proton coupled electron transfer might be controlled by the protonation state of the amino acids[23-25]. The protein shell of iNOSoxy or myoglobin would also mediate proton transfers in this reaction, which could act as a local buffer counteracting the change in bulk pH and make the reaction relatively less dependent on pH, as observed.

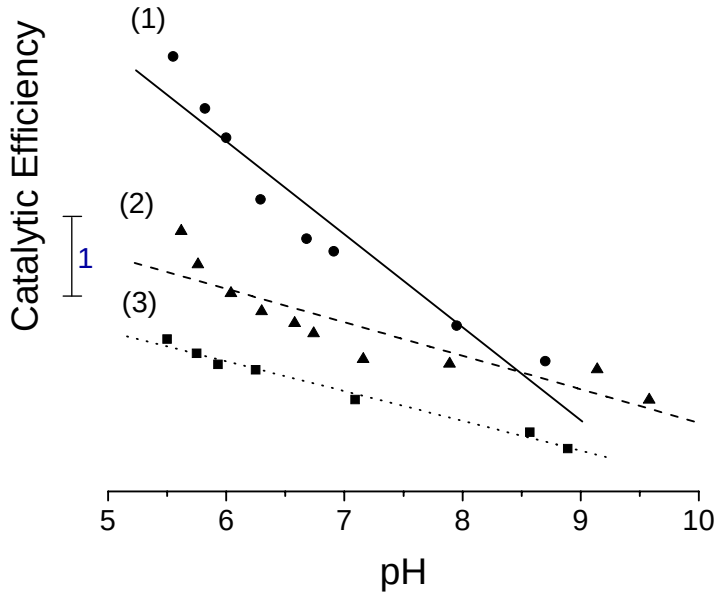

Figure 3.10 Catalytic efficiency of nitromethane catalytic reduction as a function of pH in the presence of 0.1mM nitromethane mediated by (1) Hm/DDAB/PG, (2) iNOSoxy/DDAB/PG, and (3) Mb/DDAB/PG

3.3.4 Final products of hemin-mediated catalysis versus hemoprotein-mediated catalysis

Bulk electrolysis experiments coupled with mass spectrometric analysis as we used in the previous study show that the final product of hemin or myoglobin-mediated catalysis is methyl hydroxylamine. The number of electrons per nitromethane molecule in the electroreduction is close to 4 to 1 in both cases. The trials are shown in Table 3.2.

We also did the experiment with iNOSoxy/DDAB electrode. Unfortunately, because of the vigorous convection applied in the bulk electrolysis, iNOSoxy/DDAB film was washed off quickly, and the experiment could not finish successfully.

Table 3.2 The ratio of electron to nitromethane molecule

		Total electrons passed	Total nitromethane molecules reduced	Electrons per molecule	
Mb/DDAB	Trial 1	7.20×10^{18}	1.54×10^{18}	4.68	4.45 ± 0.22
	Trial 2	7.33×10^{18}	1.65×10^{18}	4.44	
	Trial 3	7.62×10^{18}	1.80×10^{18}	4.23	
Hm/DDAB	Trial 1	7.12×10^{18}	1.58×10^{18}	4.51	4.53 ± 0.13
	Trial 2	6.59×10^{18}	1.41×10^{18}	4.67	
	Trial 3	7.98×10^{18}	1.81×10^{18}	4.41	

The results show that the final products of the electrocatalysis mediated by hemin or hemoprotein are the same. Therefore, the reaction mechanisms for these catalysts are likely the same as we proposed in last chapter with heme as the major player.

3.4 Conclusion

iNOSoxy-mediated electroreduction of nitromethane shows highest catalytic ability close to the bare hemin-facilitated one. Low K_m of iNOSoxy indicates a high heme binding affinity to a catalytically active form derived from the substrate. This is likely facilitated by the thiolate fifth ligand of heme and flanking residues around heme binding site. The scan rate dependency study shows that the protein shells of myoglobin and iNOSoxy control the mass transfer to the active site. Furthermore, the pH dependency study implies that the residues close to the heme binding site may mediate proton transfer or act as proton donors to assist the catalytic transformations.

Comparing electroactivation of nitromethane catalyzed by two distinct hemoprotein and bare hemin illustrates the effects caused by the protein shell and iron ligation as well as the effects caused by residues around the heme site.

3.5 References

1. Dai, Z.; Xu, X.; Ju, H., Direct electrochemistry and electrocatalysis of myoglobin immobilized on a hexagonal mesoporous silica matrix. *Anal Biochem* **2004,** 332, (1), 23-31.

2. Immoos, C. E.; Chou, J.; Bayachou, M.; Blair, E.; Greaves, J.; Farmer, P. J., Electrocatalytic reductions of nitrite, nitric oxide, and nitrous oxide by thermophilic cytochrome P450 CYP119 in film-modified electrodes and an analytical comparison of its catalytic activities with myoglobin. *J Am Chem Soc* **2004,** 126, (15), 4934-42.

3. Lu, H.; Li, Z.; Hu, N., Direct voltammetry and electrocatalytic properties of catalase incorporated in polyacrylamide hydrogel films. *Biophys Chem* **2003,** 104, (3), 623-32.

4. Alatorre Ordaz, A. B., Fethi, The electrocatalytic reduction of organohalides by myoglobin and hemoglobin in a biomembrane-like film and its application to the electrochemical detection of pollutants: new trends and discussion. *Sensors and Actuators B: Chemical* **1999,** 59, (2-3), 128-133.

5. Boutros, J.; Bayachou, M., Myoglobin as an efficient electrocatalyst for nitromethane reduction. *Inorg Chem* **2004,** 43, (13), 3847-53.

6. White, K. A.; Marletta, M. A., Nitric oxide synthase is a cytochrome P-450 type hemoprotein. *Biochemistry* **1992,** 31, (29), 6627-31.

7. Ghosh, D. K.; Stuehr, D. J., Macrophage NO synthase: characterization of isolated oxygenase and reductase domains reveals a head-to-head subunit interaction. *Biochemistry* **1995,** 34, (3), 801-7.

8. Iyanagi, T., Structure and function of NADPH-cytochrome P450 reductase and nitric oxide synthase reductase domain. *Biochem Biophys Res Commun* **2005,** 338, (1), 520-8.

9. Bayachou, M.; Boutros, J. A., Direct electron transfer to the oxygenase domain of neuronal nitric oxide synthase (NOS): exploring unique redox properties of NOS enzymes. *J Am Chem Soc* **2004,** 126, (40), 12722-3.

10. Renodon, A.; Boucher, J. L.; Wu, C.; Gachhui, R.; Sari, M. A.; Mansuy, D.; Stuehr, D., Formation of nitric oxide synthase-iron(II) nitrosoalkane complexes: severe restriction of access to the iron(II) site in the presence of tetrahydrobiopterin. *Biochemistry* **1998,** 37, (18), 6367-74.

11. Gadda, G.; Fitzpatrick, P. F., Mechanism of nitroalkane oxidase: 2. pH and kinetic isotope effects. *Biochemistry* **2000,** 39, (6), 1406-10.

12. DeMaster, E. G.; Raij, L.; Archer, S. L.; Weir, E. K., Hydroxylamine is a vasorelaxant and a possible intermediate in the oxidative conversion of L-arginine to nitric oxide. *Biochem Biophys Res Commun* **1989,** 163, (1), 527-33.

13. Beranova, P.; Chalupsky, K.; Kleschyov, A. L.; Schott, C.; Boucher, J. L.; Mansuy, D.; Munzel, T.; Muller, B.; Stoclet, J. C., Nomega-hydroxy-L-arginine homologues and hydroxylamine as nitric oxide-dependent vasorelaxant agents. *Eur J Pharmacol* **2005,** 516, (3), 260-7.

14. Wu, C.; Zhang, J.; Abu-Soud, H.; Ghosh, D. K.; Stuehr, D. J., High-level expression of mouse inducible nitric oxide synthase in Escherichia coli requires coexpression with calmodulin. *Biochem Biophys Res Commun* **1996,** 222, (2), 439-44.

15. Nassar, A.-E. F. B., J. M.; Stuart, J. D.; Rusling, J. F., Catalytic Reduction of Organohalide Pollutants by Myoglobin in a Biomembrane-like Surfactant Film. *Journal of the American Chemical Society* **1995,** 117, (44), 10986-10993.

16. Dunn, A. R.; Belliston-Bittner, W.; Winkler, J. R.; Getzoff, E. D.; Stuehr, D. J.; Gray, H. B., Luminescent ruthenium(II)- and rhenium(I)-diimine wires bind nitric oxide synthase. *J Am Chem Soc* **2005,** 127, (14), 5169-73.

17. Udit, A. K.; Belliston-Bittner, W.; Glazer, E. C.; Nguyen, Y. H.; Gillan, J. M.; Hill, M. G.; Marletta, M. A.; Goodin, D. B.; Gray, H. B., Redox couples of inducible nitric oxide synthase. *J Am Chem Soc* **2005,** 127, (32), 11212-3.

18. Rafferty, S. P.; Guillemette, J. G.; Berghuis, A. M.; Smith, M.; Brayer, G. D.; Mauk, A. G., Mechanistic and structural contributions of critical surface and internal residues to cytochrome c electron transfer reactivity. *Biochemistry* **1996,** 35, (33), 10784-92.

19. Nassar, A. E.; Rusling, J. F.; Kumosinski, T. F., Salt and pH effects on electrochemistry of myoglobin in thick films of a bilayer-forming surfactant. *Biophys Chem* **1997,** 67, (1-3), 107-16.

20. Zhang, Z.; Rusling, J. F., Electron transfer between myoglobin and electrodes in thin films of phosphatidylcholines and dihexadecylphosphate. *Biophys Chem* **1997,** 63, (2-3), 133-46.

21. Guto, P. M.; Rusling, J. F., Enzyme-like kinetics of ferryloxy myoglobin formation in films on electrodes in microemulsions. *J Phys Chem B* **2005,** 109, (51), 24457-64.

22. Scheiner, S., Proton transfers in hydrogen-bonded systems. Cationic oligomers of water. *J. Am. Chem. Soc.* **1981,** 103, 315-320.

23. Liu, H. H.; Tian, Z. Q.; Lu, Z. X.; Zhang, Z. L.; Zhang, M.; Pang, D. W., Direct electrochemistry and electrocatalysis of heme-proteins entrapped in agarose hydrogel films. *Biosens Bioelectron* **2004,** 20, (2), 294-304.

24. Feng, J. J.; Zhao, G.; Xu, J. J.; Chen, H. Y., Direct electrochemistry and electrocatalysis of heme proteins immobilized on gold nanoparticles stabilized by chitosan. *Anal Biochem* **2005,** 342, (2), 280-6.

25. Yamazaki, I.; Araiso, T.; Hayashi, Y.; Yamada, H.; Makino, R., Analysis of acid-base properties of peroxidase and myoglobin. *Adv. Biophys.* **1978,** 11, 249-281.

26. Huang, H.; Hu, N.; Zeng, Y.; Zhou, G., Electrochemistry and electrocatalysis with heme proteins in chitosan biopolymer films. *Anal Biochem* **2002,** 308, (1), 141-51.

27. Huang, H.; He, P.; Hu, N.; Zeng, Y., Electrochemical and electrocatalytic properties of myoglobin and hemoglobin incorporated in carboxymethyl cellulose films. *Bioelectrochemistry* **2003,** 61, (1-2), 29-38.

CHAPTER IV

CATALYTIC ELECTROREDUCTION OF ALIPHATIC NITROALKANES MEDIATED: A COMPARATIVE STUDY OF INOSOXY AND HEMIN AS HEME-CATALYSTS

4.1 Introduction

Most nitroalkanes are toxic,[1] and some are even found to be carcinogenic[2-6] and genotoxic[7]. Nitromethane is an example of nitroalkanes that are potent carcinogens.[8] Also, 1-nitropropane has demonstrated mutagenic activity[7, 9, 10] in cells though no link to carcinogenicity has been established even with chronic exposure.[9] Some of the secondary nitroalkanes such as 2-nitrobutane and 3-nitropentane may cause significant incidence of hepatocarcinoma with metastasis in the lungs, and have also been found to be more carcinogenic than their corresponding primary nitroalkanes.[11] 2-nitropropane is another well-known hepatocarcinogen,[12-14] and its mutagenicity has been studied widely using animal models.[10, 15-18]

The types of cancer caused by nitroalkanes are different for, but the key step in each carcinogenic process always involves a biotransformation of the nitroalkane into a more

reactive compound. One possible metabolic pathway could be anaerobic nitro-reduction catalyzed by cytochrome P450 xenobiotic metabolizing enzymes through electron transfer producing alkyl hydroxylamines as the final product. This is in agreement with some research of the anaerobic metabolism of nitro compounds using biological samples.[19, 20]

Previously we tested nitromethane anaerobic electroreduction mediated by myoglobin, hemin, and iNOSoxy. Our results indicate that electro-activation of nitromethane can be catalyzed by hemin or hemoproteins, and the catalytic function of the heme may reflect the metabolic pathway of nitromethane activation by P450 metabolizing enzymes under anaerobic conditions. Mass spectroscopy shows that the catalytic reduction of nitromethane under these conditions reduces the nitro group to hydroxylamine, possibly through our proposed pathway, Scheme 4.1. Hence, we propose that nitroalkanes with different alkyl groups may also be catalytically reduced to hydroxylamines through a similar catalytic mechanism.

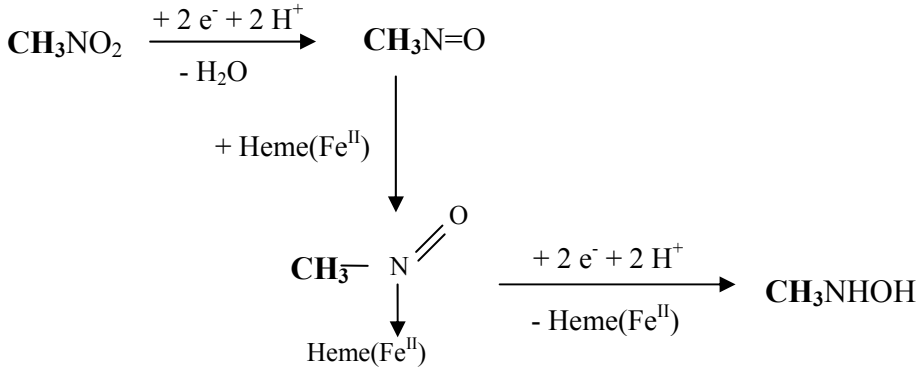

Scheme 4.1 Proposed heme-catalyzed electroreduction of nitromethane

The size of the alkyl group might affect the mass transport in diffusion-controlled electrochemical techniques such as cyclic voltammetry. The different alkyl groups in

nitroalkanes may also affect the chemical properties of their nitro groups, therefore exhibiting effects on catalytic reduction. Because of these potential changes in chemical properties, we examined four different substrates in this study, nitromethane, nitroethane, 1-nitropropane, and 2-nitropropane, Scheme 4.2.

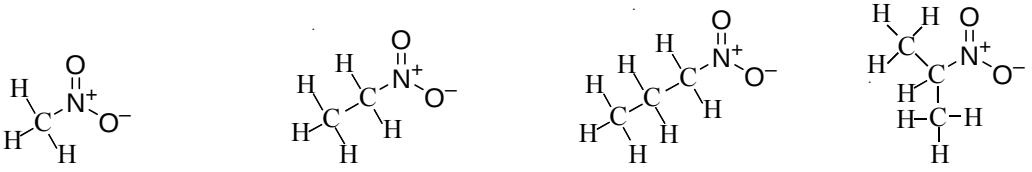

nitromethane nitroethane 1-nitropropane 2-nitropropane

Scheme 4.2 Structures of the nitroalkanes used in the study

In this part, the various nitroalkanes are tested on Hm/DDAB/PG and iNOSoxy/DDAB/PG electrodes, and catalytic currents from cyclic voltammetry are used as the expressions of the catalysis. Mass spectrometry is used to identify the products of heme-mediated electroreduction of these 4 nitroalkanes. The catalytic efficiencies of different substrates are contrasted and effects of factors such as substrate concentration, scan rate of cyclic voltammetry, and pH, are discussed.

4.2 Experimental design

4.2.1 Material

Hemin, Nitromethane, Nitroethane, 1-Nitropropane, and 2-nitropropane are purchased from Sigma and used without further process. Didodecyldimethyl-ammonium bromide (DDAB) is from Acros Organics. Oxygenase domain of inducible nitric oxide synthase (iNOSoxy) is expressed and purified in our laboratory using the procedure described in chapter 3.

Nitrogen, compressed from PRAXAIR. Deionized water is obtained from a Barnstead Nanopure system with a resistivity greater than 18 MΩ · cm. Pyrolytic graphite (Advanced Ceramics) is the material for the working electrodes. Homemade working electrodes are prepared as in reference.[21]

4.2.2 Methods

The hemin and iNOSoxy modification of electrodes have been described in chapter 3. Electrochemical techniques employed and the apparatus are the same as chapter 2.

Bulk electrolysis is performed at -1.0 V vs. Ag/AgCl under constant stirring for 1 hour. A large surface PG electrode modified with Hm/DDAB or iNOSoxy/DDAB is used as a working electrode. The starting concentration of nitroalkane is 1.96 mM in 5 mL of solution, and the concentration of nitroalkane after the electrolysis is estimated using an electrochemical method. The consumption of nitroalkane is derived from the difference between the initial amount and final amount. The total charge passed during the electrolysis is recorded. The total number of electrons per nitroalkane molecule can therefore be calculated.

A mass spectrometric method is employed to identify the product after the bulk electrolysis. The solution after electrolysis is infused into an electro spray ionization triple quadrupole (ESI-QQQ) mass spectrometer (Micromass Quattro II). The product is identified by the m/z ratio on the mass spectrum.

4.3 Results and discussion

4.3.1 Direct electroreduction of nitroalkanes on a DDAB/PG and catalytic electroreduction of nitroalkanes mediated by Hm/DDAB/PG and iNOSoxy/DDAB/PG

Figure 4.1 shows the electroreduction of nitroalkanes on DDAB/PG electrodes. Since there is no catalyst involved, we label these processes as direct reductions or non-mediated reductions. The reduction current response for the various nitroalkanes are in the order of nitromethane > nitroethane > 1-nitropropane > 2- nitropropane, and the reductive potentials from positive to negative are 1-nitropropane (-1.133 V), nitromethane (-1.195 V), nitroethane (-1.217 V), and 2- nitropropane (-1.221 V). The hemin-mediated catalytic reductions (Figure 4.2) show that the current intensities are in the same order of that of direct reduction, and the potential from positive to negative follows the order 1-nitropropane (-0.972 V), 2-nitropropane (-0.979 V), nitromethane (-1.001 V), and nitroethane (-1.042 V). The reduction currents of iNOSoxy-mediated reactions (Figure 4.3) follow the same order as the direct reductions, and the reduction potentials also show the same order as for the direct reductions but at much positive potentials: 1-nitropropane (-1.024 V), nitromethane (-1.049 V), nitroethane (-1.056 V), and 2-nitropropane (-1.058 V). In addition, the potentials of iNOSoxy-mediated electroreductions are very close to each other.

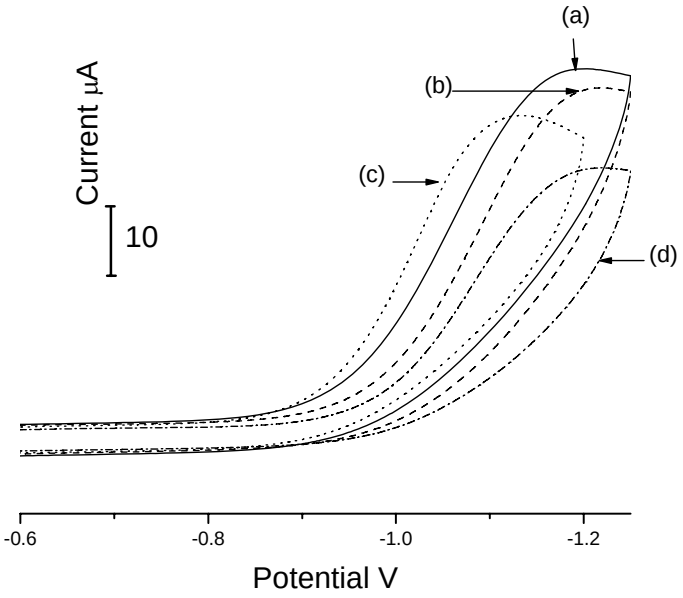

Figure 4.1 Cyclic Voltammograms of DDAB/PG electrode in pH 5.5 buffer at 150 mV/s in the presence of nitroalkanes. (a) 0.2 mM nitromethane, (b) 0.2 mM nitroethane, (c) 0.2 mM 1-nitropropane, and (d) 0.2 mM 2-nitropropane.

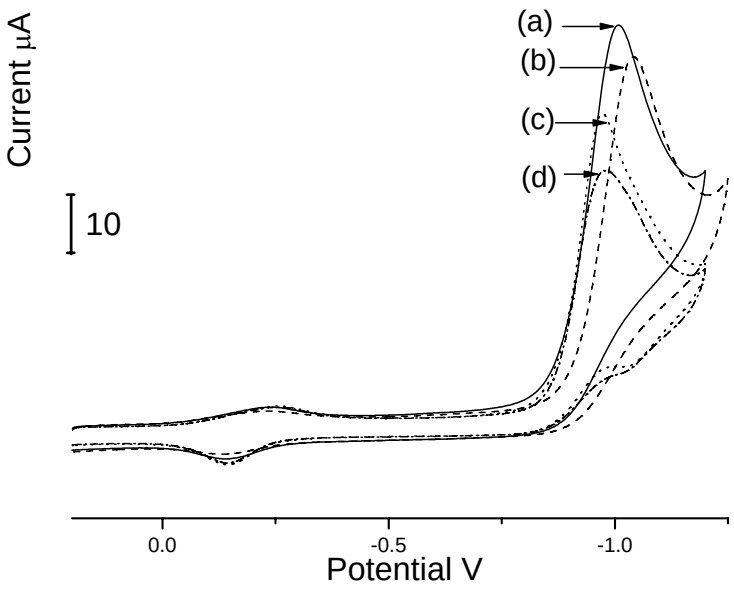

Figure 4.2 Cyclic Voltammograms of Hm/DDAB/PG electrode in pH 5.5 buffer at 150 mV/s in the presence of nitroalkanes. (a) 0.2 mM nitromethane, (b) 0.2 mM nitroethane, (c) 0.2 mM 1-nitropropane, and (d) 0.2 mM 2-nitropropane.

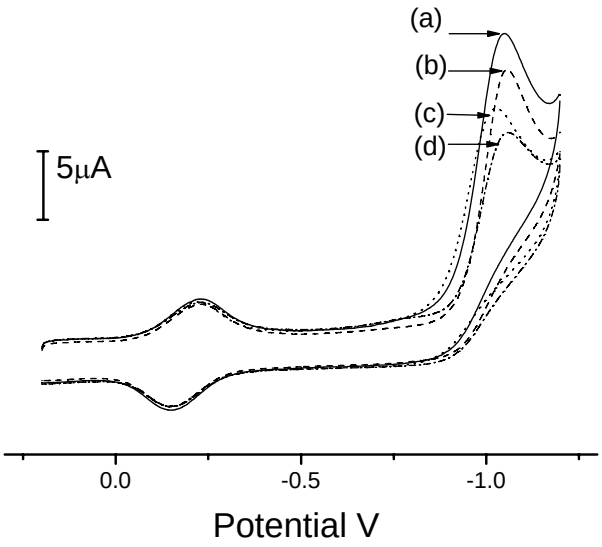

Figure 4.3 Cyclic Voltammograms of iNOSoxy/DDAB/PG electrode in pH 5.5 buffer at 150 mV/s in the presence of nitroalkanes. (a) 0.2 mM nitromethane, (b) 0.2 mM nitroethane, (c) 0.2 mM 1-nitropropane, and (d) 0.2 mM 2-nitropropane.

The current intensities of direct electroreductions on the DDAB/PG and the heme-facilitated electroreduction (Figure 4.2 and Figure 4.3) exhibit the same trend in that smaller nitroalkanes have higher catalytic currents. An obvious reason is that the diffusion that controls mass transport plays to the advantage of small molecules, Table 4.1. To see the effect of molecular size of the nitroalkane substrate, we examined and compared the effect of scan rate of catalytic reduction of the various nitroalkanes.

Table 4.1 Hydrodynamic radiuses of the alkyl groups[22]

	methyl	ethyl	propyl	isopropyl
r (nm)	0.20	0.225	0.25	0.30

For heme-mediated reduction of the four nitroalkane substrates, the reduction peaks in the voltammograms all shift to positive potentials compared to the direct reductions. The same is true for hemin-mediated catalysis but the current intensities are relatively larger. The shift of the reductions to positive potentials and the increase of reaction rate are typical features for electrocatalytic process. Therefore, hemin and iNOSoxy are efficient electrocatalysis for the electroreductions of the 4 nitroalkane substrates.

The direct reduction potentials follow the order of nitromethane, nitroethane, and 2-nitropropane. This trend may be explained by the inductive and hyperconjugative effects of alkyl groups.[23] Alkyl groups are considered as electron-donating to the nitro group, and the inductive effect (+I) follows the order $-CH_3 < -CH_2CH_2CH_3 < -CH_2CH_3 < -CH(CH_3)_2$. The effect increases the negative charge on the nitro group therefore make the reduction more difficult. However, 1-nitropropane is unique among the 4 substrates. It shows the most positive potential in both direct electroreduction and heme-mediated ones.

A possible reason is that the reduction of 1-nitropropane, with the smallest dielectric constant among the 4 nitroalkanes, is favorable on our electrodes modified with hydrophobic DDAB films. Stabilized intermediates derived from this nitroalkane relative to the other 3 substrates may also play a role in these reductions at positive potentials.

One may notice that the hemin-mediated 2-nitropropane displays the largest shift of reduction potential from –1.221 V to –0.979 V among all the nitroalkane substrates. The hemin catalyst in the reaction lowers the activation energy of 2-nitropropane reduction more than those of the other 3 substrates. It is possible that in the heme-mediated reduction, 2-nitropropane forms the hemin ferrous 2-nitrosopropane complex that can be reduced at low potential, and the mediation by hemin may also compensate for the inductive effects that makes 2-nitropropane hard to reduce.

4.3.2 Identification of the products of the hemin-mediated electroreduction of nitroalkanes

It is critical to know the products of the catalytic electroreduction and number of electrons consumed per substrate molecule so that the mechanism of the catalysis can be derived. To find out the ratio of electron to nitroalkane molecules, we perform bulk electrolysis using each of the 4 nitroalkane substrates. From the total electrons passed and total amount of nitroalkane consumed, one can calculate the electrons per molecule. The results of this work are listed in Table 4.2. The products of catalytic electroreduction of nitroalkanes are identified by mass spectrometry (Figure 4.4) using the solution after bulk electrolysis (Table 4.3).

Table 4.2 The ratio of electron to nitroalkane molecule

	Total electrons passed	Total molecules reduced	Electrons per molecule
nitromethane	8.45×10^{18}	1.93×10^{18}	4.38
nitroethane	7.15×10^{18}	1.69×10^{18}	4.23
1-nitropropane	7.54×10^{18}	1.81×10^{18}	4.17
2-nitropropane	7.07×10^{18}	1.63×10^{18}	4.34

Table 4.3 The products of catalytic electroreduction of nitroalkanes

	The products of catalytic electroreduction
nitromethane	methyl hydroxylamine (CH_3-NHOH)
nitroethane	ethyl hydroxylamine (C_2H_5-NHOH)
1-nitropropane	propyl hydroxylamine (C_3H_7-NHOH)
2-nitropropane	isopropyl hydroxylamine ($(CH_3)_2$C-NHOH)

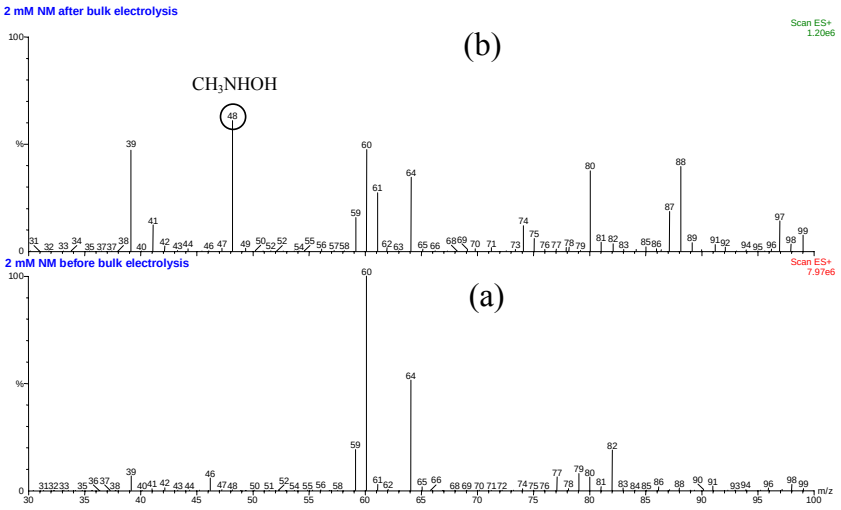

Figure 4.4A Mass spectra of 2 mM nitromethane in the buffer solution (a) before and (b) after the bulk electrolysis.

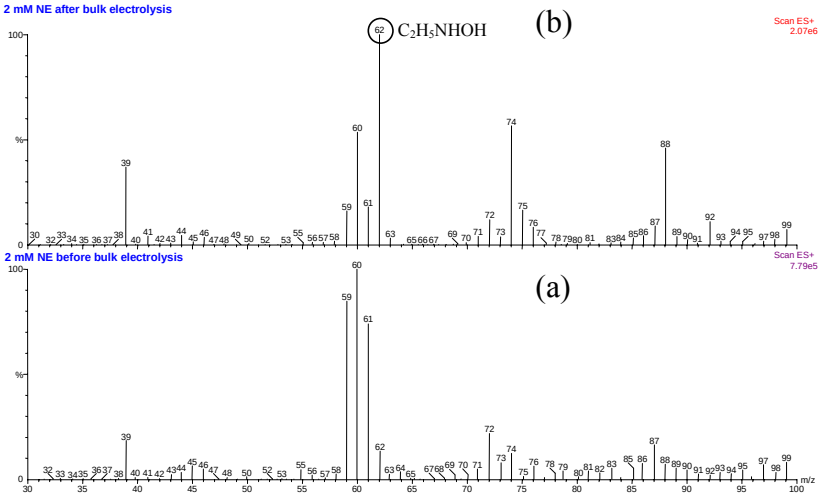

Figure 4.4B Mass spectra of 2 mM nitroethane in the buffer solution (a) before and (b) after the bulk electrolysis.

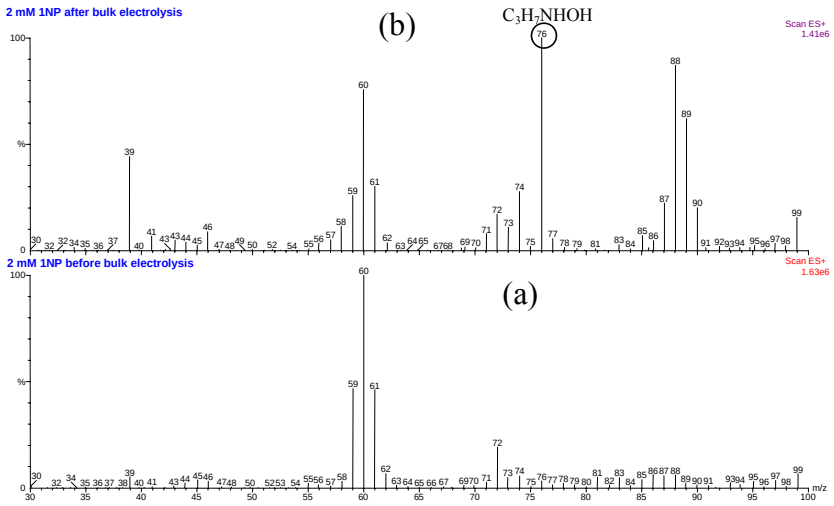

Figure 4.4C Mass spectra of 2 mM 1-nitropropane in the buffer solution (a) before and (b) after the bulk electrolysis.

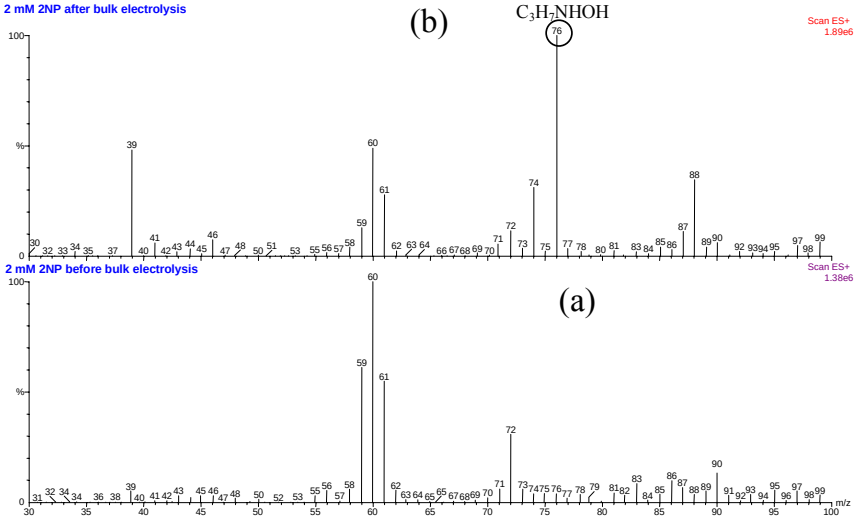

Figure 4.4D Mass spectra of 2 mM 2-nitropropane in the buffer solution (a) before and (b) after the bulk electrolysis.

Since the mass spectrometric results show that the reduction products of nitroalkanes are exclusively the corresponding alkyl hydroxylamine, and the ratio of electrons to nitroalkane molecules is close to 4 for each substrate, the possible mechanism of the catalysis may be similar to Scheme 4.1. We can therefore describe the electroreductions by the following generalized scheme (Scheme 4.3).

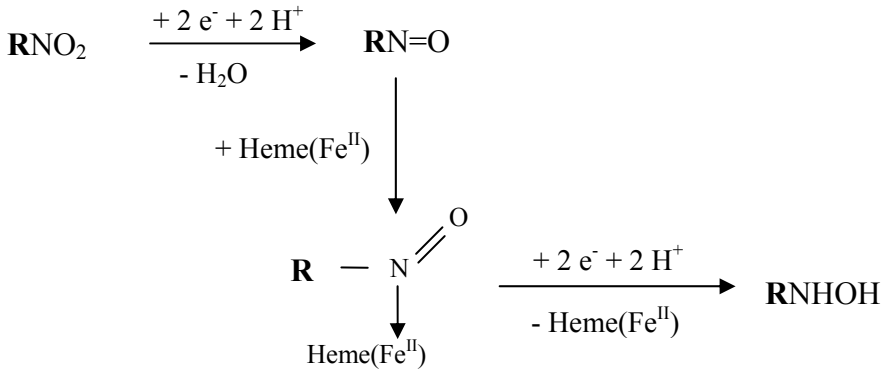

Scheme 4.3 Heme-catalyzed electroreduction of nitroalkanes

4.3.3 The effect of substrate concentration

The catalytic current increases as the concentration of substrate increases, Figure 4.5. One can see that the first redox couple Fe^{III}/Fe^{II}, which is caused by the surface confined hemin is not affected by the addition of nitroalkanes. Therefore, we can use the reductive wave of I_0 as an indication of the amount of hemin in the film. To eliminate the effect that is caused by the slight difference among electrodes, we use the ratio of I_{cat} / I_0 and referred it as catalytic efficiency. This way we can compare the catalysis of different nitroalkanes with different electrodes. From the plot of catalytic efficiencies as functions of substrate concentration, Figure 4.6 and Figure 4.7, one can see that the catalytic efficiencies increase steadily at low concentrations and tend to reach maximum at high

concentrations. This catalysis saturation behavior fits Michaelis-Menten enzyme kinetics, Equation 4.1.

$$V = \frac{V_{\max} \times [S]}{K_m + [S]} \qquad \text{(Michaelis-Menten Equation)} \qquad (4.1)$$

Since we use the normalized catalytic current, I_{cat} / I_0, as the measurement of the velocity of the reaction, Figure 4.6 and 4.7 can be treated as Michaelis-Menten plot. To obtain the kinetic parameters of the catalyst, we perform the non-linear regression using Michaelis-Menten equation and we can estimate the K_m values for each substrate and each catalyst system, Table 4.4.

Table 4.4 K_m values of hemin and iNOSoxy for different nitroalkane substrates from the non-linear regression of the Mechaelis-Menten plots

		nitromethane	nitroethane	1-nitropropane	2-nitropropane
Hemin	K_m (mM)	4.4 ±0.50	4.04 ±0.25	6.03 ±0.39	6.11 ±0.69
	k_{cat} (s^{-1})	68.3 ± 6.3	55.6 ± 4.8	45.8 ± 3.7	39.5 ± 4.1
	k_{cat}/K_m ($s^{-1}\cdot mM^{-1}$)	15.6	13.8	7.6	6.5
iNOSoxy	K_m (mM)	1.81±0.17	2.14±0.31	2.06±0.12	2.76±0.29
	k_{cat} (s^{-1})	28.1±2.2	26.3±1.9	23.1±1.7	20.7±1.6
	k_{cat}/K_m ($s^{-1}\cdot mM^{-1}$)	16.5	12.3	11.2	7.5

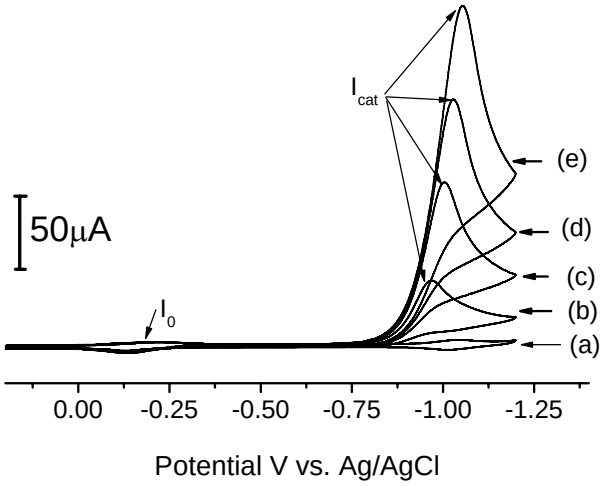

Figure 4.5 Cyclic voltammograms (a) 0 mM, (b) 0.3 mM, (c) 0.8 mM, (d) 1.3 mM, and (e) 2.0 mM of nitromethane electroreduction mediated by Hm/DDAB/PG in pH 5.5 buffer at 0.15 V/s.

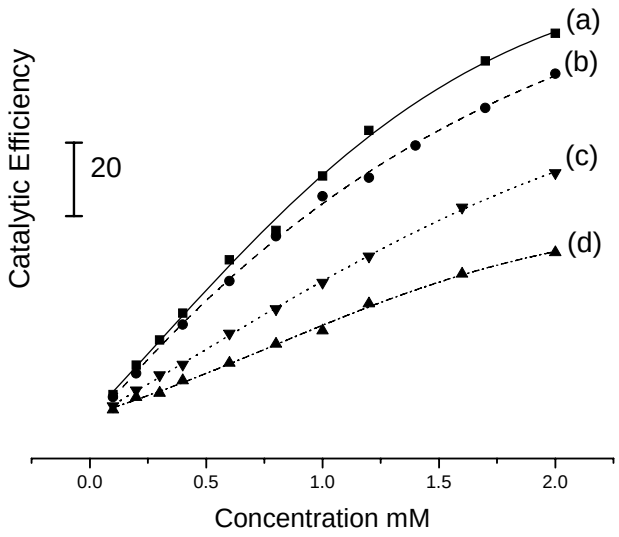

Figure 4.6 Catalytic efficiency as a function of nitroalkane concentration for Hm/DDAB/PG electrode. (a) nitromethane (b) nitroethane (c) 1-nitropropane (d) 2-nitropropane

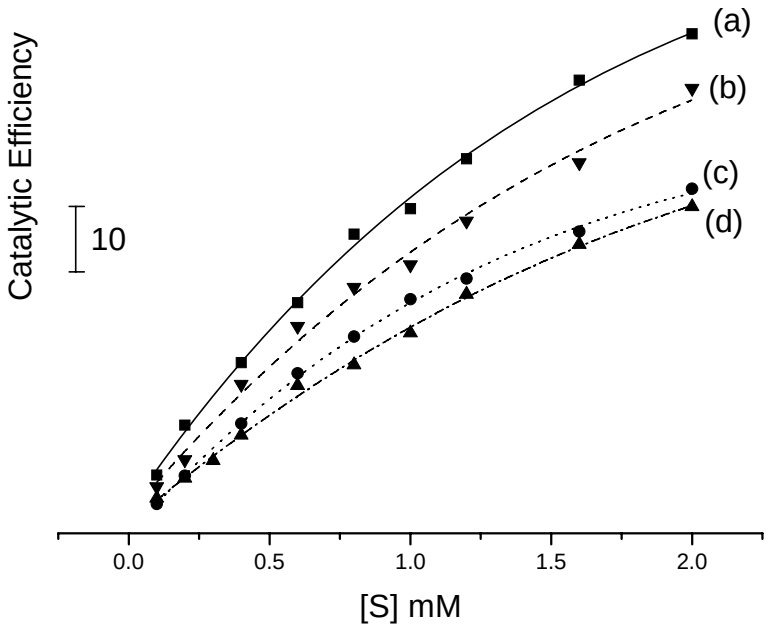

Figure 4.7 Catalytic efficiency as a function of nitroalkane concentration for iNOSoxy/DDAB/PG electrode. (a) nitromethane (b) nitroethane (c) 1-nitropropane (d) 2-nitropropane

Comparing the K_m of nitroalkane substrates in hemin-catalyzed reduction, nitromethane and nitroethane have similar smaller values, whereas 1-nitropropane and 2-nitropropane both have relatively larger values. Steric effects may contribute to this trend. Therefore, the larger K_m can be rationalized by the steric hindrance caused by the larger alkyl groups in the substrate-catalyst interaction process. This effect may cause a difference between smaller and larger nitroalkanes or between straight versus branched nitroalkanes because of their different geometric arrangements. This observation is consistent with previous reports that indicate the formation rate of the heme ferrous nitrosoalkane in solution is slower for larger nitroalkanes such as 2-nitropropane.[24]

The other Michaelis-Menten parameter k_{cat} can be obtained by non-linear regression of the Michaelis-Menten plot using the electrochemical format of Michaelis-Menten equation, as described in Chapter 2. The k_{cat} and the k_{cat}/K_m of each substrate indicate that hemin can catalyzed the electroreduction of smaller nitroalkane more efficiently than larger ones, and linear nitroalkane 1-nitropropane has higher turnover rate than the branched one.

In both case of hemin and iNOSoxy-mediated activation of different nitroalkanes, the catalytic efficiency follows the order: nitromethane > nitroethane > 1-nitropropane > 2-nitropropane, Figure 4.6 and 4.7, Our results suggest that the smaller the nitroalkane, the higher the catalytic efficiency. In addition, branched nitroalkanes show slightly lower rates of catalysis than their linear counterparts.

The K_m constants of nitroalkanes electroreduction for hemin as a catalyst are significantly larger than that for iNOSoxy. The proximal thiolate ligand of the iNOSoxy heme group help stabilize the trans-ligand, and the flanking residues around the binding

site also facilitate the binding of intermediates during turnover. These conditions are not met for bare hemin and thus large K_m value results.

4.3.4 The effect of scan rate

Scan rate of cyclic voltammetry defines the timescale within which the catalytic reaction is observed as well as substrate and product transports by diffusion. Increase of scan rate shortens the timescale and the catalysis is monitored very early in the process (less catalytic turnovers). As we seen in Figure 4.8, I_{ca}/I_0 decreases with logarithm of scan rate. Catalytic efficiencies of hemin-mediated electroreduction as a function of scan rate (Figure 4.8) shows the same trend for all the substrates, and within the same range of scan rate, the catalytic efficiencies of the 4 substrates follows the order nitromethane > nitroethane > 1-nitropropane > 2-nitropropane. Therefore, the size of the substrate molecule plays an important role in the catalysis. More of this will be discussed when we present our results of digital simulation of the catalytic process.

The catalytic efficiencies of iNOSoxy-mediated reduction of nitroalkane substrates show the expected decreasing trend with increasing scan rate, Figure 4.9. At low scan rate region (<1 V/s), the catalytic efficiencies of iNOSoxy-mediated reductions decrease faster than the efficiencies of the same reaction catalyzed by hemin. From scan rate 1V/s to 20V/s, the catalytic efficiency only exhibits only a slight decrease for all 4 substrates.

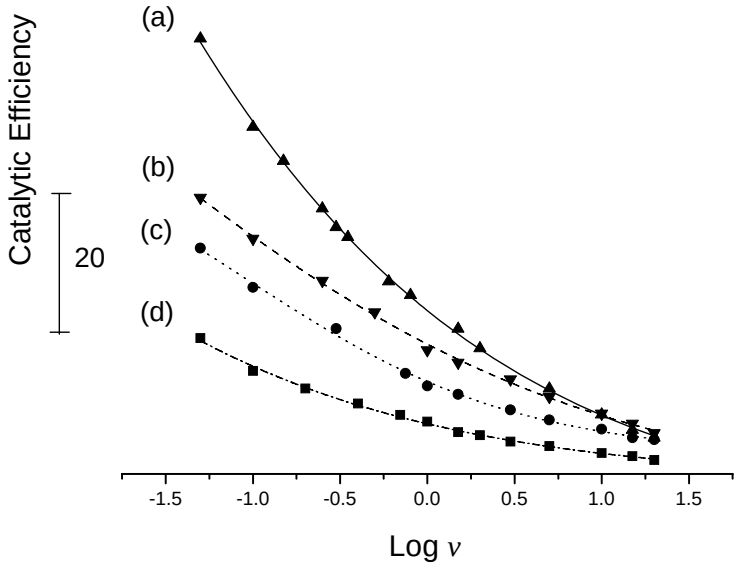

Figure 4.8 Catalytic efficiency as a logarithmic function of scan rate for Hm/DDAB/PG in pH5.5 buffer in the presence of 0.2 mM nitromethane. (a) nitromethane (b) nitroethane (c) 1-nitropropane (d) 2-nitropropane

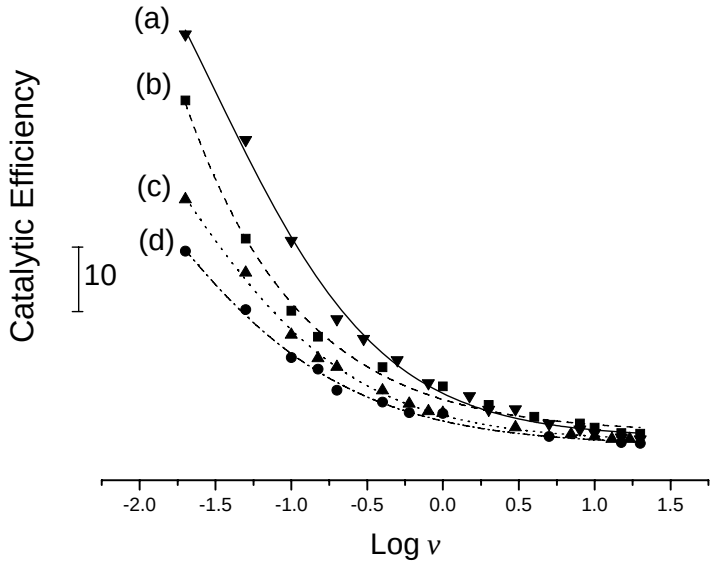

Figure 4.9 Catalytic efficiency as a logarithmic function of scan rate for iNOSoxy/DDAB/PG in pH5.5 buffer in the presence of 0.2 mM nitromethane. (a) nitromethane (b) nitroethane (c) 1-nitropropane (d) 2-nitropropane

4.3.5 The effect of pH

The catalytic electroreduction of nitroalkane is a 4-electron 4-proton process. The proton availability will obviously affect the efficiency of the catalysis. As seen in Figure 4.10 and Figure 4.11, catalytic efficiencies decrease with increasing pH. However, the trend of decrease for each substrate is irregular and unique, pointing to other factors that affect the catalytic reduction at different pHs other than proton availability.

Nitroalkanes are polar and slightly acidic in aqueous medium. Primary and secondary nitroalkanes can dissociate into nitronate anions and protons, Equation 4.2. The aci-nitro tautomerism of nitroalkane shows the equilibria of nitronic acid, $R_1R_2C{=}NO_2H$ (aci form), nitroalkane, and the nitronate anion $R_1R_2C{=}NO_2^-$ in neutral or basic medium, Equation 4.3.[25]

$$R_1R_2CH\text{-}NO_2 + H_2O \underset{k_{-1}}{\overset{k_1}{\rightleftharpoons}} R_1R_2C{=}NO_2^- + H_3O^+ \qquad (4.2)$$

$$R_1R_2C{=}NO_2H \underset{k_{-2}}{\overset{k_2}{\rightleftharpoons}} R_1R_2C{=}NO_2^- + H^+ \underset{k_1}{\overset{k_{-1}}{\rightleftharpoons}} R_1R_2CH\text{-}NO_2 \qquad (4.3)$$

Because of the intramolecular proton transfer, the nitro group can transform into several other functional groups. These unique chemical properties may play a role in the catalytic electroreduction of nitroalkanes. As shown in Nielsen's work,[25] pH is closely related to the tautomerization (equation 2) of nitroalkanes. Since the nitronate anion of nitroalkane is not electro reducible,[25] the ionization of nitroalkane should have an effect on the electroreduction. The ionization constant pK_a^{nitro} ($K_a = k_1/k_{-1}$) and pK_a^{Aci} ($K_a = k_2/k_{-2}$) for different nitroalkanes reported by Nielsen[25] are in Table 4.5.

Table 4.5 Ionization constant of nitroalkanes and nitronic acids in water[25]

nitroalkane	pK_a^{nitro}	pK_a^{Aci}
nitromethane	10.21	3.25
nitroethane	8.5	4.4
1-nitropropane	8.98	4.6
2-nitropropane	7.68	5.1

Since the ionization is much weaker for the nitro form of nitroalkane than the aci form, the catalytic efficiency in acidic and neutral media would not be affected too much by the ionization of nitroalkanes. However, in basic media, nitroalkanes will transform to nitronic acids and make the electroreduction process difficult. For hemin-mediated reductions, Figure 4.10a shows nitromethane having the sharpest decrease from pH 9 to pH 10.5, and the catalytic efficiency declining slopes (pH >9) follow the order nitromethane > nitroethane > 1-nitropropane > 2-nitropropane. This order fits the pK_a^{Aci} values of the aci form nitroalkanes.

We also tested the iNOSoxy-mediated catalytic reduction in the pH range from 5.35 to 10.00. The trends of the catalytic electroreduction for all the nitroalkane substrates were similar. Results show that while iNOSoxy-mediated catalytic reductions are dependent on protons, the dependence is less pronounced compared to hemin-mediated catalysis. The protein shell of iNOSoxy very likely plays a role in mediating proton transfers, which could act as a local buffer counteracting the change in bulk pH.

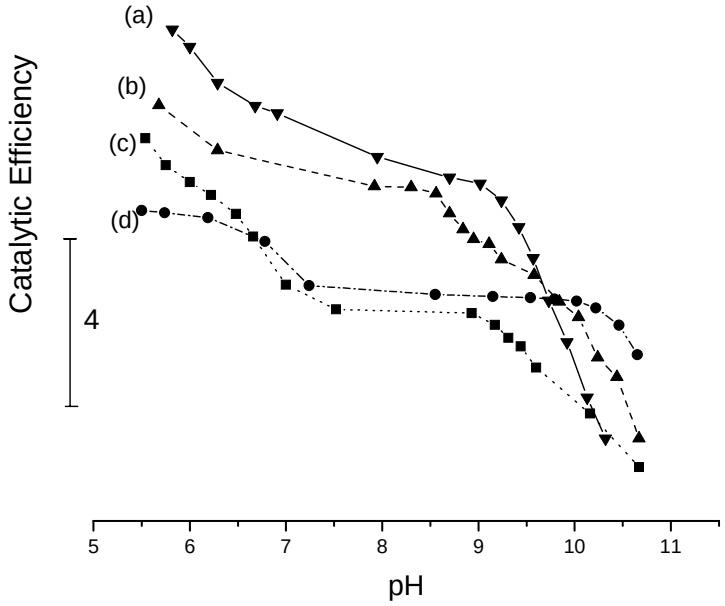

Figure 4.10 Catalytic efficiency as a function of pH for the nitroalkane electroreduction on Hm/DDAB/PG electrodes. (1) 0.2 mM nitromethane, (2) 0.2 mM nitroethane, (3) 0.2 mM 1-nitropropane, and (4) 0.2 mM 2-nitropropane.

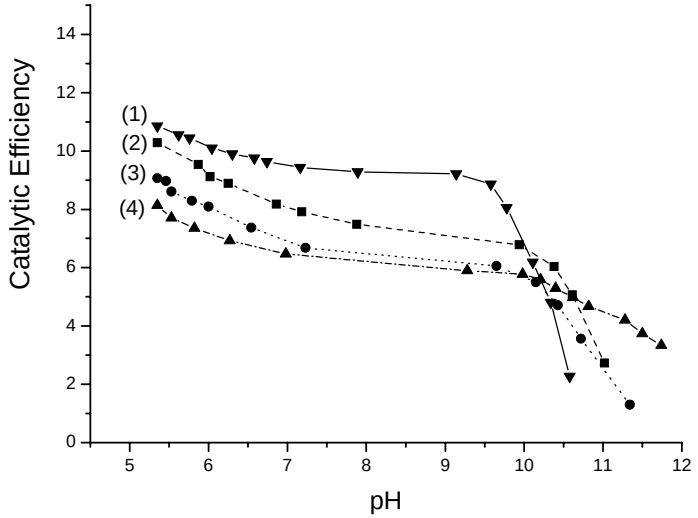

Figure 4.11 Catalytic efficiency as a function of pH for the nitroalkane electroreduction on iNOSoxy/DDAB/PG electrodes. (1) 0.2 mM nitromethane, (2) 0.2 mM nitroethane, (3) 0.2 mM 1-nitropropane, and (4) 0.2 mM 2-nitropropane.

4.3.6 Estimation of heterogeneous and homogeneous reaction rates

To further shed light on the mechanism and to assess the kinetics of catalytically initiated steps, we decided to carry out digital simulation of the voltammetric response of each substrate and catalytic system.

To test our working mechanism of heme-mediated nitroalkane electroreduction for all four substrates, we used digital simulation to calculate voltammetric response and fit our experimental data. We only show the results of hemin-mediated reduction.

The heme-mediated electroreduction of nitroalkanes involves multiple steps of chemical and electrochemical reactions as proposed in our previous study, and can be generalized as shown in Equation 4.4 to 4.7. The rate constant of each step can be adjusted in the program until a satisfactory fit to experimental data is achieved. The results from the simulations are tabulated in Table 4.6. The detailed simulation procedure is showed in Chapter 2. The simulated voltammograms are shown in Figure 4.12.

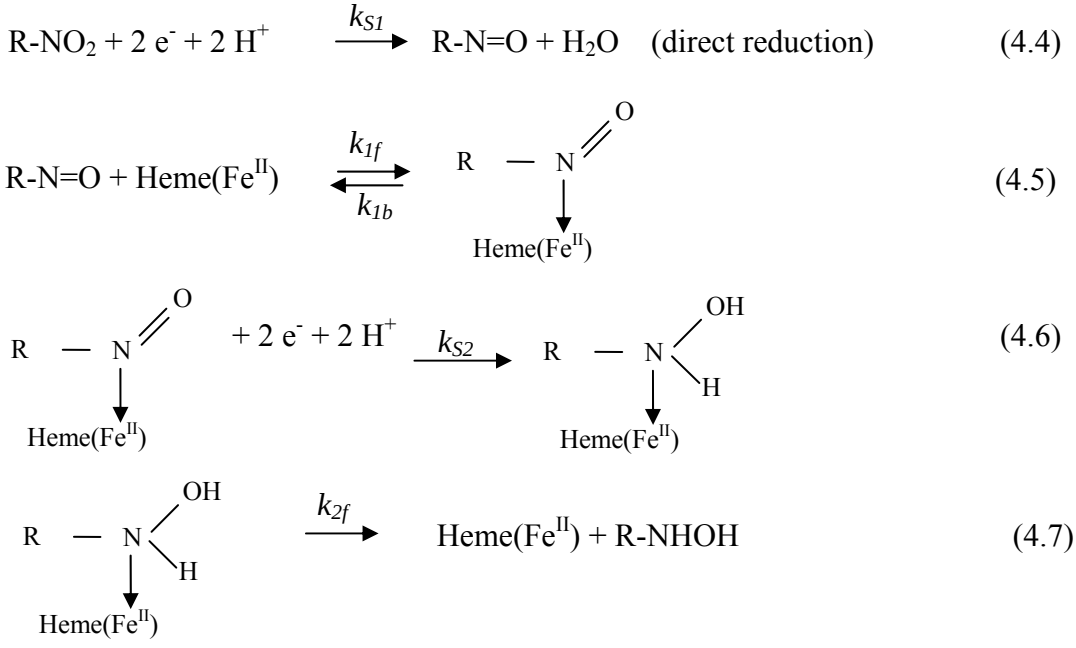

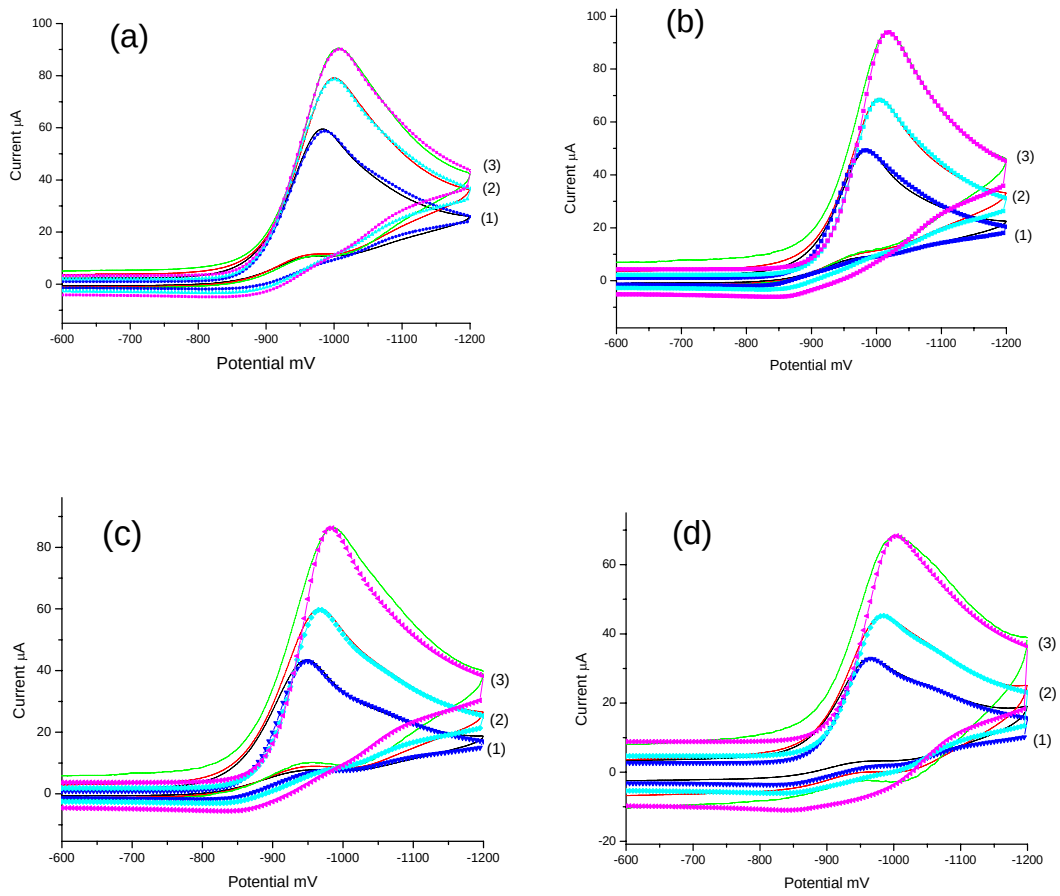

Figure 4.12 Digisim® simulation of cyclic voltammograms. (■) simulated voltammogram, (—) experimental voltammogram

(a) Cyclic voltammogram of Hm/DDAB/PG in the presence of 0.4 mM nitromethane at (1) 200 mV/s, (2) 400 mV/s, and (3) 600 mV/s.

(b) Cyclic voltammogram of Hm/DDAB/PG in the presence of 0.4 mM nitroethane at (1) 200 mV/s, (2) 400 mV/s, and (3) 800 mV/s.

(c) Cyclic voltammogram of Hm/DDAB/PG in the presence of 0.4 mM 1-nitropropane at (1) 200 mV/s, (2) 400 mV/s, and (3) 800 mV/s.

(d) Cyclic voltammogram of Hm/DDAB/PG in the presence of 0.4 mM 2-nitropropane at (1) 200 mV/s, (2) 400 mV/s, and (3) 800 mV/s.

Table 4.6 Digisim® simulation parameters of hemin-catalyzed nitroalkane electroreductions.

	k_{1f} ($s^{-1} \cdot M^{-1}$)	k_{1b} (s^{-1})	k_{2f} (s^{-1})	k_{S1} (cm/s)	k_{S2} (cm/s)
nitromethane	2×10^4	20	70	3.8×10^{-7}	0.01
nitroethane	2×10^4	25	55	3.3×10^{-7}	0.01
1-nitropropane	1.5×10^4	44	46	2.5×10^{-7}	0.01
2-nitropropane	1.5×10^4	50	40	2.1×10^{-7}	0.01

For all the substrates, the direct electroreduction of nitroalkane is sluggish (k_{S1} is in 10^{-7} range), whereas the hemin-mediated electroreduction is fast (the rate constant k_{S2} is 0.01). It is common for a catalyzed reaction. The catalyst-substrate complex formation rate k_{1f} for smaller nitroalkanes (CH_3NO_2 and $CH_3CH_2NO_2$) is faster and slower for the larger ones. The catalyst-substrate complex dissociation rate k_{1b} follows the order nitromethane<nitroethane<1-nitropropane<2-nitropropane. The simulation results nicely agreed with the arguments that in our previous discussion.

In addition, the results showed that the reaction rate of each step can fit perfectly to the Michaelis-Menten parameters (Table 4.4) as we know that by definition, k_{2f} is equal to k_{cat} and K_m is equal to $(k_{1b} + k_{2f}) / k_{1f}$. To show the relationship between Mechaelis-Menten parameters and reaction rate constants, we put the results from digital simulation and the results from Mechaelis-Menten analysis side by side in Table 4.7.

Table 4.7 The parameters derived from digital simulation and non-linear regression of Mechaelis-Menten plots.

	Digital simulation			Mechaelis-Menten analysis	
	k_{1f} ($s^{-1}\cdot M^{-1}$)	k_{1b} (s^{-1})	k_{2f} (s^{-1})	K_m (mM)	k_{cat} (s^{-1})
nitromethane	2×10^4	20	70	4.4 ±0.50	68.3 ± 6.3
nitroethane	2×10^4	25	55	4.04 ±0.25	55.6 ± 4.8
1-nitropropane	1.5×10^4	44	46	6.03 ±0.39	45.8 ± 3.7
2-nitropropane	1.5×10^4	50	40	6.11 ±0.69	39.5 ± 4.1

Digital simulation of heme-mediated electroreduction of nitroalkanes confirms our generalized mechanism of electrocatalysis. In addition, the rate constants of elementary steps of the electroreduction as derived from digital simulations over a range of scan rate agree very well with the numbers found for k_{cat} and K_m derived from simple Mechaelis-Menten analysis.

Simulated catalytic efficiency is obtained by dividing the simulated catalytic current (using a proposed mechanism scheme) by the simulated hemin(FeII) current without substrate. The simulated catalytic efficiency as a function of scan rate result is shown in Figure 4.13. The simulated curve fits our experimental data well as shown in Figure 4.13. This great fit of simulated curve to experimental data over a range of scan rates is an indication of the validity of the proposed mechanism as reported in the previous section.

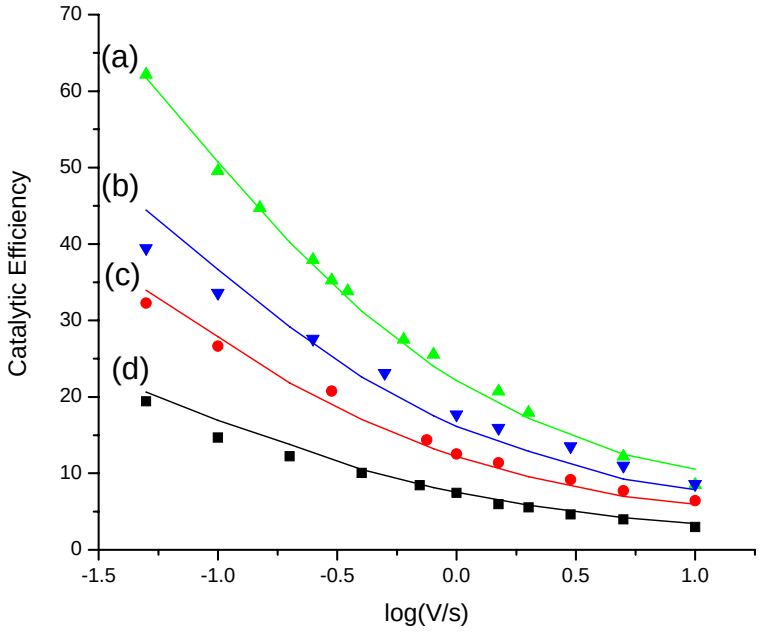

Figure 4.13 Simulated scan rate dependency curve with experimental data (a) nitromethane (b) nitroethane (c) 1-nitropropane (d) 2-nitropropane

4.4 Conclusion

Mass spectrometry shows that heme-mediated electroreductions of nitromethane, nitroethane, 1-nitropropane and 2-nitropropane produce the corresponding alkyl hydroxylamines as the final product. The intrinsic properties of aliphatic nitroalkanes affect their electroreduction process. The potential of catalytic peak differences among the various nitroalkanes seem to match inductive effect of alkyl groups connected to the nitro group. The size and shape of the substrate have a clear effect on the turnover rate. Smaller nitroalkanes exhibit higher turnover rates as compared to the larger ones. The K_m value of hemin catalyst for each nitroalkane substrate indicates the stability of the catalyst-substrate intermediate complex, which is likely, a heme-nitrosoalkane complex; smaller nitroalkanes such as nitromethane and nitroethane exhibit higher stability. The study of pH catalysis dependency shows that the catalytic reduction is affected by the intrinsic ionization of the nitronic acid. Digisim simulations of cyclic voltammograms not only estimate the reaction rate of each elementary step of our proposed mechanism of the electrocatalysis, but also reinforce and validate the parameters derived from non-linear regression fitting of Michaelis-Menten plots.

4.5 References

1. Hryhorczuk, D. O.; Aks, S. E.; Turk, J. W., Unusual occupational toxins. *Occup Med* **1992,** 7, (3), 567-86.

2. Conaway, C. C.; Nie, G.; Hussain, N. S.; Fiala, E. S., Comparison of oxidative damage to rat liver DNA and RNA by primary nitroalkanes, secondary nitroalkanes, cyclopentanone oxime, and related compounds. *Cancer Res* **1991,** 51, (12), 3143-7.

3. Dayal, R.; Gescher, A.; Harpur, E. S.; Pratt, I.; Chipman, J. K., Comparison of the hepatotoxicity in mice and the mutagenicity of three nitroalkanes. *Fundam Appl Toxicol* **1989,** 13, (2), 341-8.

4. Lewis, T. R.; Ulrich, C. E.; Busey, W. M., Subchronic inhalation toxicity of nitromethane and 2-nitropropane. *J Environ Pathol Toxicol* **1979,** 2, (5), 233-49.

5. Fiala, E. S.; Czerniak, R.; Castonguay, A.; Conaway, C. C.; Rivenson, A., Assay of 1-nitropropane, 2-nitropropane, 1-azoxypropane and 2-azoxypropane for carcinogenicity by gavage in Sprague-Dawley rats. *Carcinogenesis* **1987,** 8, (12), 1947-9.

6. Haas-Jobelius, M.; Coulston, F.; Korte, F., Effects of short-term inhalation exposure to 1-nitropropane and 2-nitropropane on rat liver enzymes. *Ecotoxicol Environ Saf* **1992,** 23, (3), 253-9.

7. Goggelmann, W.; Bauchinger, M.; Kulka, U.; Schmid, E., Genotoxicity of 2-nitropropane and 1-nitropropane in Salmonella typhimurium and human lymphocytes. *Mutagenesis* **1988,** 3, (2), 137-40.

8. Zhang, Z.; Rusling, J. F., Electron transfer between myoglobin and electrodes in thin films of phosphatidylcholines and dihexadecylphosphate. *Biophys Chem* **1997,** 63, (2-3), 133-46.

9. Cunningham, M. L.; Matthews, H. B., Relationship of hepatocarcinogenicity and hepatocellular proliferation induced by mutagenic noncarcinogens vs carcinogens. II. 1- vs 2-nitropropane. *Toxicol Appl Pharmacol* **1991,** 110, (3), 505-13.

10. George, E.; Burlinson, B.; Gatehouse, D., Genotoxicity of 1- and 2-nitropropane in the rat. *Carcinogenesis* **1989,** 10, (12), 2329-34.

11. Fiala, E. S.; Sodum, R. S.; Hussain, N. S.; Rivenson, A.; Dolan, L., Secondary nitroalkanes: induction of DNA repair in rat hepatocytes, activation by aryl sulfotransferase and hepatocarcinogenicity of 2-nitrobutane and 3-nitropentane in male F344 rats. *Toxicology* **1995,** 99, (1-2), 89-97.

12. Fiala, E. S.; Conaway, C. C.; Mathis, J. E., Oxidative DNA and RNA damage in the livers of Sprague-Dawley rats treated with the hepatocarcinogen 2-nitropropane. *Cancer Res* **1989,** 49, (20), 5518-22.

13. Sodum, R. S.; Fiala, E. S., N2-amination of guanine to 2-hydrazinohypoxanthine, a novel in vivo nucleic acid modification produced by the hepatocarcinogen 2-nitropropane. *Chem Res Toxicol* **1998,** 11, (12), 1453-9.

14. Sodum, R. S.; Nie, G.; Fiala, E. S., 8-Aminoguanine: a base modification produced in rat liver nucleic acids by the hepatocarcinogen 2-nitropropane. *Chem Res Toxicol* **1993,** 6, (3), 269-76.

15. Andrae, U.; Homfeldt, H.; Vogl, L.; Lichtmannegger, J.; Summer, K. H., 2-Nitropropane induces DNA repair synthesis in rat hepatocytes in vitro and in vivo. *Carcinogenesis* **1988,** 9, (5), 811-5.

16. Deng, X. S.; Tuo, J.; Poulsen, H. E.; Loft, S., 2-Nitropropane-induced DNA damage in rat bone marrow. *Mutat Res* **1997,** 391, (3), 165-9.

17. Fiala, E. S.; Sohn, O. S.; Li, H.; El-Bayoumy, K.; Sodum, R. S., Inhibition of 2-nitropropane-induced rat liver DNA and RNA damage by benzyl selenocyanate. *Carcinogenesis* **1997,** 18, (9), 1809-15.

18. Hussain, N. S.; Conaway, C. C.; Guo, N.; Asaad, W.; Fiala, E. S., Oxidative DNA and RNA damage in rat liver due to acetoxime: similarity to effects of 2-nitropropane. *Carcinogenesis* **1990,** 11, (6), 1013-6.

19. Harada, N.; Omura, T., Participation of cytochrome P-450 in the reduction of nitro compounds by rat liver microsomes. *J Biochem (Tokyo)* **1980,** 87, (5), 1539-54.

20. Jonen, H. G.; Oesch, F.; Platt, K. L., 4-Hydroxylation of nitrofurantoin in the rat. A 3-methylcholanthrene-inducible pathway of a relatively nontoxic compound. *Drug Metab Dispos* **1980,** 8, (6), 446-51.

21. Boutros, J.; Bayachou, M., Myoglobin as an efficient electrocatalyst for nitromethane reduction. *Inorg Chem* **2004,** 43, (13), 3847-53.

22. Charoenkwan Kraiya, P. S., Dennis H. Evans, Revisiting the heterogeneous electron-transfer kinetics of nitro compounds. *Journal of Electroanalytical Chemistry* **2004,** 563, 203–212.

23. Wheeler, O. H., Polarographic Reduction of Ortho Alkyl Nitrobenzenes. *Can. J. Chem* **1963,** 41, 192-194.

24. Renodon, A.; Boucher, J. L.; Wu, C.; Gachhui, R.; Sari, M. A.; Mansuy, D.; Stuehr, D., Formation of nitric oxide synthase-iron(II) nitrosoalkane complexes: severe restriction of access to the iron(II) site in the presence of tetrahydrobiopterin. *Biochemistry* **1998,** 37, (18), 6367-74.

25. Feuer, H., The chemistry of nitro and nitroso groups. *Robert E. Krieger Publishing Company, Huntington, New York* **1981,** Chapter 7, 349-486.

Appendix A

Cyclic Voltammetry

Cyclic voltammetry (CV) is a potentiodynamic electrochemical technique. In a cyclic voltammetry experiment the working electrode potential is scanned linearly versus time as shown in the potential waveform plot. When the scan reaches a set point of potential, the potential scan is inverted. This inversion can be set multiple times during one single experiment. The current passing through the working electrode is recorded versus the potential applied to give the cyclic voltammogram. The waveform and resulting voltammogram is shown in Figure A1.

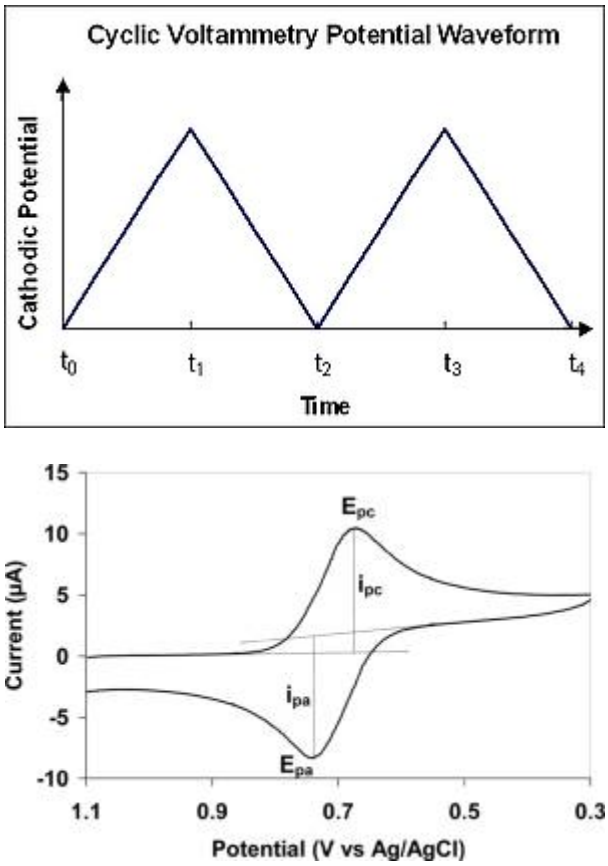

Figure A1 Waveform and resulting voltammogram of cyclic voltammetry (CV)

Appendix B

Demonstration of fabricating PG working electrodes

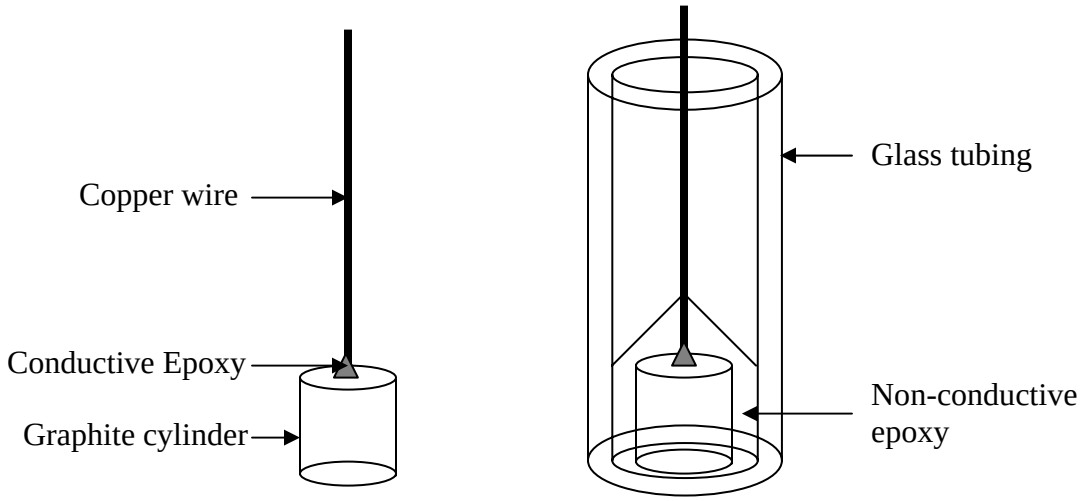

Figure B Fabrication of the PG working electrode.

Appendix C

DigiSim® simulation

DigiSim is a simulation software developed by BASi for cyclic voltammetry. DigiSim can be used to simulate any electrochemical mechanism that can be expressed in terms of single or multiple electron transfer reactions and first- and second-order homogenous reactions. In addition, DigiSim can generate dynamic concentration profiles and can fit simulated data to imported experimental data.[1]

Mechanism used to fit our cyclic voltammogram:

$CH_3NO_2 + 2e = CH_3NO$

$Fe^{II} + CH_3NO = Fe^{II}CH_3NO$

$Fe^{II}CH_3NO + 2e = Fe^{II}CH_3NHOH$

$Fe^{II}CH_3NHOH = Fe^{II} + CH_3NHOH$

$Fe^{II} + e = Fe^{I}$

(1) Copyright © Bioanalytical Systems, Inc.